SHARE

SEVENTH FRAMEWORK PROGRAMME

Grant Agreement no. 226967
Seismic Hazard Harmonization in Europe
Project Acronym: SHARE

SP 1-Cooperation

Collaborative project: Small or medium-scale focused research project

THEME 6: Environment

Call: ENV.2008.1.3.1.1 Development of a common methodology and tools to evaluate earthquake hazard in Europe

D2.5 – Seismic loss scenarios for sample European cities and regions

Due date of deliverable: 30.11.2012
Actual submission date: 15.03.2013

Start date of project: 2009-06-01 Duration: 42

Universita degli Studi di Pavia (UPAV)
H. Crowley, M. Colombi,

Laboratorio National de Engenharia Civil (LNEC)
M.L. Sousa, A. Carvalho, E. Coehlo

Aristotle University of Thessaloniki (AUTH)
E. Riga, K. Pitilakis, A. Anastasiadis, D. Pitilakis, M. Manakou, A. Karatzetzou, Stavroula Fotopoulou

Kandilli Observatory and Earthquake Research Institute (KOERI)

Revision: 2

Dissemination Level		
PU	Public	x
PP	Restricted to other programme participants (including the Commission Services)	
RE	Restricted to a group specified by the consortium (including the Commission Services)	
CO	Confidential, only for members of the consortium (including the Commission Services)	

TABLE OF CONTENTS

TABLE OF CONTENTS 2
1. Introduction 11
2. Seismic Risk Assessment 11
2.1. Analytical approach 12
2.1.1. Building damage 12
2.1.2. Social losses 14
2.1.3. Economic losses 15
2.2. Empirical approach 16
3. Regional seismic risk applications 16
3.1. Italy 16
3.1.1. Seismic hazard assessment 17
3.1.2. Exposure 24
3.1.3. Vulnerability 26
3.1.4. Seismic Risk 28
3.2. Marmara Region 38
3.2.1. Seismic hazard assessment 39
3.2.2. Exposure 42
3.2.3. Vulnerability 44
3.2.4. Seismic Risk 45
4. Urban seismic risk applications 48
4.1. Thessaloniki 48
4.1.1. Seismic hazard assessment 48
4.1.2. Exposure 55
4.1.3. Vulnerability 58
4.1.4. Seismic Risk 60
4.2. Lisbon 75
4.2.1. Seismic hazard assessment 77
4.2.2. Exposure 84
4.2.3. Vulnerability 90
4.2.4. Seismic Risk 93
5. Conclusion 101
REFERENCES 103
ANNEX A – Seismic zonation for the first Portuguese earthquake resistant codes 108
ANNEX B – Parameters of building damage model 109
ANNEX C – Parameters of social loss model 112

LIST OF FIGURES

Figure 2.1 (a) performance point of a low rise concrete moment resisting frame designed with moderate code (b) expected displacement response overlaid with the fragility curves (c) discrete building damage probability 14
Figure 3.1 : a) Level 1 – region limits, b) Level 2 – province limits, c) Level 3 – municipality limits 16
Figure 3.2: Seismic hazard map in terms of PGA ordinates for a return period of 475 years (0.05° resolution) 18
Figure 3.3: Elastic design spectra for soil classes A-E for an Italian municipality 20
Figure 3.4: SHARE seismic hazard maps in terms of PGA ordinates for a return period of 475 years. (a) model 1 (b) model 2 21
Figure 3.5: SHARE UHS for an Italian municipality estimated with the model 1 and model 2 21
Figure 3.6: Comparative map. Difference between SHARE model 1 and SHARE model 1 Fixed seismic hazard in terms of Sa(4) ordinates for a return period of 475 years. 22
Figure 3.7: Comparative maps. Difference between SHARE model 1 and NTC08 seismic hazard in terms of (a) PGA and (b) Sa(0.5) ordinates for a return period of 475 years... 23
Figure 3.8: Comparative maps. Difference between SHARE model 2 and NTC08 seismic hazard in terms of (a) PGA and (b) Sa(0.5) ordinates for a return period of 475 years... 23
Figure 3.9: Comparative maps. Difference between SHARE model 1 and SHARE model 2 seismic hazard in terms of (a) PGA and (b) Sa(0.5) ordinates for a return period of 475 years. 24
Figure 3.10: Comparison between NTC08 elastic design spectrum and SHARE UHS, model 1 and model 2, for an Italian municipality. 24
Figure 3.11: Percentages of (a) masonry (b) non seismically designed reinforced concrete (c) seismically designed reinforced concrete buildings in each municipality 25
Figure 3.12: Distribution of population throughout Italy 26
Figure 3.13: Proportion of (a) masonry and (b) reinforced concrete buildings for each number of storeys obtained from a sample of buildings in Catania (Faccioli and Pessina, 2000). (NI means the storey number was unknown) 27
Figure 3.14: (a) Plot of three different capacity curves for different vulnerability classes (b) Fragility curves of a low rise reinforced concrete seismically designed (c=10%) building 28
Figure 3.15: Comparison of the conditional seismic risk for a return period of 475 years in term of percentage of (a) no damaged buildings (b) slight damage buildings (c) moderate damaged buildings (d) extensive damaged buildings and (e) collapsed buildings. SHARE model 1 versus NTC08. 29
Figure 3.16: Comparison of the percentages of casualties (a) level 1 (b) level 2 (c) level 3 (d) level 4. SHARE model 1 versus NTC08. 30
Figure 3.17: Comparison of the conditional seismic risk for a return period of 475 years in term of percentage of (a) no damaged surface area (b) slight damaged surface area (c)

moderate damaged surface area (d) extensive damaged surface area and (e) collapsed surface area. SHARE model 1 versus NTC08. 31
Figure 3.18: Comparison of the Mean Damage Ratio. SHARE model 1 versus NTC08. 31
Figure 3.19: Comparison of the conditional seismic risk for a return period of 475 years in term of percentage of (a) no damaged buildings (b) slight damage buildings (c) moderate damaged buildings (d) extensive damaged buildings and (e) collapsed buildings. SHARE model 2 versus NTC08. 32
Figure 3.20: Comparison of the percentages of casualties (a) level 1 (b) level 2 (c) level 3 (d) level 4. SHARE model 2 versus NTC08. 33
Figure 3.21: Comparison of the conditional seismic risk for a return period of 475 years in term of percentage of (a) no damaged surface area (b) slight damaged surface area (c) moderate damaged surface area (d) extensive damaged surface area and (e) collapsed surface area. SHARE model 2 versus NTC08. 34
Figure 3.22: Comparison of the Mean Damage Ratio. SHARE model 2 versus NTC08. 34
Figure 3.23: Comparison of the conditional seismic risk for a return period of 475 years in term of percentage of (a) no damaged buildings (b) slight damage buildings (c) moderate damaged buildings (d) extensive damaged buildings and (e) collapsed buildings. SHARE model 1 versus SHARE model 2. 35
Figure 3.24: Comparison of the percentages of casualties (a) level 1 (b) level 2 (c) level 3 (d) level 4. SHARE model 1 versus SHARE model 2. 36
Figure 3.25: Comparison of the conditional seismic risk for a return period of 475 years in term of percentage of (a) no damaged surface area (b) slight damaged surface area (c) moderate damaged surface area (d) extensive damaged surface area and (e) collapsed surface area. SHARE model 1 versus SHARE model 2. 37
Figure 3.26: Comparison of the Mean Damage Ratio. SHARE model 1 versus SHARE model 2. 37
Figure 3.27 Location of the Marmara Region at Province level 38
Figure 3.28 Location of the Marmara Region at Sub-Province level 39
Figure 3.29 Seismic hazard maps in terms of macroseismic intensity for a return period of 72 years (0.05° resolution) 41
Figure 3.30 Seismic hazard maps in terms of macroseismic intensity for a return period of 475 years (0.05° resolution) 41
Figure 3.31 Seismic hazard maps in terms of macroseismic intensity for a return period of 2475 years (0.05° resolution) 42
Figure 3.32 Number of buildings of type of reinforced concrete, mid rise and pre1980 43
Figure 3.33 Distribution of population in Turkey on the basis of Landscan data 44
Figure 3.34 Intensity based vulnerability curves for the general mid rise (bold dashed lines) and high-, and low-rise R/C frame type and masonry buildings (thin solid lines) in Turkey 45
Figure 3.35 Province based building damage distribution corresponding to 475 years return period. Chart size indicates total number of damaged buildings 46

Figure 3.36 Province based building damage distribution (Damage states D3+D4+D5) corresponding to 475 years return period. Chart size indicates total number of buildings. 46
Figure 3.37 Province based loss ratio corresponding to 475 years return period 47
Figure 3.38 Province based loss ratio corresponding to 475 years return period 48
Figure 4.1: Study area in SYNER-G case study. Red lines illustrate Urban Audit SCDs boundaries. 48
Figure 4.2: PGA_{rock} zones for the Metropolitan area of Thessaloniki for a mean return period Tm=475 years based on seismic hazard results from SRM-LIFE. 49
Figure 4.3: SHARE UHS for Thessaloniki, compared to EC8 Type 1 rock spectra for the two PGA_{rock} values for Thessaloniki from SRM-LIFE (rock site conditions). 50
Figure 4.4: Map of EC8 site classes for Thessaloniki compiled utilizing all available geological, geophysical and geotechnical information. Grey polygons illustrate the building blocks of the study area. 51
Figure 4.5: Map of new site classes for Thessaloniki compiled utilizing all available geological, geophysical and geotechnical information. Grey polygons illustrate the building blocks of the study area. 52
Figure 4.6: EC8 Type 1 elastic response spectra for soil classes B and C and for PGA_{rock}=0.2g or 0.24g (Hazard 1). 53
Figure 4.7: (a) SHARE rock UHS for Thessaloniki amplified with the current (Hazard 4) and the improved (Hazard 5) EC8 soil amplification factors, (b) SHARE rock UHS for Thessaloniki amplified with the soil amplification factors of the new classification system (Hazard 6). All spectra refer to a return period T=475 years. 54
Figure 4.8: Elastic Response Spectra of Thessaloniki 1978 accelerograms recorded at City Hotel compared to various code spectra. 55
Figure 4.9: Building blocks of Thessaloniki study area. 56
Figure 4.10: Classification of the RC buildings of the study area based on the BTM of Table 4.4 (Kappos et al. 2006). The first letter of each building type refers to the height of the building (L: low, M: medium, H: high), while the second letter refers to the seismic code level of the building (N: no, L: low, M: medium, H: high). 58
Figure 4.11: Plot of representative pushover curves for high-rise R/C frames designed to high codes (Kappos et al. 2006). 59
Figure 4.12: Fragility curves for mid-rise regularly infilled dual R/C systems, for (a) “low” and (b) “medium” code design, for a beta value equal to 0.4 (modified after Kappos et al. 2006). 59
Figure 4.13: Hazard 1: Seismic risk per Sub-City District for a return period of 475 years in terms of the percentage of floor area for no damaged buildings, slight damaged buildings, moderate damage buildings, extensive damaged buildings and, complete damaged buildings. 61
Figure 4.14: Hazard 1: Economic losses per Sub-City District in terms of Mean Damage Ratio (MDR). MDR for the whole study area is estimated as equal to 26.91% 62
Figure 4.15: Hazard 1: Percentages of casualties (a) level 1 (b) level 2 (c) level 3 (d) level 4. 63

Figure 4.16: Hazard 4: Seismic risk per Sub-City District for a return period of 475 years in terms of the percentage of floor area for no damaged buildings, slight damaged buildings, moderate damaged buildings, extensive damaged buildings and complete damaged buildings..... 63
Figure 4.17: Hazard 5: Seismic risk per Sub-City District for a return period of 475 years in terms of the percentage of floor area for no damaged buildings, slight damaged buildings, moderate damaged buildings, extensive damaged buildings and complete damaged buildings..... 64
Figure 4.18: Hazard 6: Seismic risk per Sub-City District for a return period of 475 years in terms of the percentage of floor area for no damaged buildings, slight damaged buildings, moderate damaged buildings, extensive damaged buildings and complete damaged buildings..... 64
Figure 4.19: Hazard 4: Economic losses per Sub-City District in terms of Mean Damage Ratio (MDR). 65
Figure 4.20: Hazard 5: Economic losses per Sub-City District in terms of Mean Damage Ratio (MDR). 65
Figure 4.21: Hazard 6: Economic losses per Sub-City District in terms of Mean Damage Ratio (MDR). 66
Figure 4.22: Hazard 4: Percentages of casualties (a) level 1 (b) level 2 (c) level 3 (d) level 4. 67
Figure 4.23: Hazard 5: Percentages of casualties (a) level 1 (b) level 2 (c) level 3 (d) level 4. 68
Figure 4.24: Hazard 6: Percentages of casualties (a) level 1 (b) level 2 (c) level 3 (d) level 4. 68
Figure 4.25: Capacity curves for the most frequent RC buildings typologies in Thessaloniki and Hazard 1 elastic and reduced demand spectra. 70
Figure 4.26: Performance points for RC4.2ML building typology located on soil class B, for Hazard 1 (current hazard) and Hazard 4 (SHARE hazard). 70
Figure 4.27: Comparative maps. Hazard 4 versus Hazard 1: Conditional seismic risk for a return period of 475 years in terms of (Hazard4-Hazard1) percentages of (a) no damaged floor area (b) slight damaged floor area (c) moderate damaged floor area (d) extensive damaged floor area and (e) complete damaged floor area. 71
Figure 4.28: Comparative map. Hazard 4 versus Hazard 1: Economic losses per Sub-City District in terms of (Hazard4-Hazard1) Mean Damage Ratio (MDR)..... 72
Figure 4.29: Comparative maps. Hazard 4 versus Hazard 1:..... 72
Figure 4.30: Portugal, Lisbon Metropolitan Area and some neighbouring counties (MAL) and Lisbon municipality..... 76
Figure 4.31: Mainland Portuguese seismic zonation (a) seismic action Type 1 (b) seismic action Type 2 [NP EN 1998-1: 2010]. 78
Figure 4.32: Shape of elastic response spectrum [EN 1998-1: 2004]. 79
Figure 4.33: Elastic response spectra for Lisbon. 79
Figure 4.34: Soil types for each parish of MAL [Carvalho et al., 2002]. 80

Figure 4.35: Elastic response spectra for Sesimbra, at bedrock and considering soil effects; seismic action Type 1. 81
Figure 4.36: Elastic response spectra for Sesimbra, at bedrock and considering soil effects; seismic action Type 2. 81
Figure 4.37: Comparison of NA of EC8 elastic response spectra and SHARE models for Lisbon. 82
Figure 4.38: Peak ground acceleration at surface for MAL and a return period of 475 years. Top: NP EN 1998-1; left: seismic action Type 1; right: seismic action Type 2. Down: SHARE; left: Model 1; right: Model 2. 83
Figure 4.39: Sa(0,3s) ordinates for MAL and a return period of 475 years. Top: NP EN 1998-1. left: seismic action Type 1; right: seismic action Type 2. Down: SHARE; left: Model 1; right: Model 2. 84
Figure 4.40: Seismic vulnerability maps for MAL; percentages of buildings per parish in each vulnerability classes. Figures (a-g) are based on **2001** inventory a) Adobe and Rubble Stone; b) Masonry before 1960; c) Masonry 1961 – 1985; d) Masonry 1986 – 2001; e) RC before 1960 f) RC 1961 – 1985 g) RC 1986 – 2001; Figure (h) is based on **2011** inventory. 88
Figure 4.41: Percentages of individuals per MAL's parish in each vulnerability class. Figures (a - g) are based on **2001** inventory; a) Adobe and Rubble Stone; b) Masonry before 1960; c) Masonry 1961 – 1985; d) Masonry 1986 – 2001; e) RC before 1960 f) RC 1961 – 1985 g) RC 1986 – 2001; Figure (h) is based on **2011** inventory. 90
Figure 4.42: (a) Example of a capacity curve (in black) and of fragility curves for 5 damage states. 92
Figure 4.43: Iterative process to obtain the peak of building response in the capacity spectrum method [Campos Costa et al., 2010]. 92
Figure 4.44: Conditional seismic risk for a hazard level of 475 years return period, measured in terms of the percentage of (a) no damaged buildings (b) slight damaged buildings (c) moderate damage buildings (d) extensive damaged buildings and (e) complete damaged buildings. Seismic Action **Type 1** of NA of EC8. 94
Figure 4.45: Percentage of casualties conditional on a 475 years return period hazard level: (a) light injury (b) hospitalization (c) severe injury and (d) killed. Seismic Action **Type 1** of NA of EC8. 95
Figure 4.46: Percentage of lost building area conditional on a 475 years return period hazard level. Seismic Action **Type 1** of NA of EC8. 95
Figure 4.47: Conditional seismic risk for a hazard level of 475 years return period, measured in terms of the percentage of (a) no damaged buildings (b) slight damaged buildings (c) moderate damage buildings (d) extensive damaged buildings and (e) complete damaged buildings. Seismic Action **Type 2** of NA of EC8. 96
Figure 4.48: Percentage of casualties conditional on a 475 years return period hazard level: (a) light injury (b) hospitalization (c) severe injury and (d) killed. Seismic Action **Type 2** of NA of EC8. 96
Figure 4.49: Percentage of lost building area conditional on a 475 years return period hazard level. Seismic Action **Type 2** of NA of EC8. 97

Figure 4.50: Comparative maps: conditional seismic risk for a hazard level of 475 years return period in terms of the percentage of (a) no damaged buildings (b) slight damaged buildings (c) moderate damage buildings (d) extensive damaged buildings and (e) complete damaged buildings. 98
Figure 4.51: Comparative maps: percentage of casualties conditional on a hazard level of 475 years return period: (a) light injury (b) hospitalization (c) severe injury and (d) killed. . 99
Figure 4.52: Comparative maps: percentage of lost building area conditional on a hazard level of 475 years return period. 100

LIST OF TABLES

Table 2.1: Description of the injury severity levels 14
Table 2.2 Casualty rates for reinforced concrete moment frame structures..... 15
Table 2.3 Casualty rates for unreinforced masonry structures..... 15
Table 3.1 Ground Type 19
Table 3.2 Values of S_S and C_C 19
Table 3.3 Values of S_T 20
Table 3.4: Vulnerability classes considered for Italian building stock in terms of construction type, number of storeys and level of seismic design..... 26
Table 4.1 Proposed Soil and Site Characterization (Pitilakis et al. 2013) 50
Table 4.2 Current and improved soil amplification factors S for the existing EC8 classification scheme (Pitilakis et al. 2012) 52
Table 4.3 Parameters of proposed acceleration response spectra (Pitilakis et al. 2013)..... 52
Table 4.4 R/C Building Typology Matrix (BTM) for Thessaloniki (Kappos et al. 2006)..... 56
Table 4.5 Loss indices for R/C structures (Kappos et al. 2003)..... 60
Table 4.6: Percentages of affected floor area per damage state for the current hazard scenario (Hazard 1), for a return period of 475 years..... 61
Table 4.7: Estimated Level 1 - Level 4 casualties for the current hazard scenario (Hazard 1), for a return period of 475 years..... 63
Table 4.8: Percentages of damaged buildings per damage state for the SHARE hazard scenarios, for a return period of 475 years. 64
Table 4.9: Mean Damage Ratios for the SHARE hazard scenarios (4-6), for a return period of 475 years 66
Table 4.10: Economic losses for the SHARE hazard scenarios (4-6), for a return period of 475 years, assuming an average replacement cost equal to 1000€/m^2 66
Table 4.11: Estimated Level 1 - Level 4 casualties for the SHARE hazard scenarios (4-6), for a return period of 475 years..... 68
Table 4.12: Percentages of damaged buildings per damage state for the current (blue) and the SHARE (red) hazard scenarios, for a return period of 475 years. 72
Table 4.13: Mean Damage Ratios for the current (blue) and the SHARE (red) hazard scenarios, for a return period of 475 years. 73
Table 4.14: Economic losses (in billions €) for the current (blue) and the SHARE (red) hazard scenarios, for a return period of 475 years. 73
Table 4.15: Estimated Level 1 - Level 4 casualties for the current (blue) and the SHARE (red) hazard scenarios, for a return period of 475 years. 73
Table 4.16: Percentages of damaged buildings per damage state for the current (blue) and the SHARE (red) hazard scenarios for a return period of 475 years, estimated with PGA-based and Sd-based fragility curves. 74
Table 4.17: Mean Damage Ratios for the current (blue) and the SHARE (red) hazard scenarios, for a return period of 475 years, estimated with PGA-based and Sd-based fragility curves..... 74

Table 4.18: Economic losses (in billions €) for the current (blue) and the SHARE (red) hazard scenarios, for a return period of 475 years, estimated with PGA-based and Sd-based fragility curves. 74
Table 4.19: Estimated Level 1 - Level 4 casualties for the current (blue) and the SHARE (red) hazard scenarios, for a return period of 475 years, estimated with PGA-based and Sd-based fragility curves. 74
Table 4.20: Comparison of damages predicted from Hazard 1 and Hazard 4 with the actual damages from Thessaloniki 1978 EQ 75
Table 4.21: Statistics for MAL [INE, 2002 and INE, 2011]. 76
Table 4.22: Reference peak ground acceleration [NP EN 1998-1: 2010]. 78
Table 4.23: Values of the parameters describing Type 1 and Type 2 elastic response spectra for Portugal; soil type A [NP EN 1998-1: 2010]. 79
Table 4.24: Vulnerability factors identified in Census 2001 [Carvalho et al., 2002; Sousa et al., 2003]. 85
Table 4.25: Vulnerability classes for MAL building stock [LESSLOSS, 2007]. 86
Table 4.26: Number of residential buildings per vulnerability class. 87
Table 4.27: Number of individuals per vulnerability class. 88
Table 4.28: Seismic risk for MAL considering the hazard specification of the NA of EC8 and SHARE hazard output. 100
Table 4.29: Relative differences of seismic risk for MAL, considering the hazard specifications of the NA of EC8 and SHARE hazard output. 101

1. Introduction

Comparative risk assessments for selected European cities and regions are the main aim of Task 2.5 in the SHARE project. This task deals with the comparison of seismic risk and loss assessment scenarios for selected European cities and regions. For what concerns regions, Italy and the Marmara region have been selected. With regards to the cities, the comparison has been carried out for Lisbon and Thessaloniki. The main goal of this task is the comparison between the final seismic risk results using local hazard studies and using the SHARE hazard output. Seismic hazard maps currently employed in those region as well as the new hazard model developed and proposed in the SHARE project have been used to estimate risk. It has to be noted that due to the fact that the same exposure and vulnerability features have been used in the calculation of the seismic risk with the different hazard results, the differences between the results are due to the influence and the impact of the hazard on the assets. It is also worthy to note that the SHARE hazard values used within this task are the results which were made available in November 2012. Because of the deadlines and the time needed to run the seismic risk analyses it was not possible to re-run the analyses with the most up-to-date SHARE results that were released at the end of the project.

Notwithstanding that, this comparison will be very useful to better appreciate and scrutinize the consequences, in terms of practical design application/assessment and seismic risk evaluation/mitigation policies, of the introduction of a new European seismic hazard model.

This deliverable describes the necessary parameters used to estimate the seismic risk focusing mainly on the differences due to the two types of hazard that have been adopted. Chapter 2 describes one of the possible ways that can be run to compute the building damage, the social losses and the economic losses of a country. Then, the following sections describe the test-bed applications developed within this task. It is possible to divide the report in two main sections: regional seismic risk applications (Chapter 3) and urban seismic risk applications (Chapter 4). The final section of each chapter provides a critical comparison of the results evaluated within this task. Finally, Chapter 5 provides a summary of the findings of this study.

2. Seismic Risk Assessment

The evaluation of seismic risk to buildings involves many disciplines from data collection to vulnerability assessment to seismic hazard assessment to social and economic sciences. In simple terms, the seismic risk can be described as the probability of loss at a given site and is obtained through the convolution of three parameters: exposure, vulnerability and seismic hazard. A fourth parameter may then be added through which the seismic risk can be related to a social or economic loss. When carrying out seismic risk assessment for a large region, or even a whole country, the exposure is generally obtained from a building census whilst the

seismic hazard is described in terms of a ground-motion parameter which should be correlated to the damage of different classes of buildings or other exposed elements through a vulnerability function.

In mathematical terms, seismic risk can be described as the unconditional probability of failure *(P*f *)* for a system with resistance *R*, under a seismic load S, using the following equation:

$$P_f = \int^{+\infty} f_s(s) F_R(S) dS \qquad 2.1$$

where f_S is the probability density function of the ground-motion parameter (which can be obtained through the derivation of the seismic hazard curve) and $F_R(S)$ is the probability that the resistance *R* is less than a given level of severity, S (often termed the fragility curve). Hence, the annual probability of collapse, for example, can be obtained by combining the probability of exceeding the resistance of the building to collapse for a given level of ground motion [F_R*(*S*)*], with the annual probability of obtaining that level of ground motion (f_S*)*, and summing this product over all possible levels of ground motion. This would allow one to estimate the mean annual probability of collapse for a given typology of buildings; this calculation would need to be repeated for each typology present in the inventory of buildings (the exposure model) and then the results would be combined considering the proportion of each building typology. Once the mean annual probability of collapse for all buildings has been calculated it can be related to economic and social losses; e.g. the mean cost of reconstructing the collapsed buildings, multiplied by the annual probability of collapse, multiplied by the total number of buildings would lead to the mean annual loss due to collapse. In the following sections the methods to compute the seismic risk assessment are briefly described. Both an analytical and an empirical method have been used.

2.1. Analytical approach

2.1.1. Building damage

To determine the seismic performance of a building a comparison between the capacity of the structure and the seismic demand is necessary. There are several methodologies to identify the so-called performance point on the capacity spectrum, and the Capacity Spectrum Method (CSM), as proposed in ATC, 40 [ATC, 1996], has been chosen to evaluate the building damage developed within this task.

The capacity spectrum method is an iterative process to estimate the performance point so that the damping of the response spectrum and the structural response are the same. The elastic response spectra are generally applied to buildings that remain elastic during the entire ground shaking time history and have elastic damping values equal to 5%. It is well known that buildings subjected to ground shaking do not remain elastic but they dissipate hysteretic energy. For this reason, reduction factors have to be applied to the elastic spectra to obtain the damped demand spectra. These reduction factors are based on the effective damping of the structure and they are different according to the domain they refer to. There are an

acceleration-domain (short period) reduction factor R_A, a velocity-domain reduction factor R_V and a displacement-domain reduction factor R_D. Both of these factors are based on the effective damping B_{eff} which is the sum between the elastic damping and the hysteretic damping of the structure. The elastic damping B_e is generally taken equal to 5%, but following Newmark and Hall (1982) recommendations, it can range from 5% (mobile homes) to 15% (wood buildings). The hysteretic damping B_h is a function of the yield and ultimate points of the capacity curve and it can be calculated as follows:

$$B_h = 63.7 \cdot \kappa \cdot \left(\frac{A_{y_i}}{A_u} - \frac{D_{y_i}}{D_u} \right) \qquad 2.2$$

where κ is a degradation factor that defines the effective amount of hysteretic damping as a function of earthquake duration and energy-absorption capacity of the structure during cyclic earthquake load. This factor depends on the duration of the ground shaking that could be short (M≤5.5), moderate (5.5 <M<7.5) or long (M≥7.5). A_{yi} and D_{yi} are obtained through an iterative process as a part of the capacity curve bilinearization.

The reduction factors, that represent the modifications to be applied to the demand spectra, can be calculated with the following formula:

$$R_A = \frac{2.12}{3.21 - 0.68 \cdot \ln(B_{eff})} \qquad 0 \le T < T_{av} \qquad 2.3$$

$$R_V = \frac{1.65}{2.31 - 0.41 \cdot \ln(B_{eff})} \qquad T_{av} \le T < T_{vd} \qquad 2.4$$

$$R_D = \frac{1.39}{1.82 - 0.27 \cdot \ln(B_{eff})} \qquad T \ge T_{vd} \qquad 2.5$$

Where T_{av} and T_{vd} are the transition building periods and they are given according to HAZUS as

$$T_{av} = \frac{S_a(T_0 = 1.0)}{S_a(T_0 = 0.3)} \quad \text{and} \quad T_{vd} = 10^{(Mw-5)/2} \qquad 2.6$$

Mw is the moment magnitude. HAZUS also modifies T_{av} in $T_{av\beta}$ where $T_{av\beta} = \frac{R_a}{R_v} T_{av}$ and usually, HAZUS does not use R_d and R_d=R_v.

Once the reduction factors are calculated and once the demand spectrum is reduced, the performance point can be estimated and it is represented by the intersection between the capacity curve and the modified response spectrum (Figure *2.1*a). The estimated displacement response is later overlaid with the fragility curves in order to compute the damage probability in each of the different damage states (Figure *2.1*b). The fragility curves are lognormally distributed and they represent the conditional probability of being in or exceeding a particular damage state given by the spectral displacement or other seismic demand parameter. Starting from cumulative fragility curves, discrete probabilities of being in each of the five different damage states can be calculated (Figure *2.1*c). It is worth noting that the parameters defining the fragility functions are strictly connected to the capacity curve of the structure.

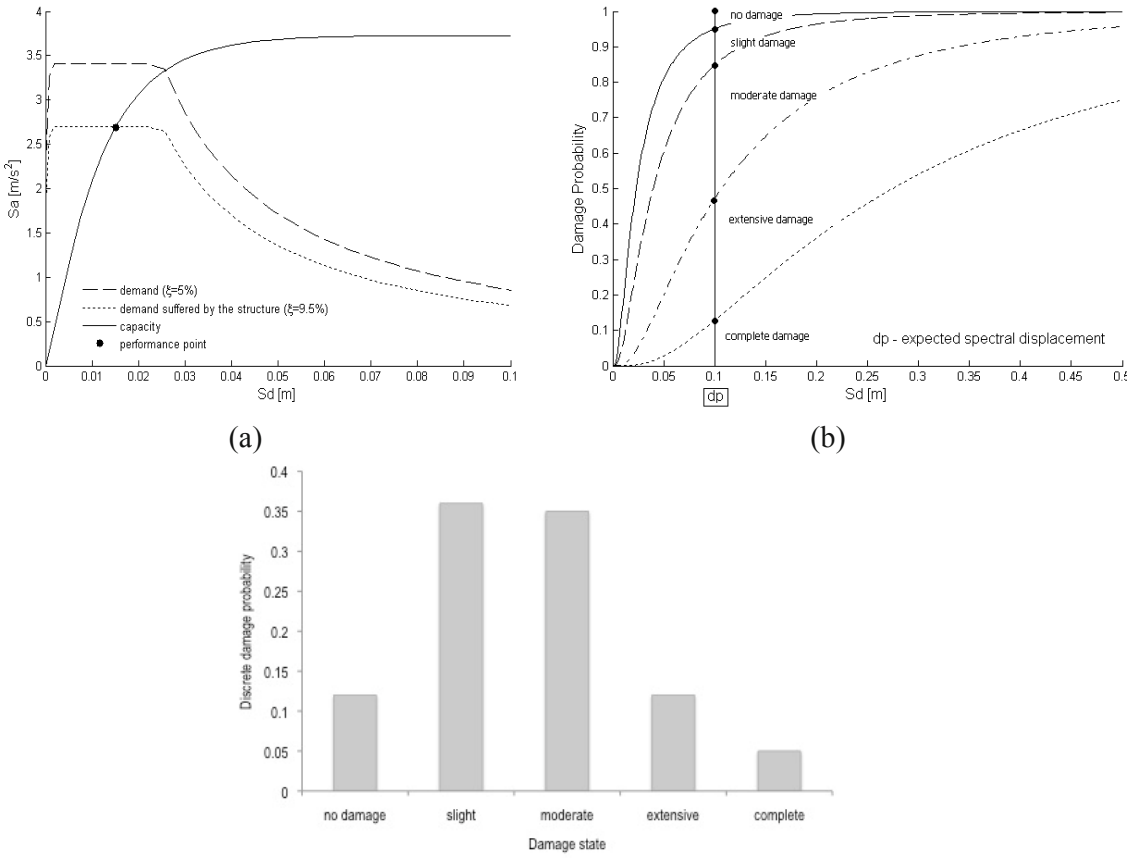

(a) (b)

(c)

Figure 2.1 (a) performance point of a low rise concrete moment resisting frame designed with moderate code (b) expected displacement response overlaid with the fragility curves (c) discrete building damage probability

2.1.2. Social losses

The casualties for any given building type, building damage level and injury severity level have been calculated using the following equation:

$$Kij = Population\ per\ Building * Number\ of\ Damaged\ Building\ in\ damage\ state\ j * Casualty\ Rate\ for\ severity\ level\ i\ and\ damage\ state\ j \quad (2.7)$$

The injury severity levels are defined according to HAZUS-MH (FEMA, 2003) by a four level injury scale and they are described in the following table.

Table 2.1: Description of the injury severity levels

Injury severity	Injury description
Level 1	Injuries requiring basic medical aid without requiring hospitalization
Level 2	Injuries requiring medical care and hospitalization, but not expected to progress into a life threatening status

Level 3	Injuries that pose an immediate life threatening condition if not treated adequately and expeditiously. The majority of these injuries result because of structural collapse and subsequent collapse or impairment of the occupants
Level 4	Instantaneously killed or mortally injured

The casualty rates used to estimate the social losses are those defined by HAZUS-MH (FEMA, 2003) and they are reported in the following tables. There are different values according to the building typology (reinforced concrete or masonry).

Table 2.2 Casualty rates for reinforced concrete moment frame structures

Injury severity	Slight damage	Moderate damage	Extensive damage	Complete damage
Level 1	0.05	0.25	1	5* - 40**
Level 2	-	0.03	0.1	1* - 20**
Level 3	-	-	0.001	0.01* - 5**
Level 4	-	-	0.001	0.01* - 10**

* the smaller values are related with partial collapse of the buildings

** the larger values are given for total collapse

Table 2.3 Casualty rates for unreinforced masonry structures

Injury severity	Slight damage	Moderate damage	Extensive damage	Complete damage
Level 1	0.05	0.35	2	10* - 40**
Level 2	-	0.04	0.2	2* - 20**
Level 3	-	-	0.002	0.02* - 5**
Level 4	-	-	0.002	0.02* - 10**

* the smaller values are related with partial collapse of the buildings

** the larger values are given for total collapse

2.1.3. Economic losses

The mean damage ratio (MDR) represents the total cost of repair divided by the cost of reconstruction. The final economic loss is then calculated by multiplying the total replacement cost with the mean damage ratio. This time instead of 5 damage classes, 4 classes have to be defined. In fact, HAZUS default values of direct economic loss for structural systems are based on the following hypotheses: the slight damage would be a loss of 2%, moderate damage of 10%, extensive damage of 50% and complete damage of 100% of the building's replacement cost. The MDR is defined as:

$$MDR = [D_1] \cdot 0.02 + [D_2] \cdot 0.1 + [D_3] \cdot 0.5 + [D_4] \cdot 1.0 \qquad 2.8$$

Where D_1, D_2, D_3 and D_4 are the percentages of surface area in damage grades slight, moderate, extensive and complete, respectively.

2.2. Empirical approach

Based on available empirical data, compilations from referenced works and engineering interpretations, the vulnerability curves can be defined and can be used to compute the loss for a certain region. The vulnerability functions describe the probability distribution of loss given an intensity measure level. These functions have been used to estimate the loss for the Marmara Region case study.

3. Regional seismic risk applications

Italy and the Marmara region have been selected to represent the European regions to be studied within the SHARE project. In the following sections seismic risk analyses for these two selected regions are described in details and a critical review of the difference between the two approaches used is presented.

3.1. Italy

Italy is a country located in the south of Europe in the middle of the Mediterranean sea. It is divided in 20 regions, which represent the first level of administrative limits, in 110 provinces, which represent the second level of administrative limits and about 8100 municipalities which represent the third level of administrative limits (Figure *3.1*). For what concerns population, about 60 millions of people live in this country nowadays. It has to be mentioned that the seismic risk analyses have been carried out taking into account the third level of exposure due to the fact that data are available at the municipality level.

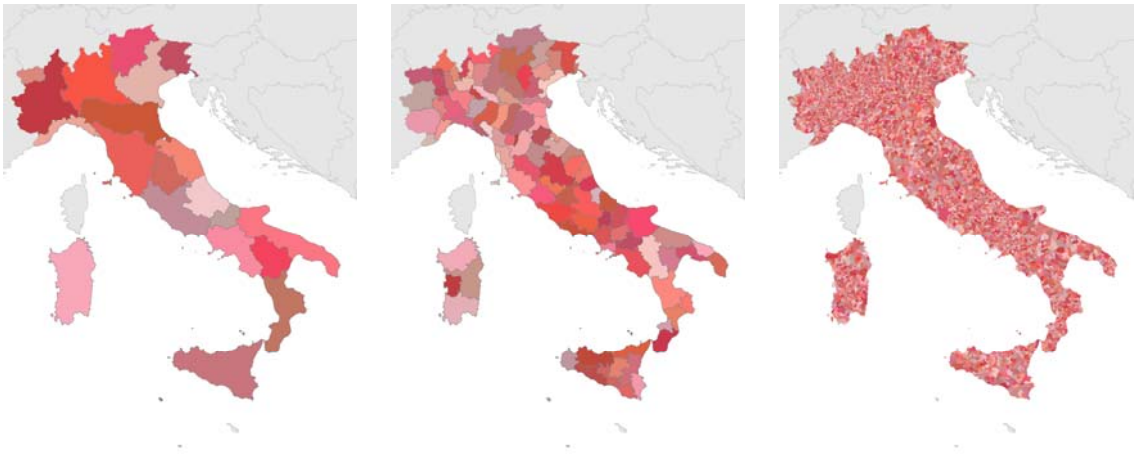

(a) (b) (c)

Figure 3.1 : a) Level 1 – region limits, b) Level 2 – province limits, c) Level 3 – municipality limits

3.1.1. Seismic hazard assessment

As mentioned before, the seismic risk has been carried out using two different types of hazard: the seismic hazard currently employed within the test-bed application countries and the new hazard model developed in SHARE. Herein, a description of the two kind of hazard is provided.

Current seismic hazard map

In 2004, a new probabilistic seismic hazard assessment for Italy, performed in terms of PGA was compiled and released, after review by an international board of experts, and became known as MPS04 (*Mappa di Pericolosità Sismica 04*: Seismic Hazard Map, in English). Following the issuing of the Prime Minister n.3519 in 2006 (*Ordinanza del Presidente del Consiglio dei Ministri,* OPCM), MPS04 is now the official reference for seismic hazard values to be used in Italy in engineering applications. The seismic hazard has been assessed for 16,852 grid points spaced at 0.05° in latitude and longitude, covering the National territory with the exception of Sardinia and some minor islands for which ad hoc studies were necessary. The seismic hazard assessment underwent a process of peer review that involved national and foreign experts in the fields of seismology and engineering.

MPS04 was computed following a logic tree approach that accounted for various sources of epistemic uncertainties such as: (i) the earthquake catalogue completeness time intervals; (ii) the seismicity rates; (iii) and the ground-motion predictive relationships. The logic tree did not include alternatives to the seismogenic source model ZS9 ("*Zonazione Sismogenetica ZS9*", *Gruppo di Lavoro* MPS04, 2004) nor the earthquake catalogue CPTI04 ("*Catalogo Parametrico dei Terremoti Italiani* 2004", *Gruppo di Lavoro* CPTI04 2004) because these input elements were obtained from a review of the existing material, including the most updated studies, and a consensus amongst the experts was reached (Montaldo et al. 2007). The ground-motion prediction equations used in the logic tree for most sources were those proposed by Sabetta and Pugliese (1996) and Ambraseys et al. (1996), while in some areas (for example in the Alps) regional equations were used. The Sabetta and Pugliese (1996) equation is based mainly on analogue records from Italian earthquakes, whilst the Ambraseys et al. (1996) equation is based on European analogue records. The seismic hazard in Italy in terms of spectral acceleration for different response periods has also been computed following the same methodology adopted to compute MPS04 within the INGV-DPC S1 Project (2007a). The results have been computed for various annual frequencies of exceedance (the reciprocal of the return period) and the results are given as the percentiles of the distribution of all possible values resulting from the logic tree. In particular, the 16th, 50th and 84th percentile maps have been produced for the whole of Italy using the 0.05° grid presenting the spectral ordinates in acceleration for various response periods from 0.1 to 2 s and for return periods varying from 30 to 2500 years; 90 maps have been produced in total. The 50^{th} percentile map for a return period of 475 years, which is plotted in Figure *3.2*, has been used to estimate the hazard and to compute the seismic risk within this project.

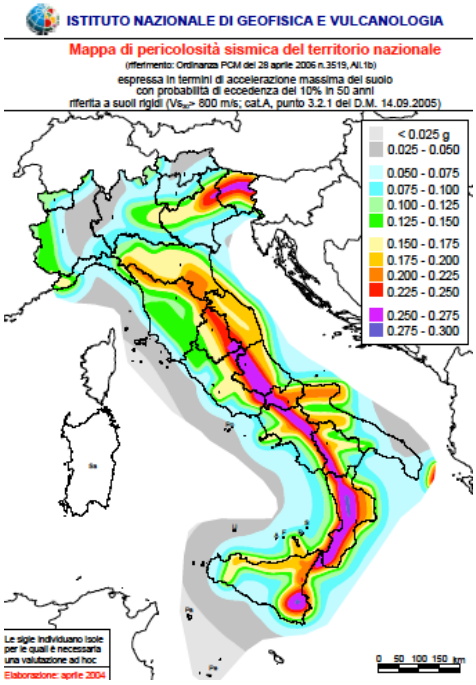

Figure 3.2: Seismic hazard map in terms of PGA ordinates for a return period of 475 years (0.05° resolution)

Starting from the PGA values, the horizontal design spectrum, which is needed to calculate the seismic risk, can be defined. The expressions of the Nuove Norme Tecniche per le Costruzioni (NTC, 2008) have been used to estimate the spectrum shape. The NTC08 have been approved in 14th January 2008 and they constitute the code currently in force in Italy. The equations used to estimate the horizontal design spectrum are shown in the following:

$$Sa(T) = a_g \cdot S \cdot \eta \cdot F_0 \cdot \left[\frac{T}{T_B} + \frac{1}{\eta \cdot F_0}\left(1 - \frac{T}{T_B}\right)\right] \qquad 0 \le T \le T_B \qquad 3.1$$

$$Sa(T) = a_g \cdot S \cdot \eta \cdot F_0 \qquad T_B < T \le T_C \qquad 3.2$$

$$Sa(T) = a_g \cdot S \cdot \eta \cdot F_0 \cdot \frac{T_C}{T} \qquad T_C < T \le T_D \qquad 3.3$$

$$Sa(T) = a_g \cdot S \cdot \eta \cdot F_0 \cdot \frac{T_C \cdot T_D}{T^2} \qquad T_D < T \qquad 3.4$$

Where:

- a_g is the peak ground acceleration (PGA) on rock soil;
- $S = S_S \cdot S_T$ is a soil factor that takes into account the soil type (S_S, see Table *3.2*) and the topography (S_T, see Table *3.3*);
- η is the damping correction factor ($\eta = 1$ for 5% viscous damping);
- F_0 is a factor which quantifies the maximum horizontal spectral amplification on bedrock. $F_0 \ge 2.2$;
- $T_C = C_C \cdot T^*_C$ where T^*_C is the corner period defining the beginning of the constant horizontal spectral velocity range and C_C is a parameter that depends on the soil type (see Table *3.2*);

- $T_B = T_C /3$ is the corner period defining the beginning of the constant spectral acceleration range;
- $T_D = 4a_g/g+1,6$ is the corner period defining the beginning of the constant spectral displacement range.

The values of a_g, F_0 and T^*_C are provided in the NTC08 as appendix for each point of the grid. This way, a specific acceleration spectrum for each Italian municipality can be computed using an interpolation between the points of the grid.

Both periods as well as the soil factor are strongly dependent on ground type. The different types of soil are distinguished using the average shear-wave velocity of the uppermost 30 m (V_{s30}) and it is divided into 5 different classes (see Table *3.1*). In the following tables the essential factors to calculate the spectra are shown.

Table 3.1 Ground Type

Ground Type	Description of stratigraphic profile	Shear wave velocity V_{s30} [m/s]
A	Rock or rock-like geological formation, incl. at most 5 meters of weaker material at the surface	>800
B	Deposits of very dense sands, gravel, or very stiff clay characterized by a gradual increase of mechanical properties with depth	360 - 800
C	Deep deposits of dense or medium-dense sand, gravel or stiff clay with thickness from several tens to many hundreds of meters	180 - 360
D	Deposits of loose-to-medium cohesionless soil, or of predominantly soft-to-firm cohesive soil	<180
E	Soil profile consisting of a surface alluvium layer with V_{s30} values of Type C or D and thickness H varying between 5-20 m underlain by stiffer material with V_{s30}>800m/s	n.a.

Table 3.2 Values of S_S and C_C

Ground Type	S_S	C_C
A	1	1
B	$1 \le 1.4 - 0.4F_0 \frac{a_g}{g} \le 1.2$	$1.10 \cdot \left(T^*_C\right)^{-0.20}$
C	$1 \le 1.7 - 0.6F_0 \frac{a_g}{g} \le 1.5$	$1.05 \cdot \left(T^*_C\right)^{-0.33}$
D	$0.9 \le 2.4 - 1.5F_0 \frac{a_g}{g} \le 1.8$	$1.25 \cdot \left(T^*_C\right)^{-0.50}$
E	$1 \le 2 - 1.1F_0 \frac{a_g}{g} \le 1.6$	$1.15 \cdot \left(T^*_C\right)^{-0.40}$

Table 3.3 Values of S_T

Topographic class	S_T
T1 = Flat field or hill side with a median slope i ≤ 15°	1.0
T2 = Hill side with a median slope i > 15°	1,2
T3 = Relief with the base larger than the ridge and median slope 15 ° ≤ i ≤ 30°	1,2
T4 = Relief with the base larger than the ridge and median slope i > 30°	1,4

An example of the elastic design spectra for soil classes A-E is shown in the following Figure.

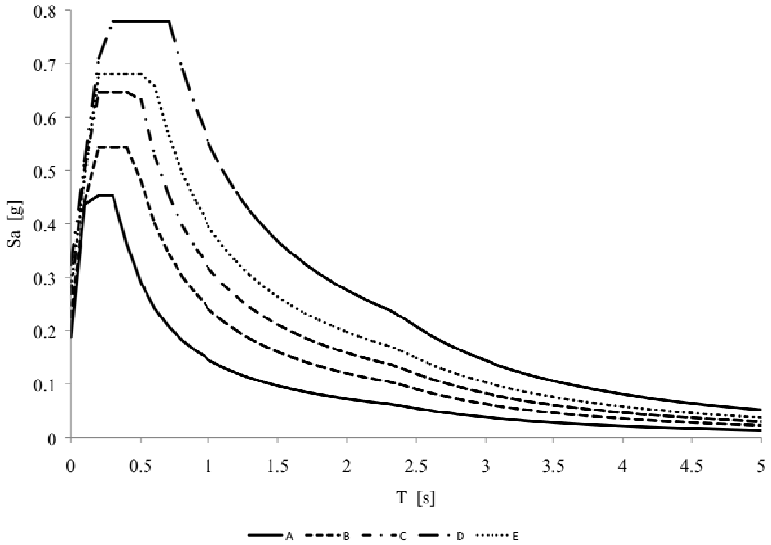

Figure 3.3: Elastic design spectra for soil classes A-E for an Italian municipality

SHARE seismic hazard map

Thanks to a close cooperation between all the partners involved in the SHARE project a new European hazard map has been developed. The results have been computed for different return periods (101, 475, 2475 and 10000 years) and they are given as the 50th percentile of the distribution of all possible values resulting from the logic tree. A 0.1° grid has been used and the spectral ordinates in acceleration for various response periods from 0 to 4 s have been calculated for each point of the grid. Two different approaches have been used in the estimation of the hazard curves according to two different ways to consider the activity rate: model 1 is based on Bayesian approach and model is based on the expert assessment (see SHARE WP5 Deliverables).

It has to be said that the hazard values shown in this deliverable are the preliminary hazard values that are available on November 2012. With regards Italy, the UHS have been produced for each point of the grid and then they have been interpolated to the municipalities' coordinates so as to have a spectrum for each Italian municipality. The interpolation was undertaken using inverse distance weighting. The PGA maps (model 1 and model 2) for a return period of 475 years are plotted in Figure 3.4.

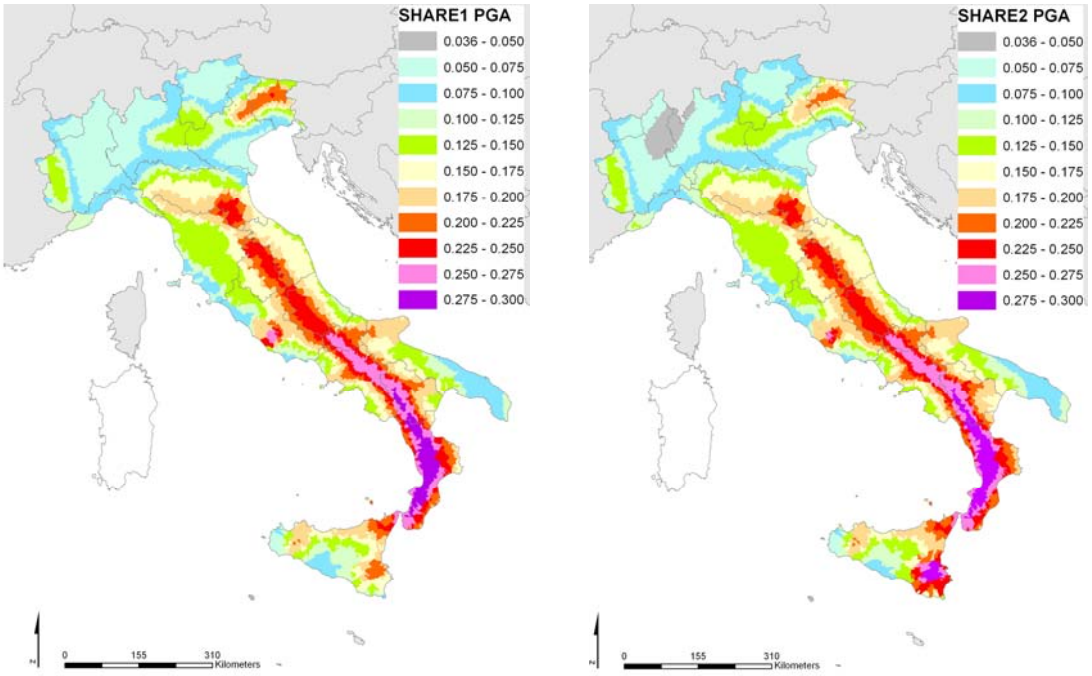

(a) (b)

Figure 3.4: SHARE seismic hazard maps in terms of PGA ordinates for a return period of 475 years. (a) model 1 (b) model 2

The UHS values have been calculated for different periods (0, 0.05, 0.1, 0.2, 0.3, 0.5, 0.75, 1, 1.5, 2, 3, 4 seconds) and in the following figure the UHS estimated with the model 1 and the UHS estimated with the model 2 are shown for an Italian municipality. In this case the two UHS are very similar.

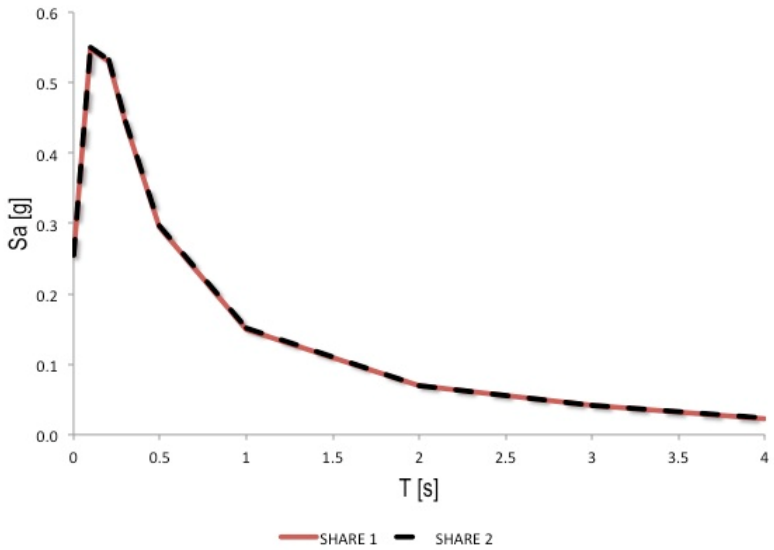

Figure 3.5: SHARE UHS for an Italian municipality estimated with the model 1 and model 2

Finally, it has to be noted that the SHARE UHS values have a minimum threshold (0.005g) built in across all periods, which is due to minimum input acceleration. Taking into consideration the Italian building stock, which is mostly characterized by buildings with low vibration periods, the UHS computed within the SHARE project are generally fine. Notwithstanding that the Italian UHS have been also calculated without a minimum threshold and in the following figure the comparison with the SHARE model 1 and the SHARE model 1 without threshold is shown for a period of 4 seconds.

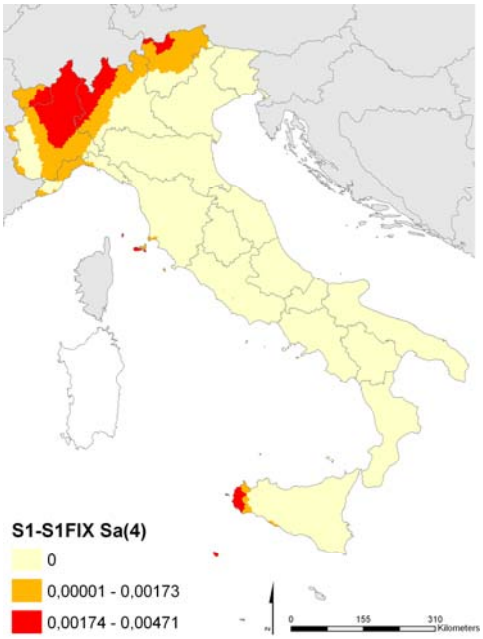

Figure 3.6: Comparative map. Difference between SHARE model 1 and SHARE model 1 Fixed seismic hazard in terms of Sa(4) ordinates for a return period of 475 years.

Comparative hazard maps

In the following figures comparative maps between NTC08 hazard and SHARE hazard calculated using model 1 (SHARE 1) and model 2 (SHARE 2) in terms of PGA and Sa(0.5) are shown. Figure 3.10 presents the comparison between NTC08 elastic design spectrum and SHARE UHS for an Italian municipality for soil class A.

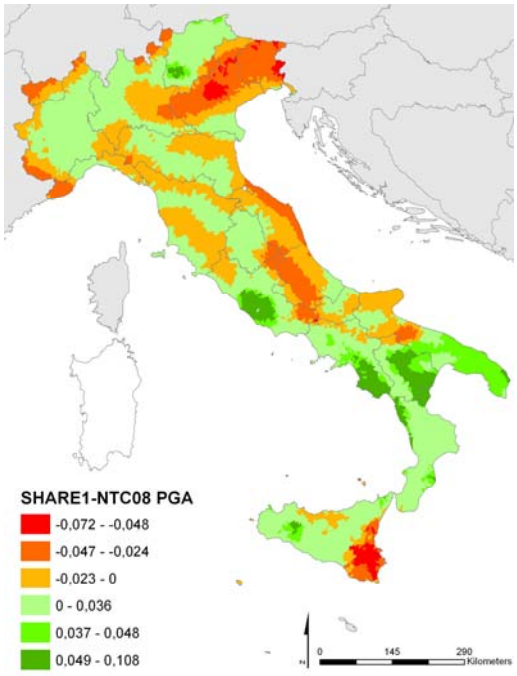

(a)

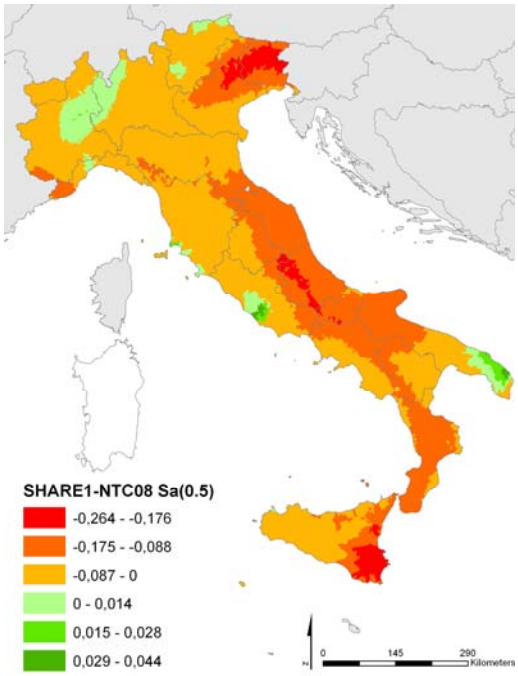

(b)

Figure 3.7: Comparative maps. Difference between SHARE model 1 and NTC08 seismic hazard in terms of (a) PGA and (b) Sa(0.5) ordinates for a return period of 475 years.

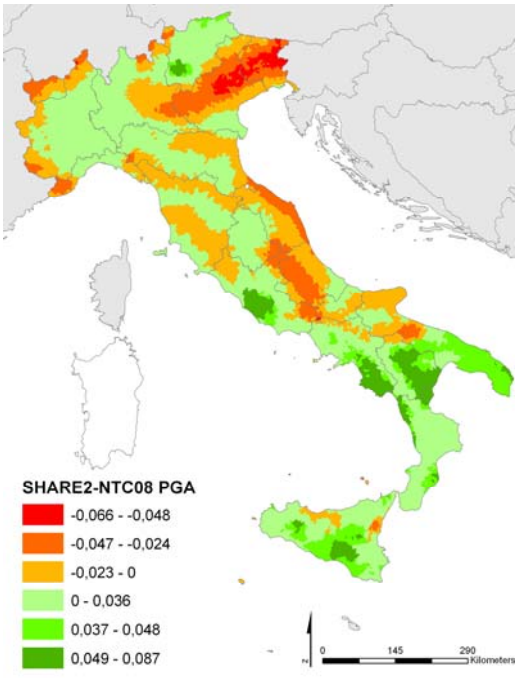

(a)

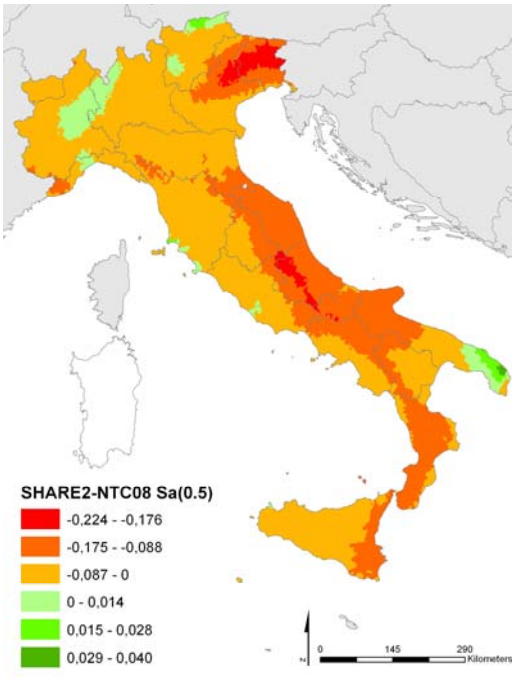

(b)

Figure 3.8: Comparative maps. Difference between SHARE model 2 and NTC08 seismic hazard in terms of (a) PGA and (b) Sa(0.5) ordinates for a return period of 475 years.

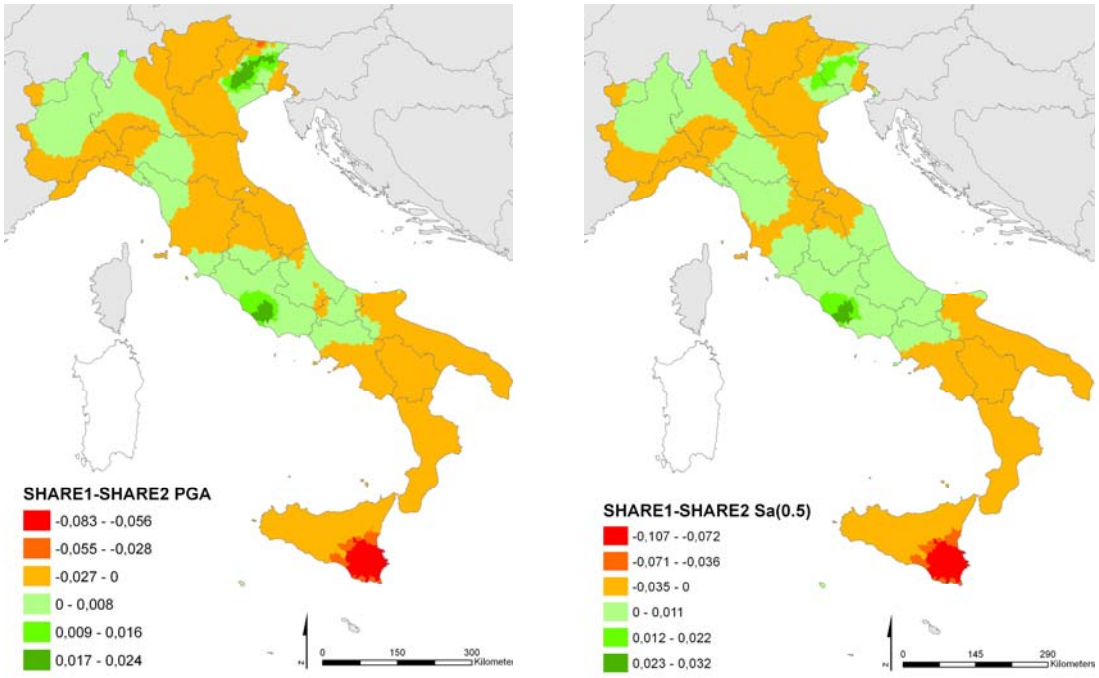

(a) (b)

Figure 3.9: Comparative maps. Difference between SHARE model 1 and SHARE model 2 seismic hazard in terms of (a) PGA and (b) Sa(0.5) ordinates for a return period of 475 years.

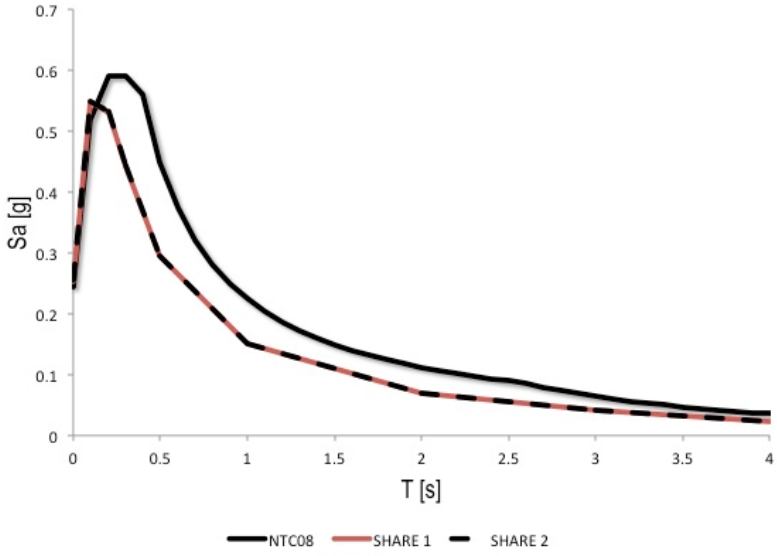

Figure 3.10: Comparison between NTC08 elastic design spectrum and SHARE UHS, model 1 and model 2, for an Italian municipality.

3.1.2. Exposure

Building exposure

The general characteristics of the Italian building stock have been obtained from the 13th General Census of the Population and Dwellings (ISTAT '91). The Census data in 1991 was

collected in terms of dwellings; however, within the Census form, each dwelling was classified as being located within a building with a certain number of dwellings (from 1 to >30), of a given construction type (RC, RC with pilotis, Masonry, Other), and with a given number of storeys (1–2, 3–5, >5). Hence, based on the Census forms compiled for all dwellings within each census tract/municipality, Meroni et al. (2000) have estimated the number of buildings classified according to the period of construction, number of storeys and the vertical structural type within each municipality. The errors associated with the use of the 1991 Census data that is based on the number of dwellings to arrive at the number of buildings are recognised by the authors and have been identified and quantified in some areas of Italy (see e.g. Frassine and Giovinazzi 2004). However, without the presence of detailed exposure data it is necessary to make some sort of hypothesis in order to obtain the number of buildings of a given construction type and with a given number of storeys. The 2001 Census has not been used herein as although this Census was specifically carried out in terms of buildings, the disaggregated data, with a level of detail congruent with that described above for the '91 data, is not currently publicly available. The percentages of masonry, seismically designed reinforced concrete and non seismically designed reinforced concrete buildings calculated within each municipality from the Census data are presented in Figure *3.11*.

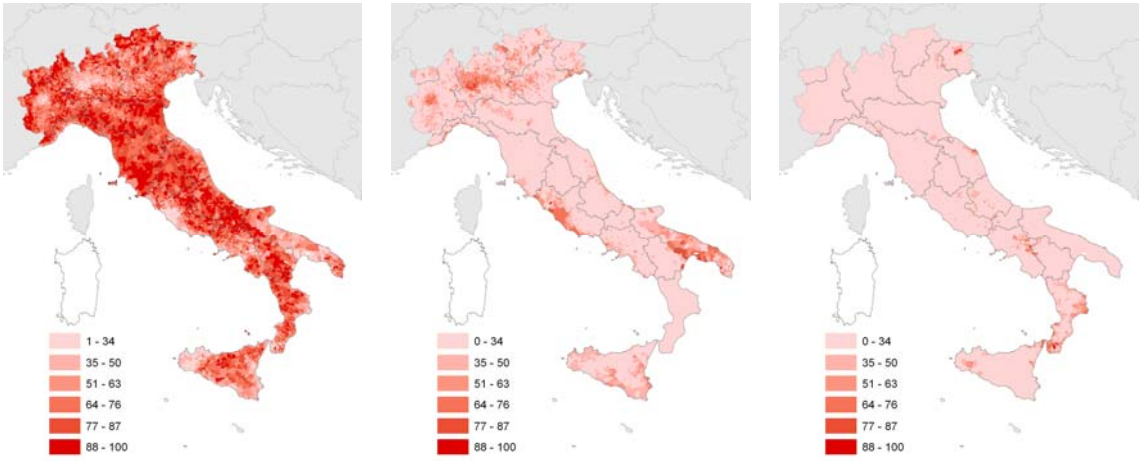

(a) (b) (c)

Figure 3.11: Percentages of (a) masonry (b) non seismically designed reinforced concrete (c) seismically designed reinforced concrete buildings in each municipality

Population exposure

The amount of the total population living in this country, is obtained from the same Census of the building stock (13th General Census of the Population and Dwellings, ISTAT 1991). About 50 millions of people lived in Italy in the beginning of the nineties and the social losses computed in this task consider this amount of population. In the following figure the distribution of people throughout Italy is shown.

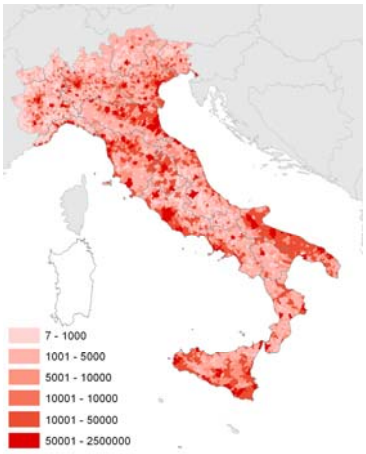

Figure 3.12: Distribution of population throughout Italy

3.1.3. Vulnerability

With regards to masonry buildings, five separate building classes have been defined as a function of the number of storeys (from 1 to 5), whilst for reinforced concrete the building classes have been defined considering the number of storeys (from 1 to 8), and the period of construction. The year of seismic classification of each municipality has then be used such that the non-seismically designed and seismically designed buildings could be separated. In this way, the evolution of seismic design in Italy and the ensuing changes to the lateral resistance and the response mechanism of the building stock could be considered. The buildings are designed considering only gravity-load design before seismic classification; following classification, depending on the seismic zone to which the municipality was assigned, a base shear coefficient has been used to design the buildings. For buildings assigned to zone 1, this coefficient has been taken as 10% of the weight, for buildings in zone 2 as 7% and for buildings in zone 3 as 4%. The influence of the infill panels on the lateral strength of the buildings is also taken into consideration and the buildings are separated into those with a regular infill panel distribution and those with an irregular infill panel distribution (i.e.with pilotis).

Table *3.4* reports the 69 vulnerability classes which it is possible to define.

Table 3.4: Vulnerability classes considered for Italian building stock in terms of construction type, number of storeys and level of seismic design

Construction Type	Number of Storeys
Masonry	
Artificial brick	1-5
Reinforced concrete	
Non seismically designed	1-8
Non seismically designed with pilotis	1-8
Seismically designed	Zone 1: 1-8

	Zone 2: 1-8
	Zone 3: 1-8
Seismically designed with pilotis	Zone 1: 1-8
	Zone 2: 1-8
	Zone 3: 1-8

As mentioned previously, the ISTAT data group the number of storeys (1–2, 3–5, >5) and 26 exposure building classes can be defined, whilst the vulnerability classes are estimated for each number of storeys separately using SPBELA methodology (Borzi et al, 2008a, 2008b). Hence, the vulnerability calculations for each number of storeys had to be aggregated to be consistent with the Census data. This was carried out based on statistics of the number of storeys of each construction type from a study of 12,503 masonry buildings and 6,494 reinforced concrete buildings in Catania (Faccioli and Pessina 2000), as reported in Figure *3.13*. These proportions were used to calculate a weighted average of the vulnerability for the exposure building class based on the vulnerability for each number of storeys separately.

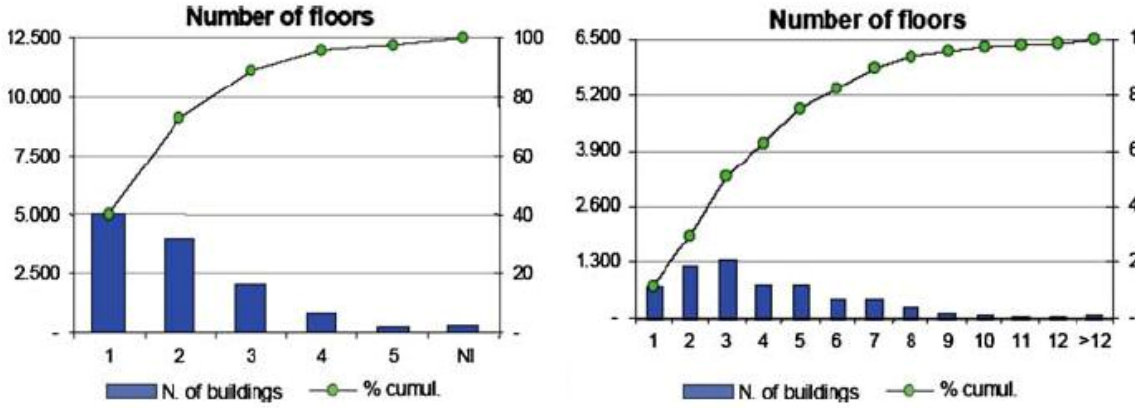

(a) (b)

Figure 3.13: Proportion of (a) masonry and (b) reinforced concrete buildings for each number of storeys obtained from a sample of buildings in Catania (Faccioli and Pessina, 2000). (NI means the storey number was unknown)

This way, it is possible to create one capacity curve for each exposure building class: 26 bilinear capacity curves have been created to estimate the seismic risk for Italy, three of which are plotted in Figure 3.14a. Furthermore, fragility curves are used to calculate the damage probability distribution for a class of structures. The parameters defining the fragility functions for a certain building type are closely connected to its capacity curve: the displacement thresholds of the limit states represent the mean of the lognormal distribution, while the standard deviation is taken equal to 0.5 for all the curves. In Figure 3.14b the fragility curves used to compute the damage probability in each one of the different damage states are shown.

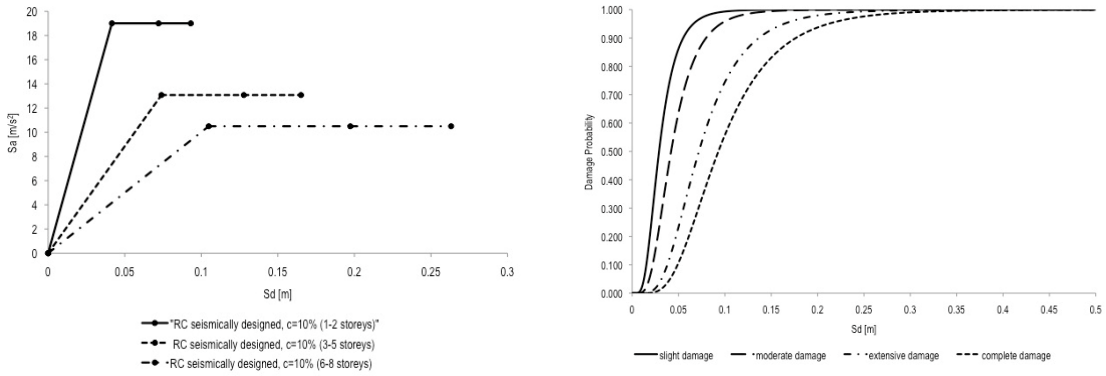

(a) (b)

Figure 3.14: (a) Plot of three different capacity curves for different vulnerability classes (b) Fragility curves of a low rise reinforced concrete seismically designed (c=10%) building

3.1.4. Seismic Risk

For what concerns the building damage, five structural damage states have been considered: no damage, slight damage, moderate damage, extensive damage and complete damage and the percentages of the damaged structures for each damage state have been computed. The production of a seismic risk map in terms of number of buildings allows the estimation of the number of people affected by the earthquake. Four levels of injury severity are taken into account from level 1 to level 4 (see Table *2.1*). The damage to the surface area is also computed and it can be very useful for the prediction of the costs required to repair the damage from earthquakes. In fact, the mean damage ratio for each municipality as it is described in Section 2.3 has been computed as an index of the economic losses. Multiplying the mean damage ratio by the reconstruction value of the surface area, the economic loss can be evaluated.

It is worth reminding that the comparison of seismic risk is based on the preliminary hazard values that are available on November 2012.

The conditional seismic risk for a return period of 475 years in terms of the percentage of damaged buildings and of the percentages of damaged surface area, the social losses and the MDR ratio have been calculated using NTC08 hazard and SHARE hazard (model 1 and model 2). Given that the main objective of this deliverable is the comparison between the impact of the different hazards on the seismic risk, comparative maps between the different approaches have been developed and shown in the following figures.

SHARE model 1 vs NTC08

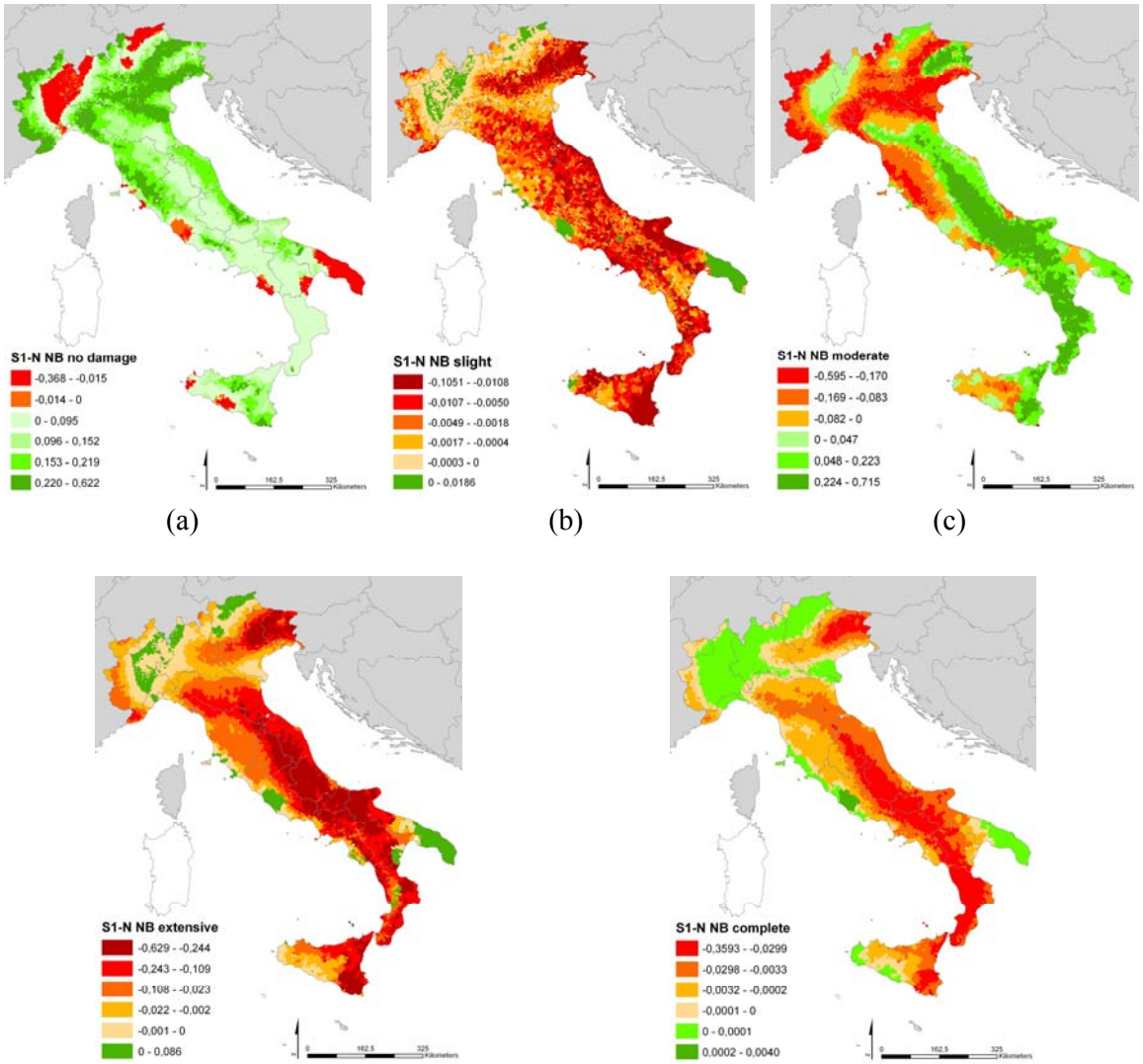

Figure 3.15: Comparison of the conditional seismic risk for a return period of 475 years in term of percentage of (a) no damaged buildings (b) slight damage buildings (c) moderate damaged buildings (d) extensive damaged buildings and (e) collapsed buildings. SHARE model 1 versus NTC08.

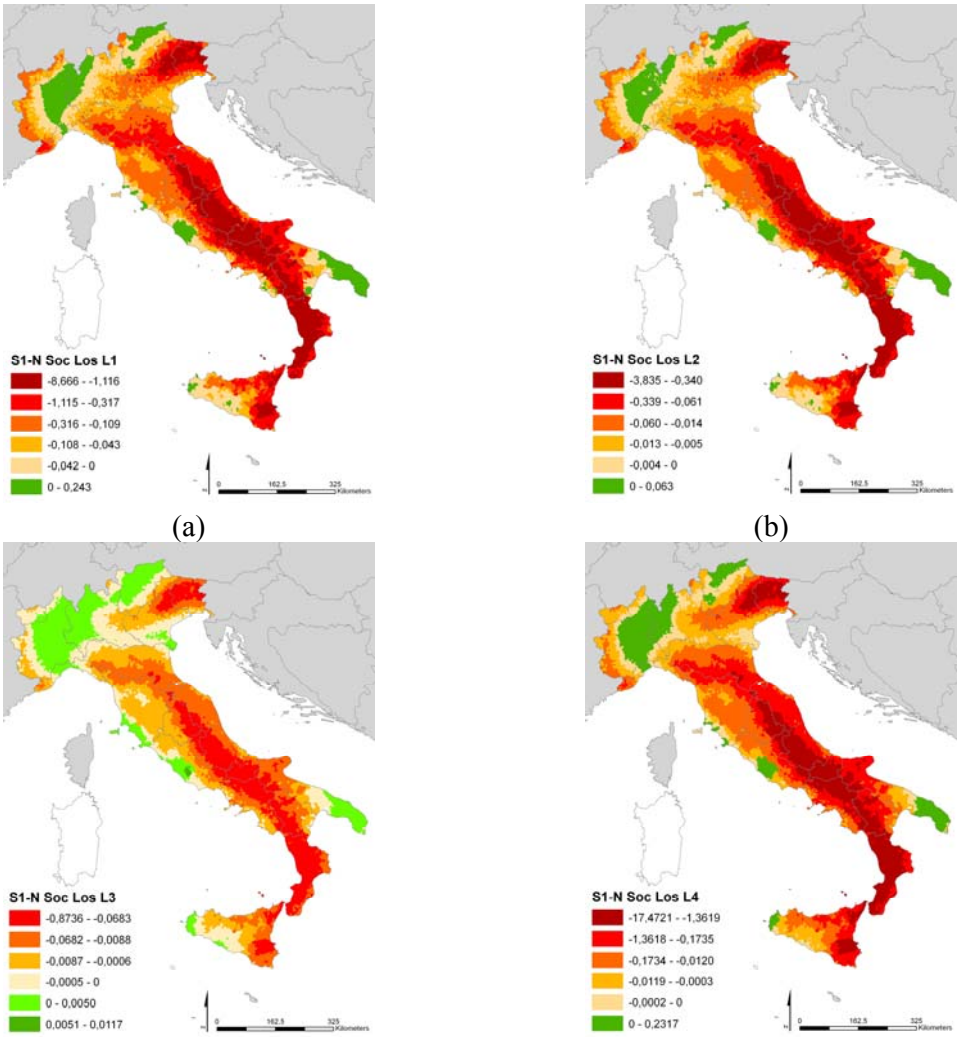

Figure 3.16: Comparison of the percentages of casualties (a) level 1 (b) level 2 (c) level 3 (d) level 4. SHARE model 1 versus NTC08.

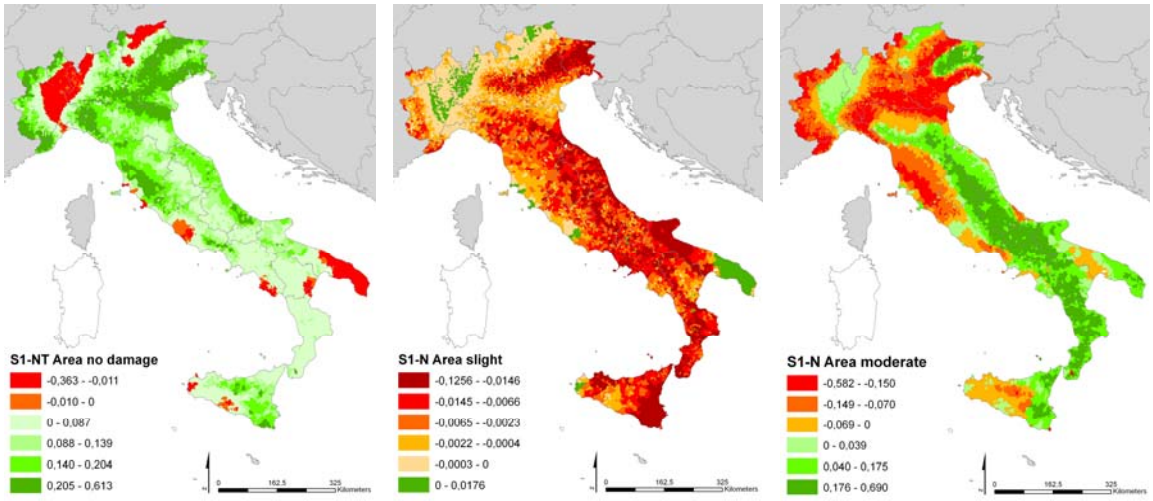

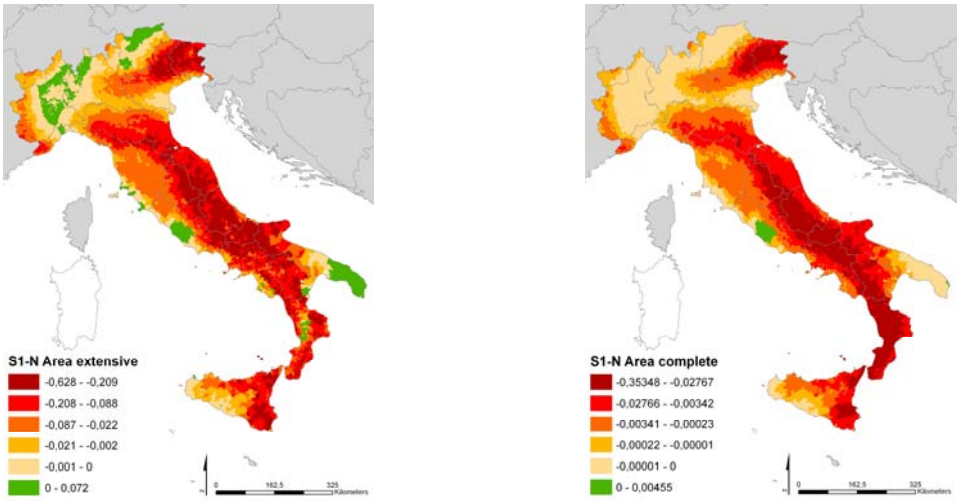

(d) (e)

Figure 3.17: Comparison of the conditional seismic risk for a return period of 475 years in term of percentage of (a) no damaged surface area (b) slight damaged surface area (c) moderate damaged surface area (d) extensive damaged surface area and (e) collapsed surface area. SHARE model 1 versus NTC08.

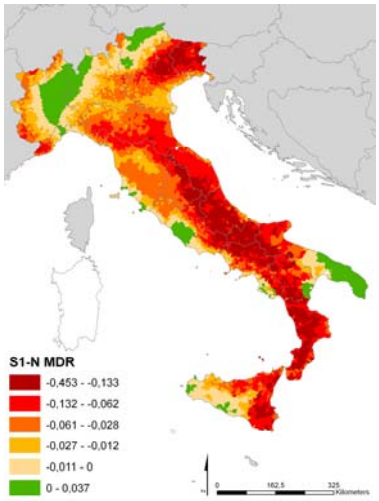

Figure 3.18: Comparison of the Mean Damage Ratio. SHARE model 1 versus NTC08.

SHARE model 2 vs NTC08

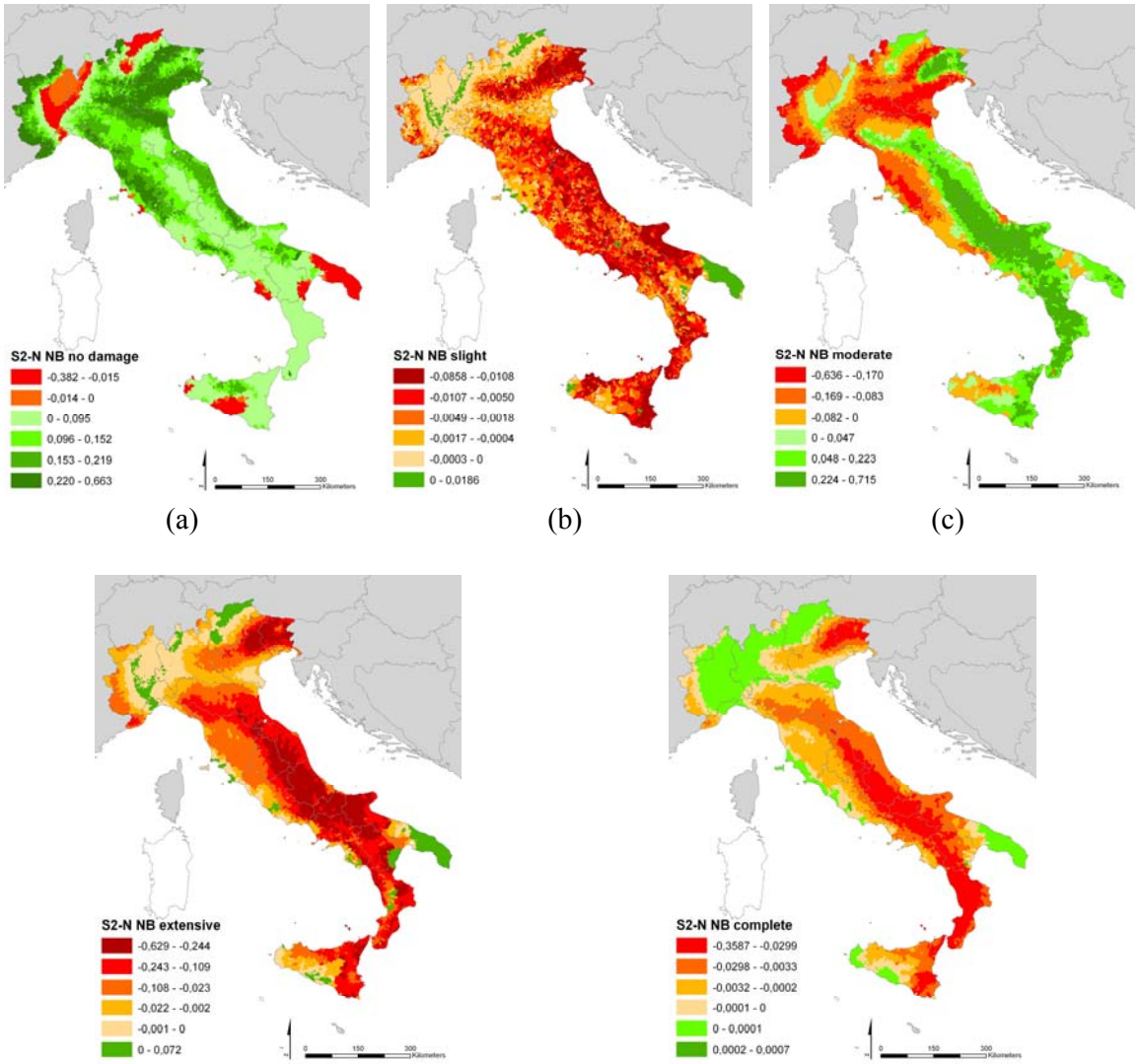

Figure 3.19: Comparison of the conditional seismic risk for a return period of 475 years in term of percentage of (a) no damaged buildings (b) slight damage buildings (c) moderate damaged buildings (d) extensive damaged buildings and (e) collapsed buildings. SHARE model 2 versus NTC08.

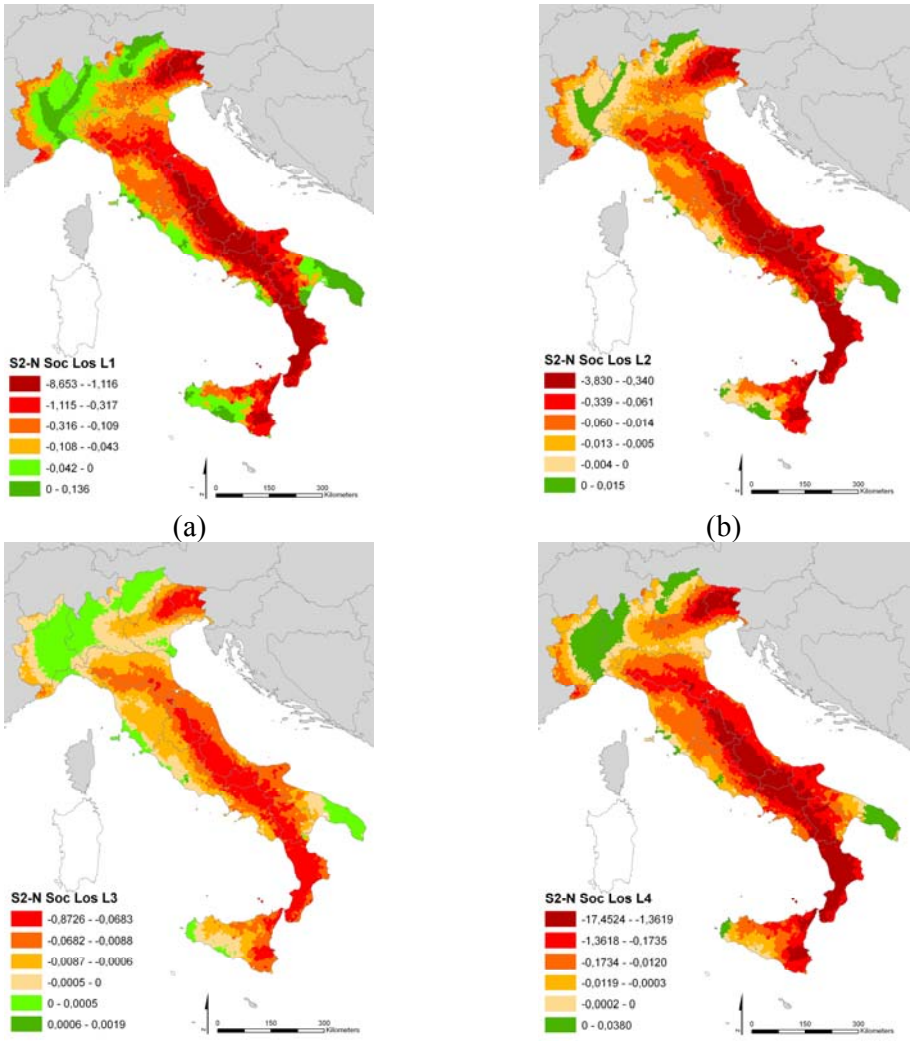

(a) (b)

(c) (d)

Figure 3.20: Comparison of the percentages of casualties (a) level 1 (b) level 2 (c) level 3 (d) level 4. SHARE model 2 versus NTC08.

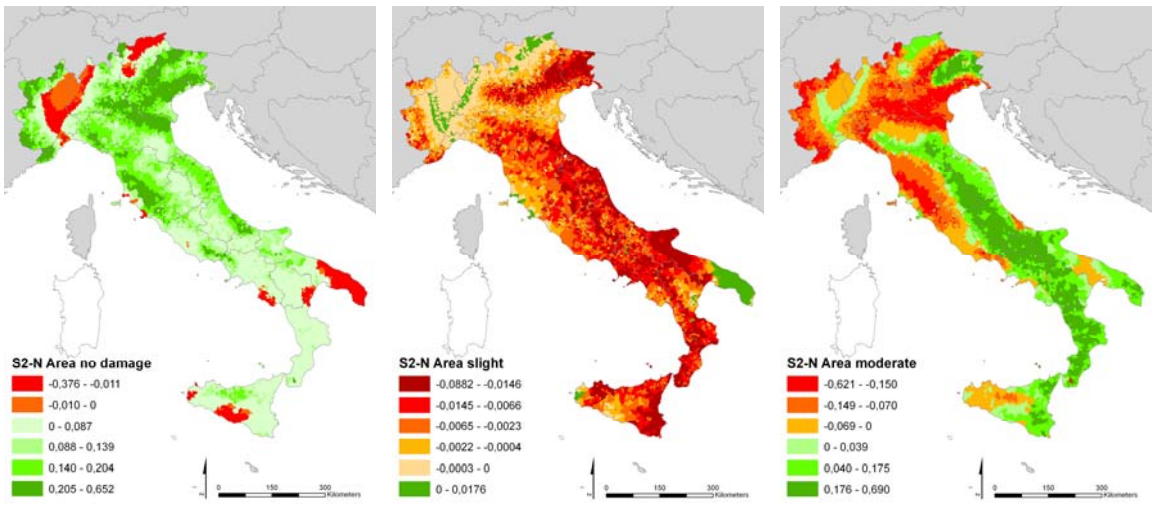

(a) (b) (c)

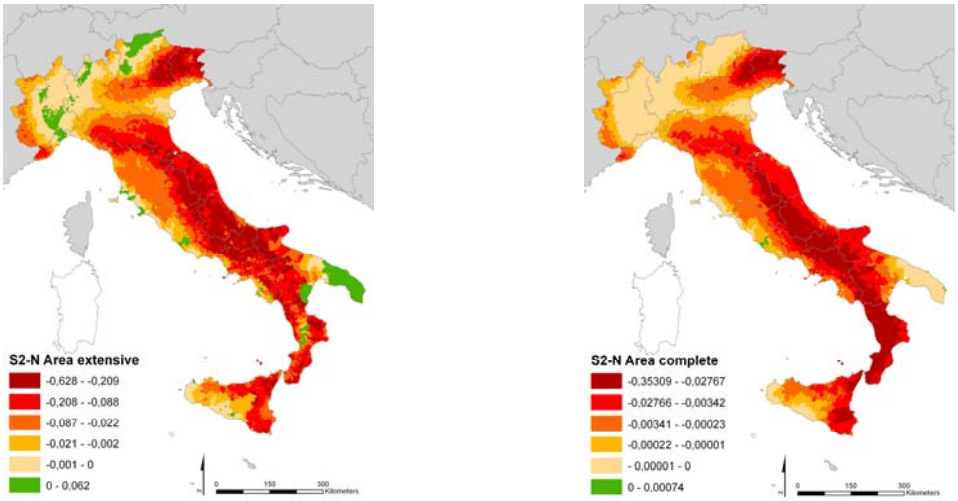

(d) (e)

Figure 3.21: Comparison of the conditional seismic risk for a return period of 475 years in term of percentage of (a) no damaged surface area (b) slight damaged surface area (c) moderate damaged surface area (d) extensive damaged surface area and (e) collapsed surface area. SHARE model 2 versus NTC08.

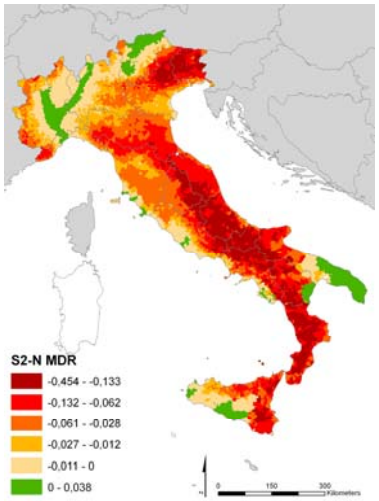

Figure 3.22: Comparison of the Mean Damage Ratio. SHARE model 2 versus NTC08.

SHARE model 1 vs SHARE model 2

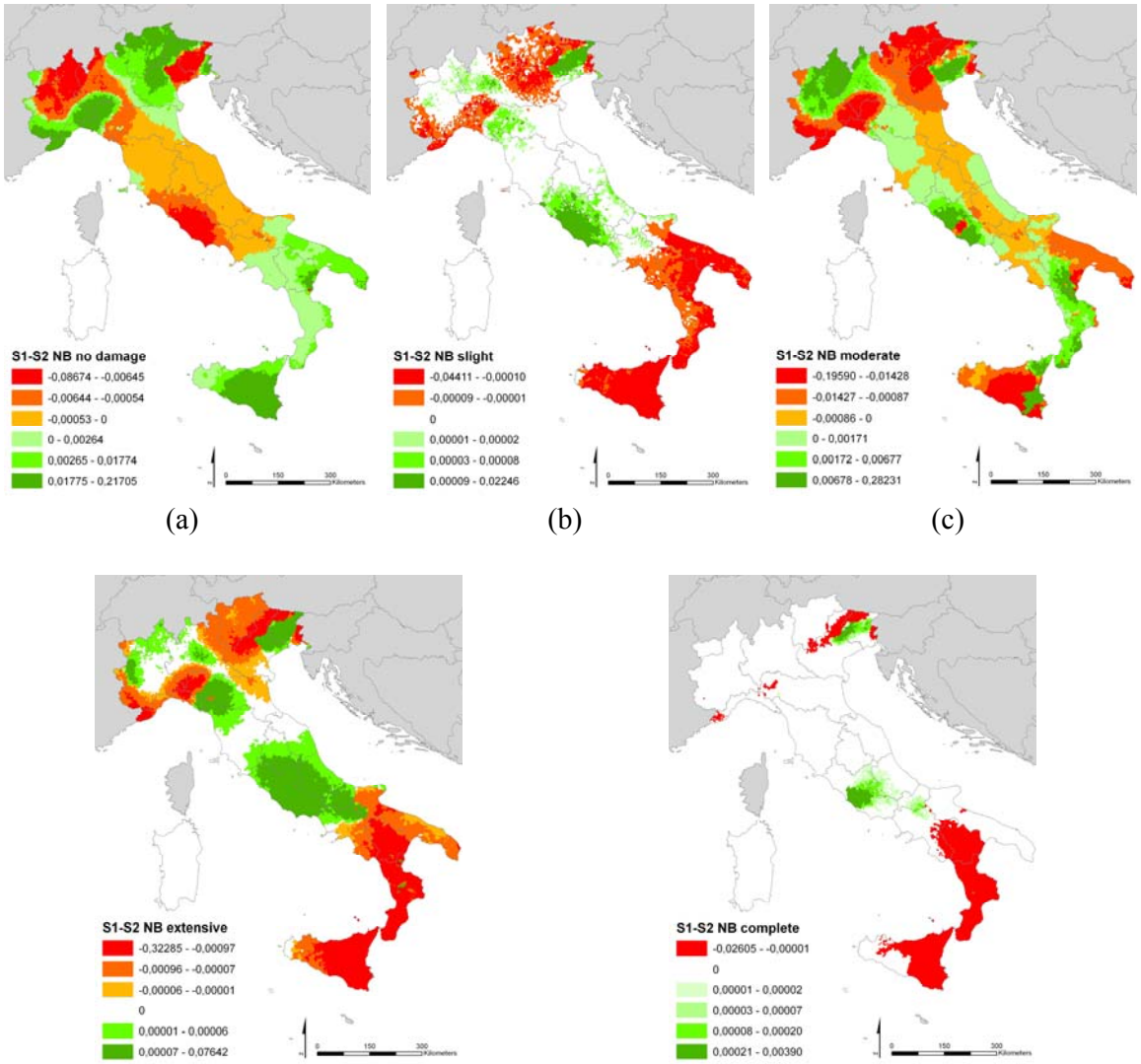

Figure 3.23: Comparison of the conditional seismic risk for a return period of 475 years in term of percentage of (a) no damaged buildings (b) slight damage buildings (c) moderate damaged buildings (d) extensive damaged buildings and (e) collapsed buildings. SHARE model 1 versus SHARE model 2.

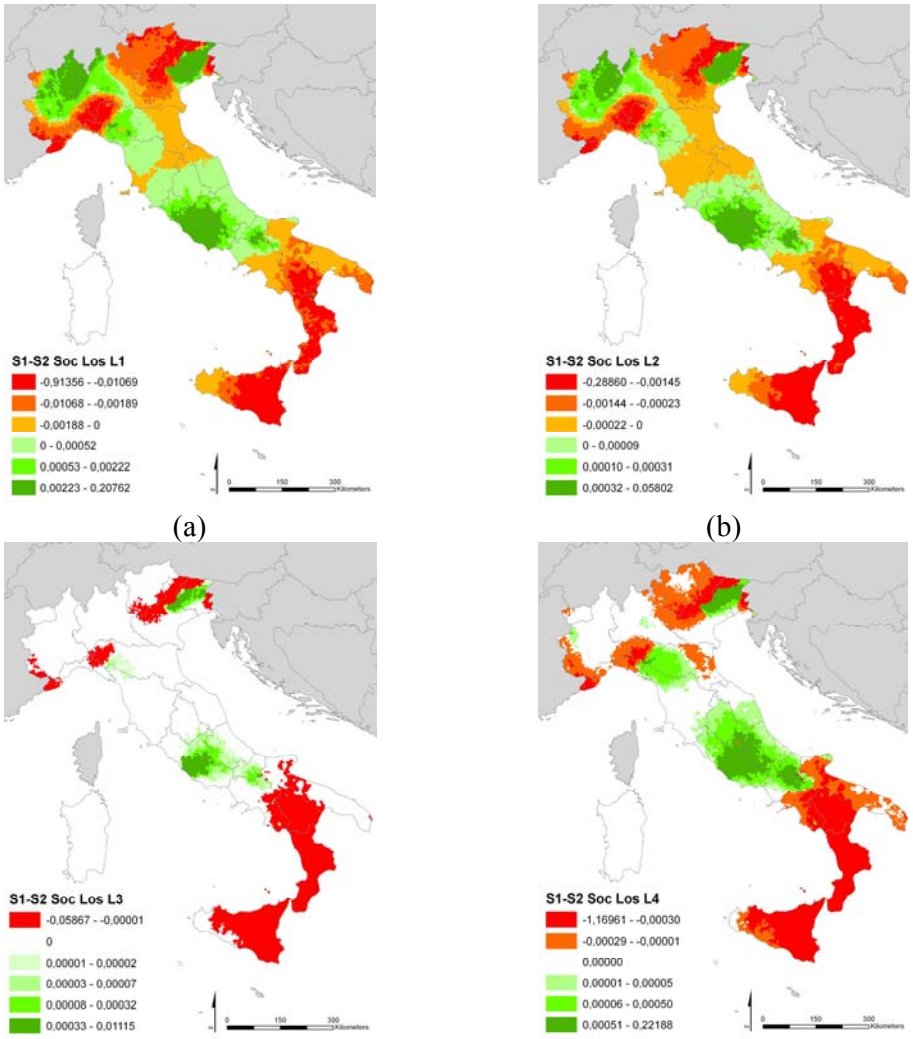

Figure 3.24: Comparison of the percentages of casualties (a) level 1 (b) level 2 (c) level 3 (d) level 4. SHARE model 1 versus SHARE model 2.

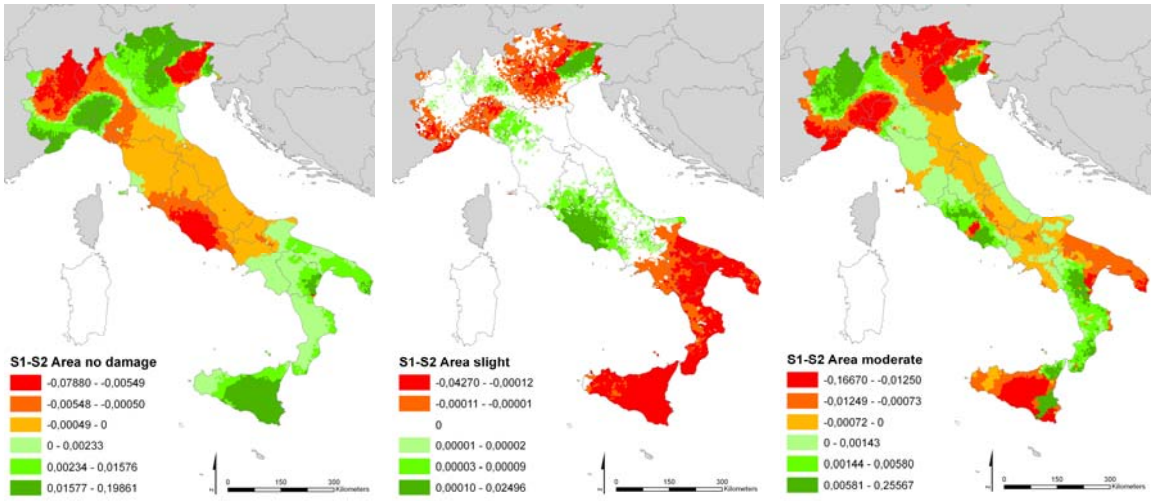

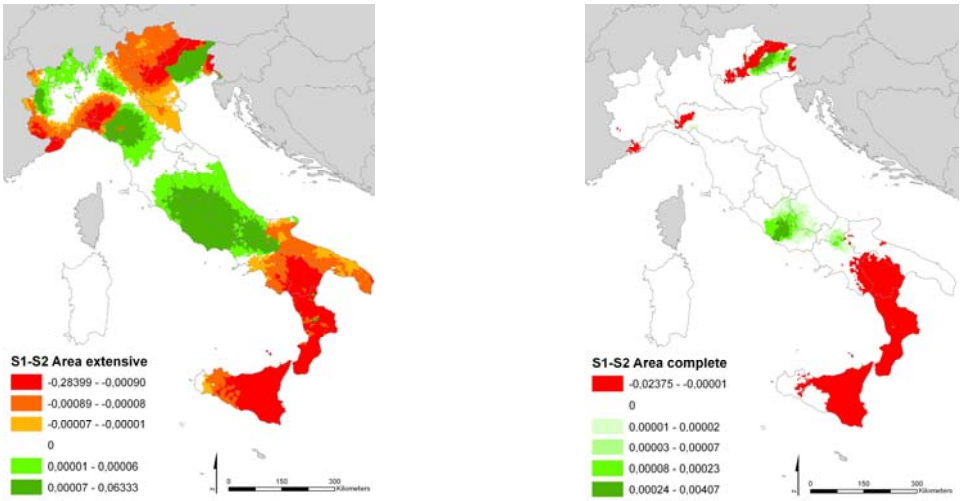

(d) (e)

Figure 3.25: Comparison of the conditional seismic risk for a return period of 475 years in term of percentage of (a) no damaged surface area (b) slight damaged surface area (c) moderate damaged surface area (d) extensive damaged surface area and (e) collapsed surface area. SHARE model 1 versus SHARE model 2.

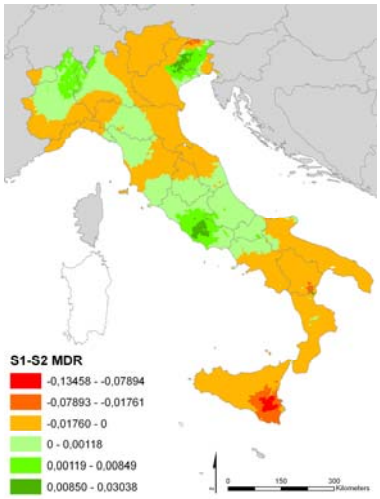

Figure 3.26: Comparison of the Mean Damage Ratio. SHARE model 1 versus SHARE model 2.

For what concerns the impact of the SHARE hazard on seismic risk assessment for Italy it can be observed that the SHARE hazard gives lower values of the seismic risk in terms of building damage, social and economic losses in the majority of Italy. As it can be seen in Figure 3.10, the SHARE UHS has much lower spectral acceleration values compared to the NTC08 hazard spectrum. This means that a lower performance point will be computed in the Capacity Spectrum Method and, subsequently, a different distribution of damage is calculated. It has to be noted (Figure 3.7 and Figure 3.8) that there is not much difference between NTC08 PGA values and SHARE PGA values, but the difference becomes significant when spectral accelerations (for instance Sa(0.5)) are considered. Due to the fact that the

fragility curves are spectral acceleration based, the difference is of great importance in the estimation of the seismic risk. These different results are likely due to different GMPEs used in the evaluation of the hazard and to the approximation that has to be done with the SHARE results passing from the grid (0.1° of resolution) to the centroid of the Italian municipality. Instead, NTC08 gives directly an acceleration spectrum for each municipality.
On the other hand, with regards to the two approaches used in SHARE, the difference between them is negligible with the exception of three areas: North-East of Italy, Rome with its neighbourhood and the South of Sicily. In the South of Sicily acceleration values are higher using model 2 and, on the contrary, in Rome and North-East the values are higher using the first approach. These differences have an impact on the final seismic risk assessment and they are mainly due to the expert opinion.

3.2. Marmara Region

Marmara Region is located in the northwest part of Turkey, with a surface area of 67.000 $km^{2.}$ The Marmara Region is surrounded by the Black Sea and Cetral Anatolia Regions to the east, The Aegean Region to the south and Greece and Bulgaria to the northwest. The borders of the Marmara Region are not in conformity with the provincial borders in many places just as in the other regions. Edirne, Kirklareli, Tekirdag, Istanbul, Kocaeli and Yalova Provinces are completely within the borders of the region. Some lands in Sakarya, Bilecik, Bursa, Balıkesir, and Çanakkale Provinces are located within the borders of the Aegean and the Black Sea Regions (Figure *3.27*). The seismic risk analyses have been carried out taking into account the two level of exposure due to the fact that data are available at the province and sub-province levels (Figure *3.27* and Figure *3.28*).

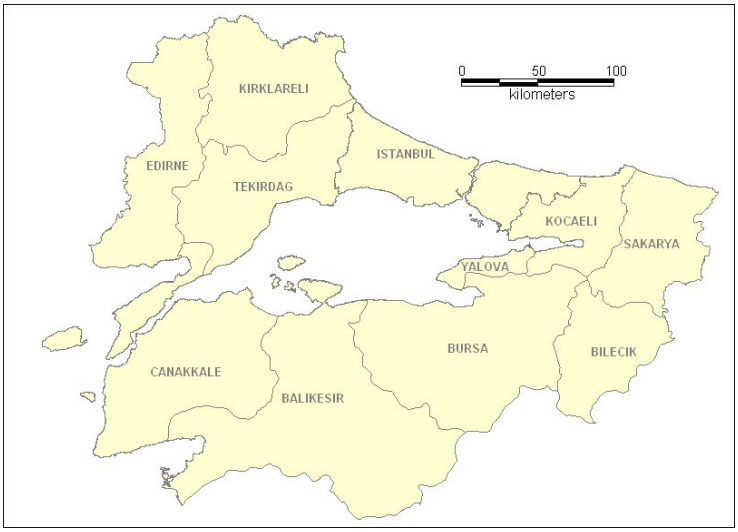

Figure 3.27 *Location of the Marmara Region at Province level*

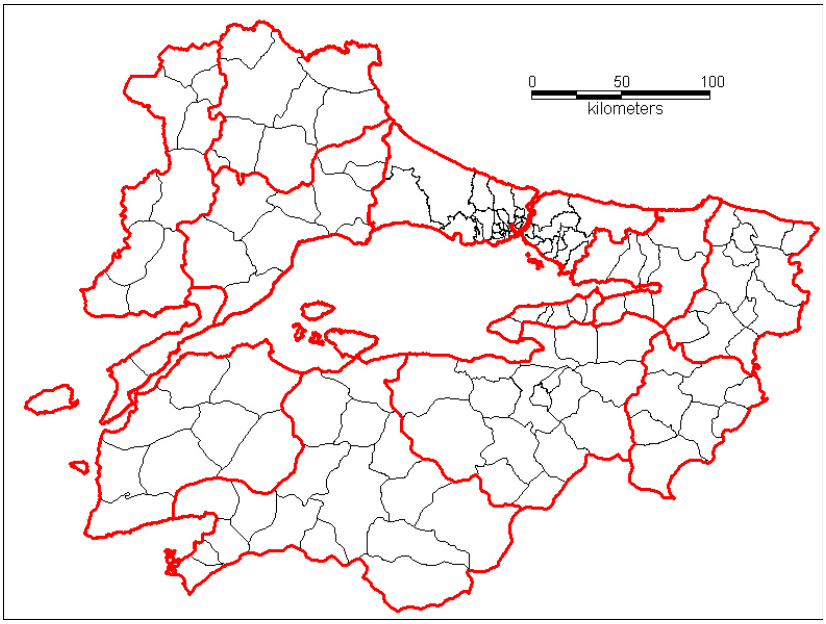

Figure 3.28 *Location of the Marmara Region at Sub-Province level*

3.2.1. Seismic hazard assessment

The intensity based seismic risk assessment for Marmara Region has been carried out in the study of "prioritization of high seismic risk provinces and public buildings for Turkey" which is not a public report. However, in this section, the methodology used in this study and the results corresponding to building damage for each damage state and the casualty estimation for each severity level will be presented for Marmara region.

Current seismic hazard map

The study of Erdik et al. (2004) forms the basis of the time dependent hazard model for the Marmara region. Earthquake occurrence and fault segmentation data in the Marmara region are adequate to constrain a time dependent characteristic model for the region. The methodology, elaborated in Erdik et al. (2003), is essentially very similar to the one developed and used by United States Geological Survey - WGCEP (http://geohazards.cr.usgs.gov/eq/index.html) for the preparation of US National Seismic Hazard Maps. The main physical ingredients of seismic hazard assessment are the tectonic setting of the region, the earthquake occurrences and the local site conditions. These regional physical features, the applicable ground motion prediction equations and the appropriate stochastic model for probabilistic hazard analysis have been considered. Owing to the geological and geo-tectonic similarity of Anatolia to the California (strike slip faults similar to North, Northeast and East Anatolian Faults), the average of Boore et al. (1997), Sadigh et.al. (1997) and Campbell et al.(2003) grund motion prediction models for Peak Ground Acceleration (PGA) and the average of Boore et. al. (1997) and Sadigh et.al. (1997) ground motion prediction models for Spectral accelerations at 0.2 sec. and 1.0 sec. periods currently used for the assessment of earthquake hazard for the Western US were utilized. Another

reason for the selection of these models was the good agreement between the instrumental intensities computed with these models with the observed macroseismic intensity distribution. The influence of the local geological structure on damage distribution due to ground-motion amplification (also called site effects) has also been considered. The 1/500,00 scale geologic map of Turkey produced by General Directorate of Mineral Research and Exploration (MTA) has been digitized and classified in terms of geological age as Quaternary, Tertiary and Mesozoic (QTM) by KOERI. The approach used for the inclusion of site effects involves using QTM classification for the assigment of Vs30 (the average shear wave velocity of the upper 30 m) values. . For southern California, Park and Elrick (1998) assigned V_{s30} values of 589 m/s, 406 m/s and 333 m/s to Mesozoic, Tertiary and Quaternary sediments respectively. Site correction according to these values is applied by Wald et al. *(*1999) in the TriNet ShakeMap alghoritm. The average shear-wave velocity in the upper 30 meters (V_{S30}) is mostly used to classify the local site conditions. The same QTM vs. V_{s30} values, together with the site correction methodology of Borcherdt (1978) were used to obtain site corrected ground motion distributions from the assigned Vs30 values for Turkey.

For the probabilistic risk assessment in this study, intensity based ground motion and Turkey-specific intensity based vulnerabilities have been used. Regression relationships between Modified Mercalli Intensity (MMI, considered essentially similar to EMS'98) and ground motion parameters PGA and PGV developed by Wald et al., (1999a and 1999b) are used to estimate intensity distribution. These relationships were developed based on data from eight significant California earthquakes with magnitudes ranging between 5.8 -7.3. The applicability of Wald et al (1999a and 1999b) model to Turkey has been evaluated by comparing the intensity distribution obtained with Boore et al. (1997) and Sadigh et al (1997) ground motion prediction equations and the instrumental intensity estimation model of Wald et al (1999a and 1999b) with observed intensity distribution of the 1999 Kocaeli earthquake. The results of the study indicate a lower future hazard for the region of the 1999 earthquake and a higher hazard for the Central Marmara Sea region corresponding to the unruptured segments of the Main Marmara Fault in the Marmara Sea, when compared to Poisson, so-called memory-less models. This finding is also in accordance with (Parsons et al, 2000) indicating heightened probabilities for a major earthquake in the Marmara Sea region based on stress transfer approach.

The seismic hazard for Marmara Region in terms of macroseismic intensity corresponding to the return period of 72, 475, and 2475 years has been presented in Figure *3.29* through Figure *3.31*.

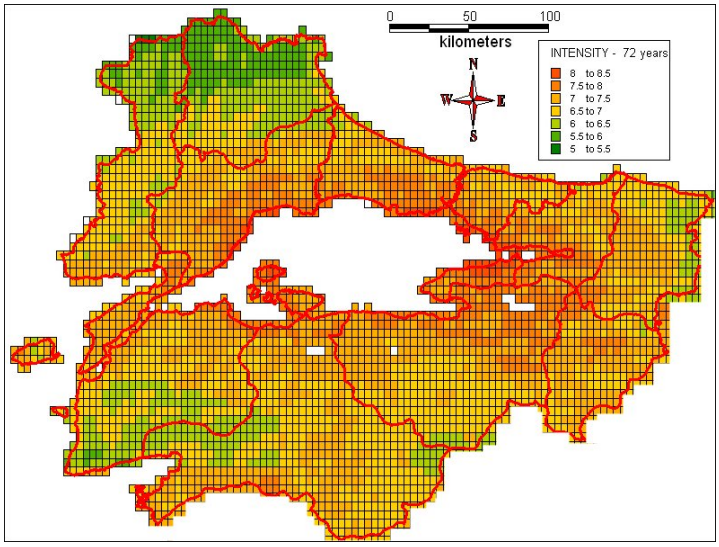

Figure 3.29 Seismic hazard maps in terms of macroseismic intensity for a return period of 72 years (0.05° resolution)

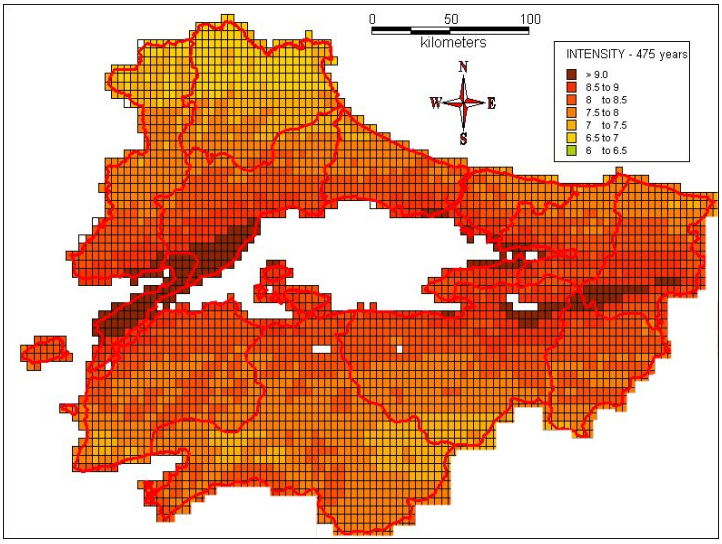

Figure 3.30 Seismic hazard maps in terms of macroseismic intensity for a return period of 475 years (0.05° resolution)

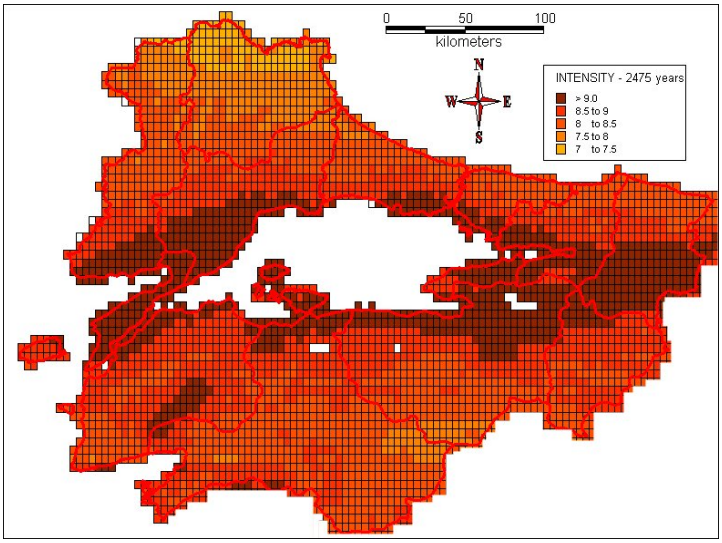

Figure 3.31 Seismic hazard maps in terms of macroseismic intensity for a return period of 2475 years (0.05° resolution)

SHARE seismic hazard map
[under development]

3.2.2. Exposure

Building exposure

The grid based building inventory dataset for Turkey has been used in this study. The data set includes the construction type, the number of stories, and the construction year. The predominant building typologies are reinforced concrete moment resisting frames with unreinforced masonry infill walls and reinforced concrete frames with shear walls and unreinforced masonry infill walls. As an example, Figure *3.32* shows the number of buildings of type of reinforced concrete, mid rise and pre1980

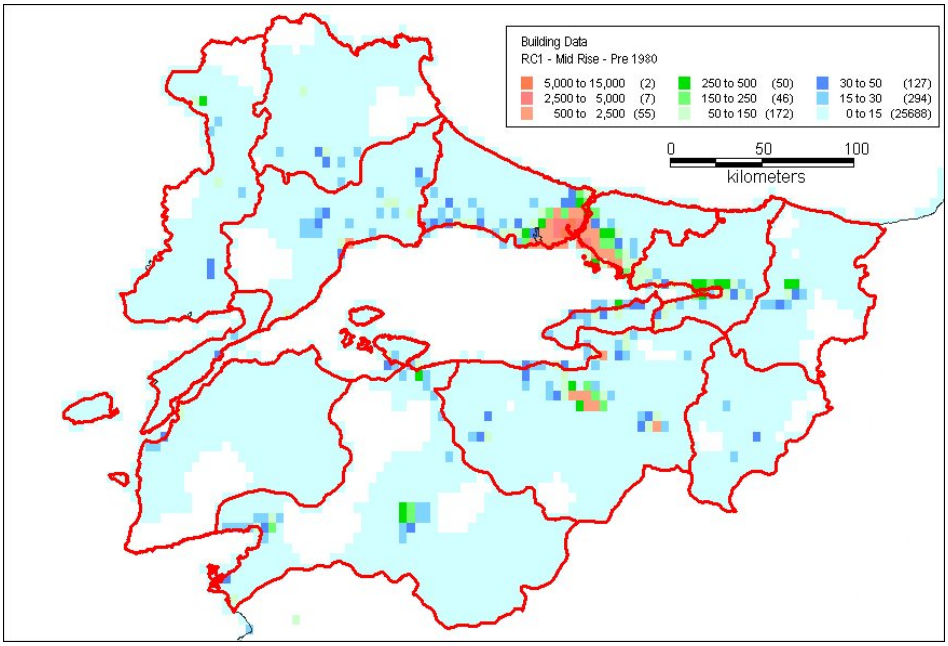

Figure 3.32 Number of buildings of type of reinforced concrete, mid rise and pre1980

Population exposure

Landscan population database for Turkey was formed in Arcview grid format, the datum of WGS84 and the grid size of 30 arc-seconds (about 1 km by 1 km in Turkey). For Marmara Region, this Landscan population database has been used (Figure *3.33*)

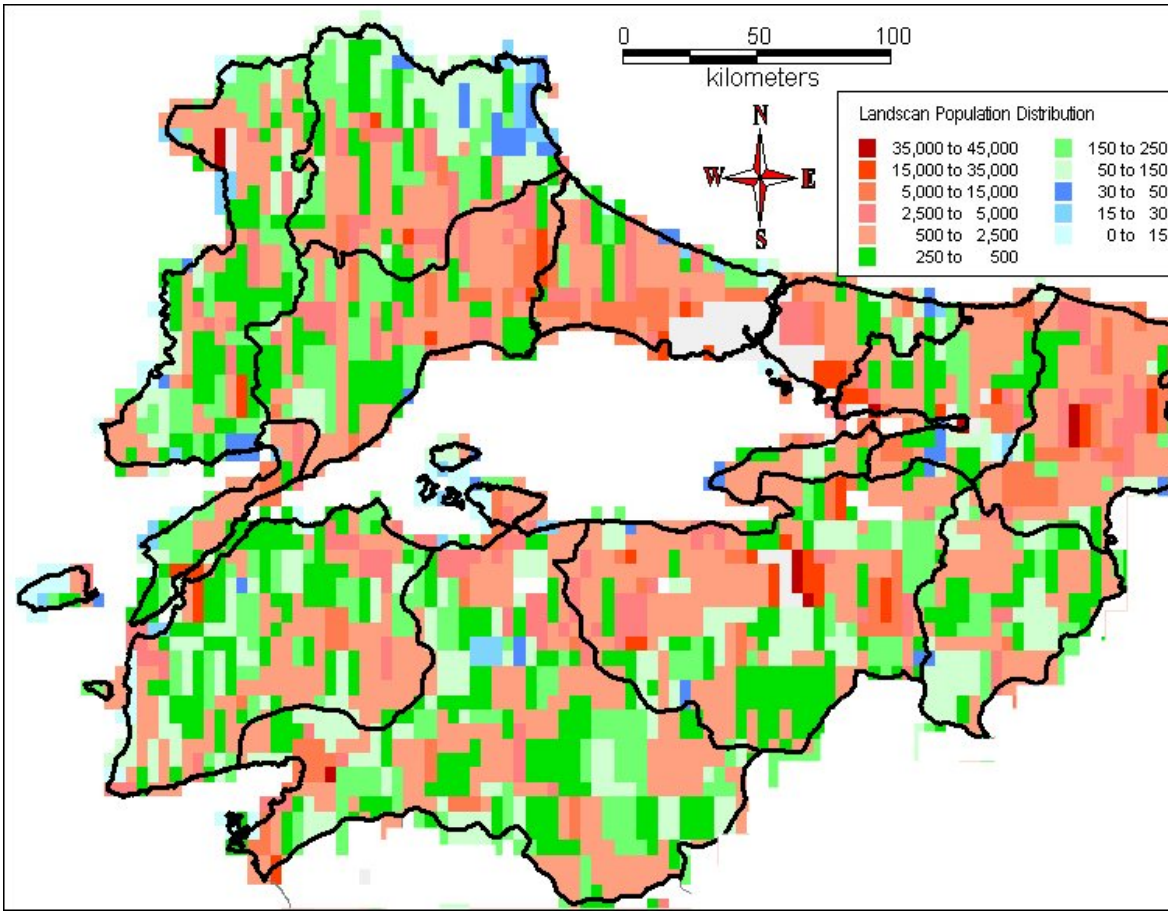

Figure 3.33 Distribution of population in Turkey on the basis of Landscan data

3.2.3. Vulnerability

The 1998 European Macroseismic Scale (EMS, 1998)**,** an updated version of the MSK-81 scale (MSK, 1981), differentiates the structural vulnerabilities into six classes (A to F). Due to deficiencies in design; concrete quality and construction practices, the bulk of the reinforced concrete building stock in Marmara Region may be considered in this vulnerability class.

Based on available empirical data, compilations from referenced works and engineering interpretations, the vulnerability curves for the general medium-rise (4-8 storey) R/C Frame type buildings in Turkey are provided in Figure *3.34* . The horizontal axis indicates the range (uncertainty) of MSK intensities and the vertical scale indicates the percentage loss for the five different damage grades, D1 through D5, as described in EMS (1998). Considering the damage level relations between low, medium and high rise R/C frame structures, the vulnerability curves for low-rise and high-rise R/C frame type buildings are obtained by half a unit left shifting of the intensity scale in the horizontal axis of the vulnerability curves of the medium rise R/C frame buildings. The resulting vulnerability curves are also illustrated in Figure *3.34*. The damage levels obtained for high-rise structures compare well with the respective ATC-13 damage factor estimates.

The vulnerability curves for masonry structures are assumed to be similar to the vulnerability curves of low-rise R/C structures.

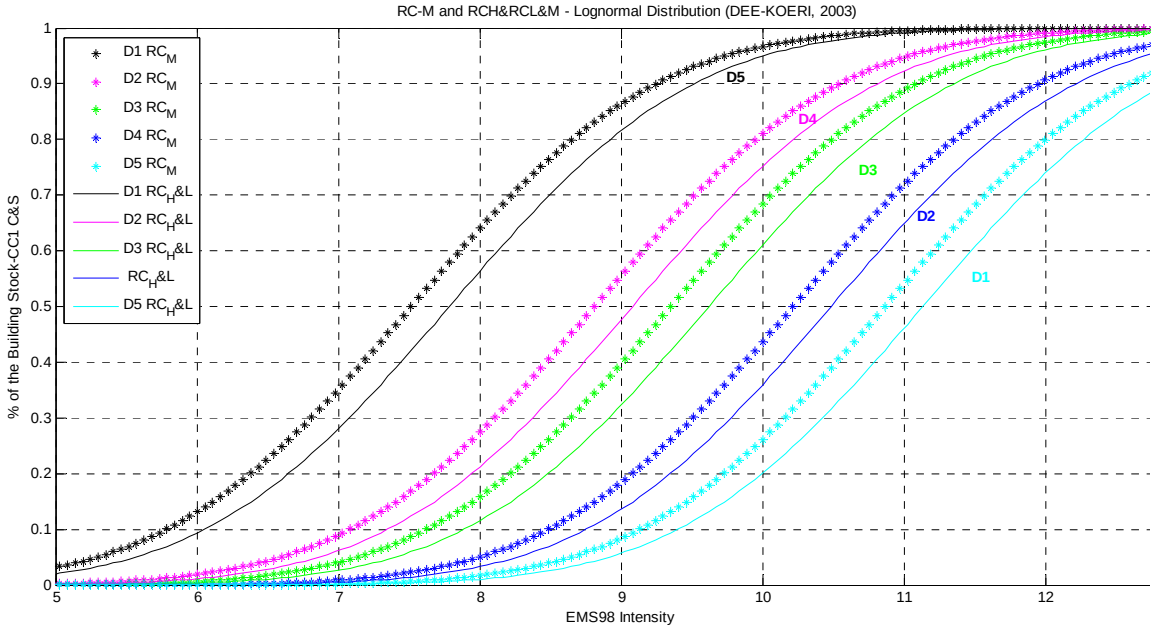

Figure 3.34 Intensity based vulnerability curves for the general mid rise (bold dashed lines) and high-, and low-rise R/C frame type and masonry buildings (thin solid lines) in Turkey

3.2.4. Seismic Risk

ELER earthquake loss assessment tools (ELER ©) developed within NERIES project JRA3 workpackage has been used for the seismic risk assessment for Marmara Region. Based on the ground motion intensity, population census, and building inventory information, the building damage and casualty estimation has been performed. The grid based building damage distributions corresponding to 475 years have been aggregated at province and sub-province levels. The province level results are presented in Figure *3.35* through Figure *3.36* in form of pie charts indicating 1) the distribution of various damages states in the total of damaged buildings and 2) the ratio of Damage States D3+D4+D5 to the total number of buildings in the province.

The grid based building damage distributions corresponding to 72, 475 and 2475 years, aggregated at province and sub-province levels have been used for the computation of province and sub-province level loss ratios (LR) and average annual loss ratios (AALR) with the help of the methodology of HAZUS-MH (FEMA 366, 2003). The province and sub-province level loss ratios corresponding to 475 years return periods are presented in Figure *3.37* through Figure *3.38*.

Current seismic risk maps

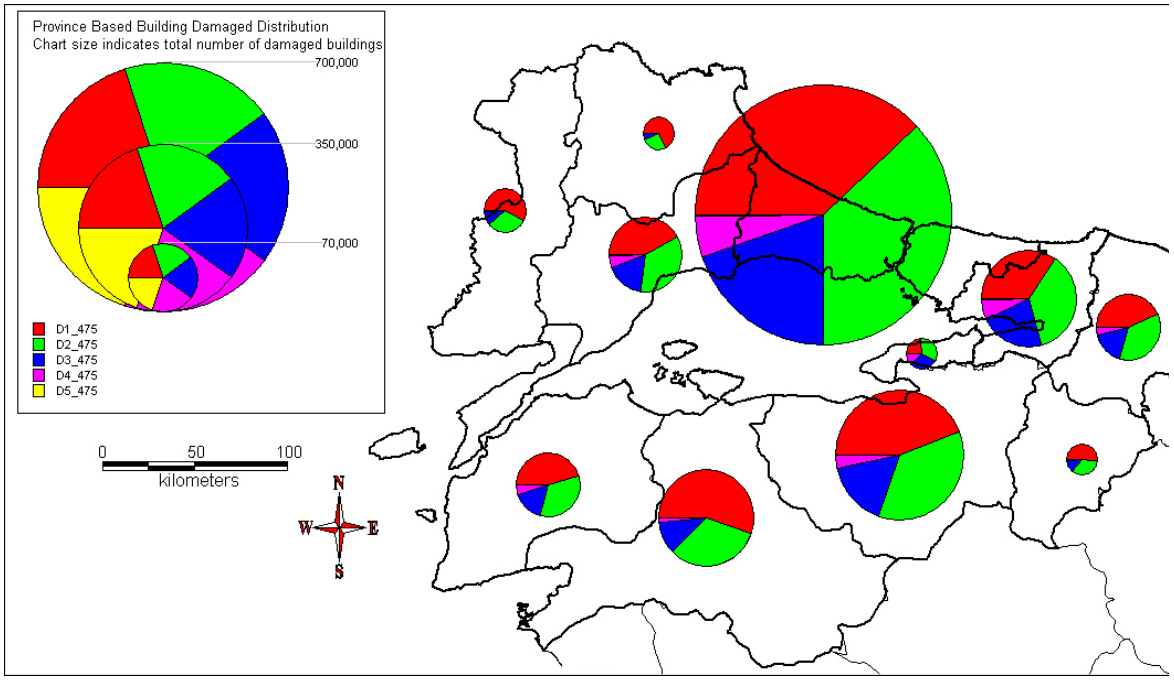

Figure 3.35 Province based building damage distribution corresponding to 475 years return period. Chart size indicates total number of damaged buildings

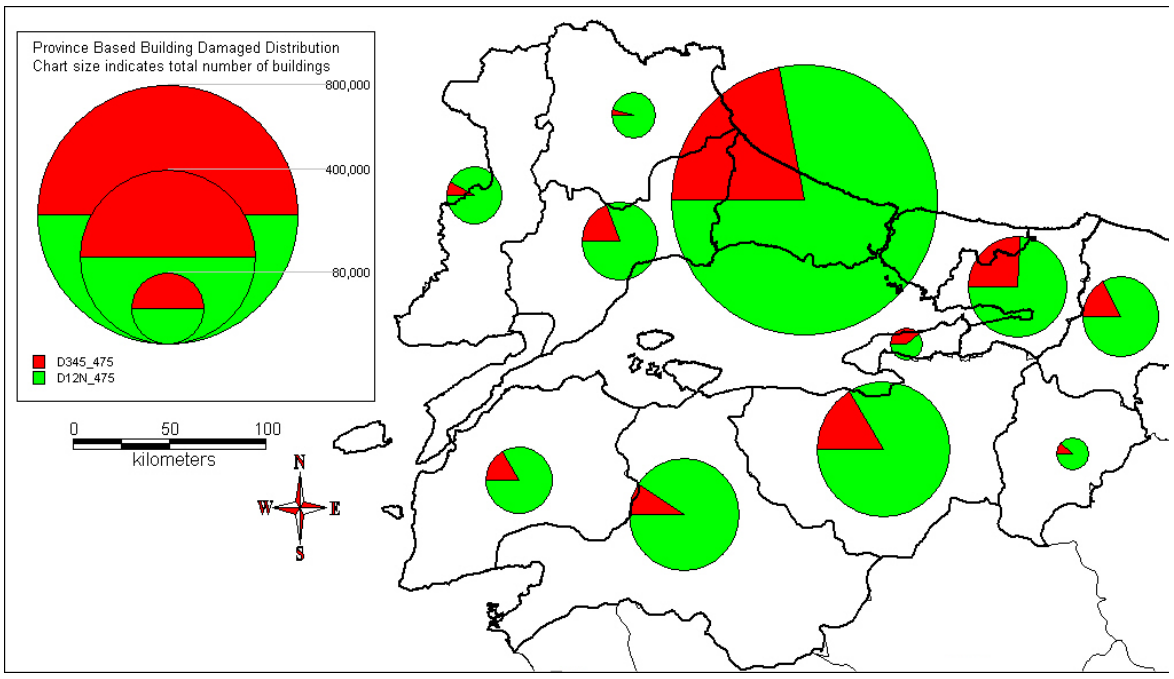

Figure 3.36 Province based building damage distribution (Damage states D3+D4+D5) corresponding to 475 years return period. Chart size indicates total number of buildings.

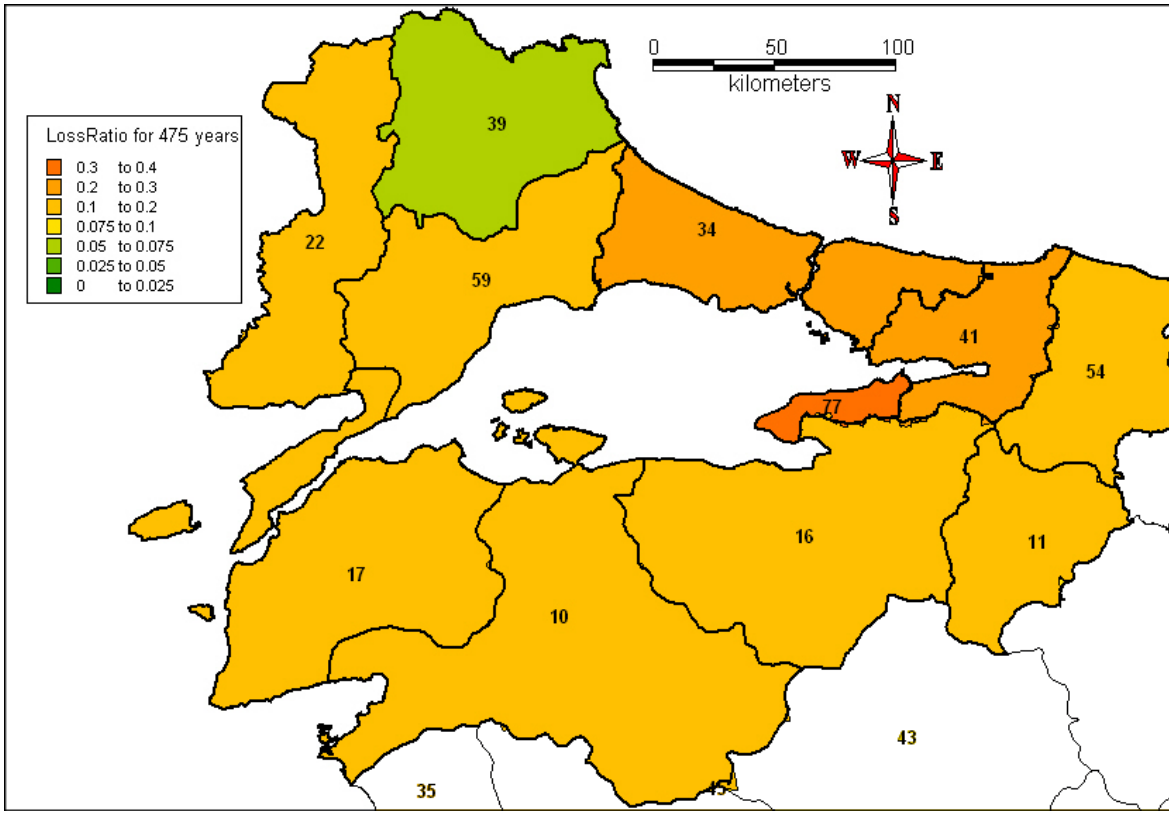

Figure 3.37 Province based loss ratio corresponding to 475 years return period

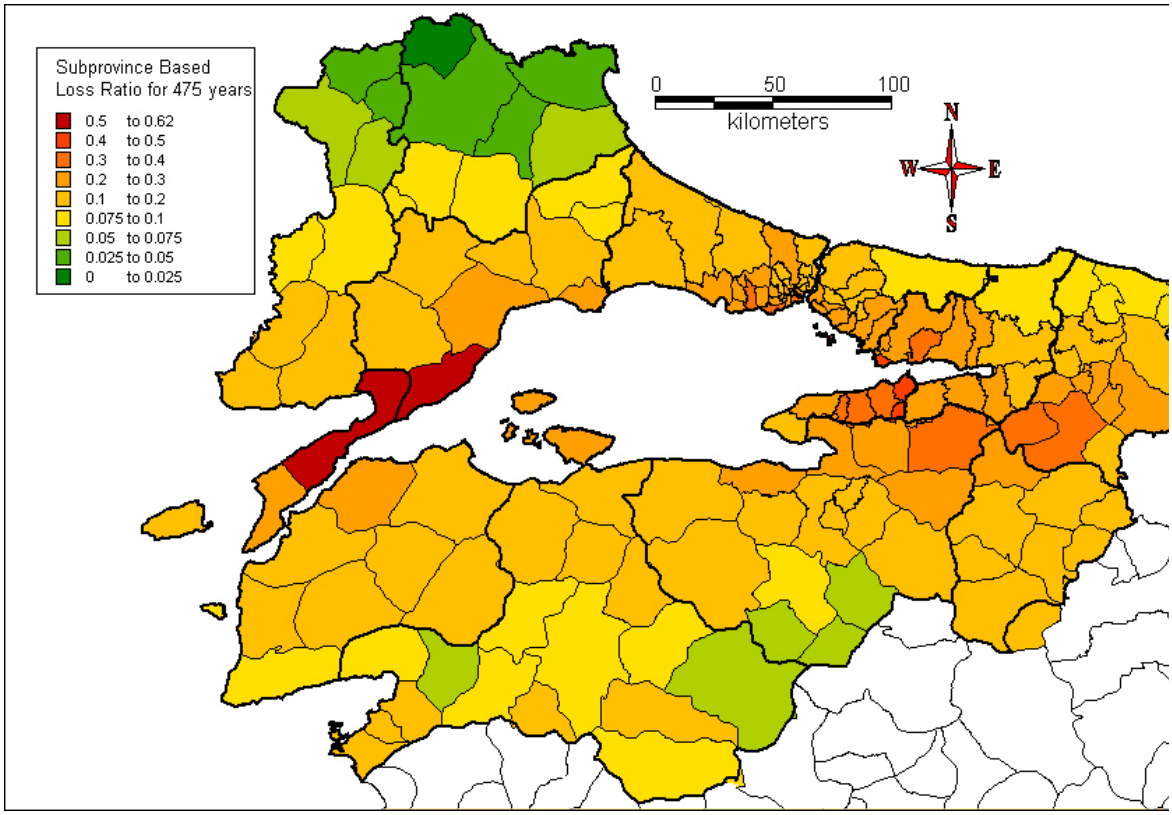

Figure 3.38 Province based loss ratio corresponding to 475 years return period

[under development]

4. Urban seismic risk applications

Thessaloniki and Lisbon have been selected to represent the European cities to be studied within the SHARE project. In the following sections seismic risk analysis for these selected cities are described in details and a critical review of the difference between the two approaches used is presented.

4.1. Thessaloniki

The city of Thessaloniki is the second largest city in Greece and the economic capital of Macedonia in northern Greece. The city has a population of 385,000 and is part of a Larger Urban Zone (LUZ) of over one million inhabitants. As study area for the estimation of seismic risk and loss assessment, the study area of the SYNER-G (http://www.vce.at/SYNER-G) FP7 European Collaborative Research Project case study was selected, since for this region a detailed inventory of the building stock is available (Kappos et al. 2008). The selected area is divided in 20 sub-city districts according to the Urban Audit (UA) database of EUROSTAT (http://www.urbanaudit.org) as shown in Figure 4.1.

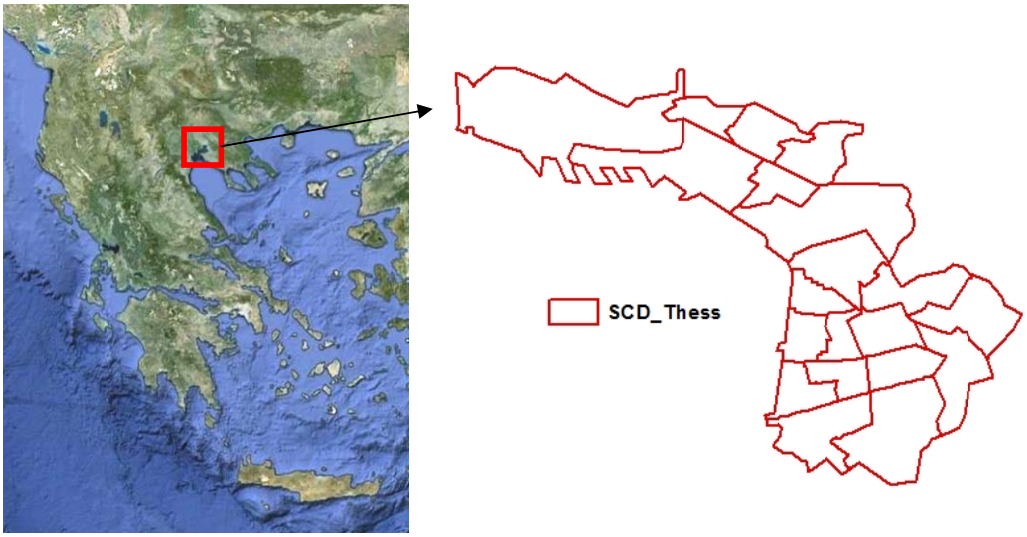

Figure 4.1: Study area in SYNER-G case study. Red lines illustrate Urban Audit SCDs boundaries.

4.1.1. Seismic hazard assessment

The seismic risk assessment was carried out using two different types of hazard, both for a mean return period Tm=475 years: (i) the seismic hazard estimated for the metropolitan area of Thessaloniki within SRM-LIFE project (Papaioannou, 2004), hereinafter referred to as "current seismic hazard", and (ii) the new hazard model developed in SHARE, hereinafter referred to as "SHARE seismic hazard". For the current hazard, the study area lies within two

zones with PGA_{rock} equal to 0.20g or 0.24g (Figure 4.2), while for the SHARE hazard, PGA_{rock} is uniform for Thessaloniki and equal to 0.20g. Concerning the hazard in terms of elastic response spectra, PGA_{rock} of current hazard is combined with EC8 Type 1 response spectrum for soil class A, while SHARE (preliminary results of the area source model provided in November 2012) provides a Uniform Hazard Spectrum (UHS) for Thessaloniki (Figure 4.3). It is observed that SHARE UHS has a much narrower plateau and lower peak spectral acceleration values compared to the current hazard spectra.

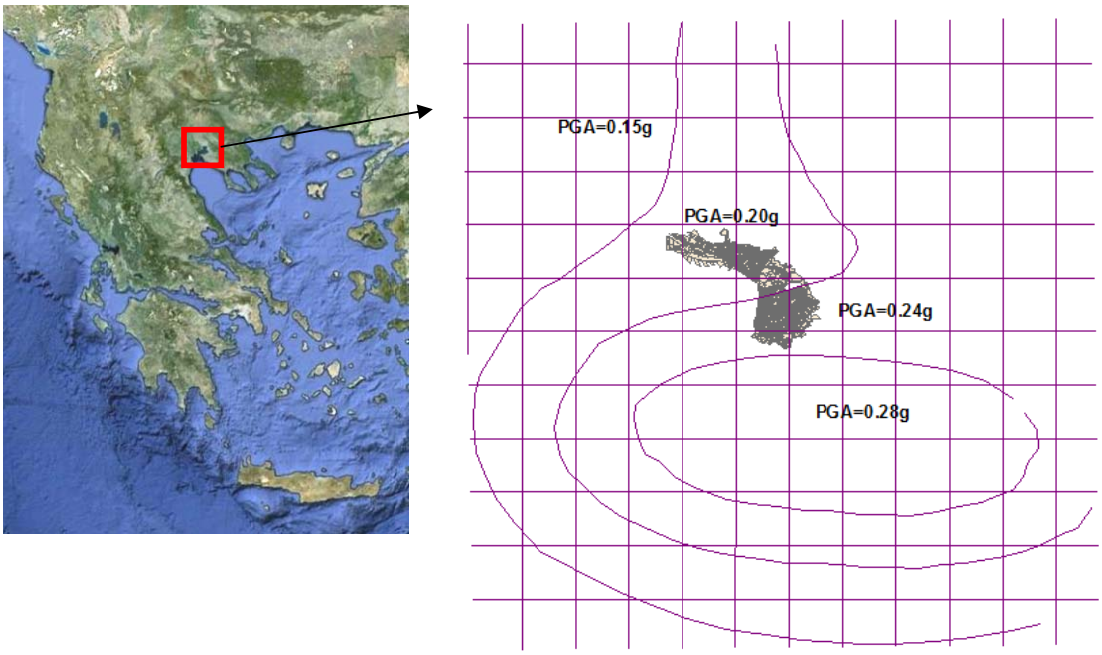

Figure 4.2: PGA_{rock} zones for the Metropolitan area of Thessaloniki for a mean return period Tm=475 years based on seismic hazard results from SRM-LIFE.

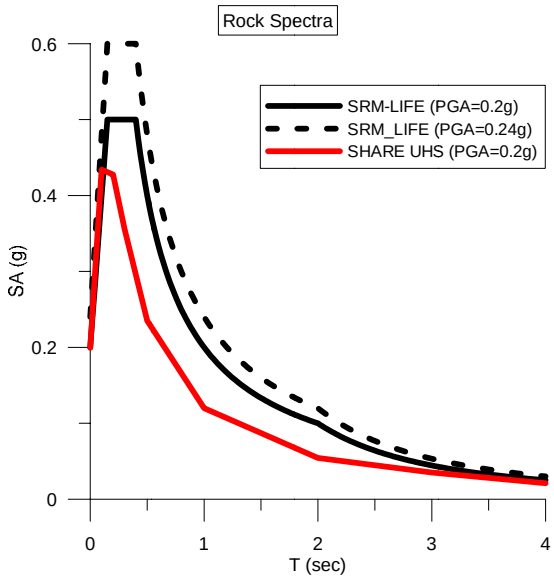

Figure 4.3: SHARE UHS for Thessaloniki, compared to EC8 Type 1 rock spectra for the two PGA_{rock} values for Thessaloniki from SRM-LIFE (rock site conditions).

For the incorporation of local site effects, two different soil classification schemes were used: the EC8 classification scheme (CEN 2004) and the new classification scheme proposed in SHARE by AUTH (Table 4.1, Pitilakis et al. 2013).

Table 4.1 Proposed Soil and Site Characterization (Pitilakis et al. 2013)

Soil Class	**Description**	**T_0 (sec)**	**Remarks**
A1	Rock formations		Vs≥1500 m/s
A2	Slightly weathered / segmented rock formations (thickness of weathered layer <5.0m)	≤0.2	Surface weathered layer: Vs≥ 200 m/sec Rock Formations: Vs ≥ 800 m/sec
	Geologic formations resembling rock formations in their mechanical properties and their composition (e.g. conglomerates)		Vs ≥ 800 m/sec
B1	Highly weathered rock formations whose weathered layer has a considerable thickness (5.0m - 30.0m)	≤0.5	Weathered layer: Vs ≥ 300 m/sec
	Soft rock formations of great thickness or formations which resemble these in their mechanical properties (e.g. stiff marls)		Vs: 400-800 m/sec N-SPT > 50, Su> 200 KPa
	Soil formations of very dense sand – sand gravel and/or very stiff/ to hard clay, of homogenous nature and small thickness (up to 30.0m)		Vs: 400-800 m/sec N-SPT > 50, Su> 200 KPa
B2	Soil formations of very dense sand – sand gravel and/or very stiff/ to hard clay, of homogenous nature and medium thickness (30.0 - 60.0m), whose mechanical properties increase with depth	≤0.8	Vs: 400-800 m/sec N-SPT > 50, Su > 200 KPa
C1	Soil formations of dense to very dense sand – sand gravel and/or stiff to very stiff clay, of great thickness (> 60.0m), whose mechanical properties and strength are constant and/or increase with depth	≤1.5	Vs: 400-800 m/sec N -SPT> 50, Su > 200 KPa
C2	Soil formations of medium dense sand – sand gravel and/or medium stiffness clay (PI > 15, fines percentage > 30%) of medium thickness (20.0 – 60.0m)	≤1.5	Vs: 200-450 m/sec N -SPT> 20, Su > 70 KPa
C3	Category C2 soil formations of great thickness (>60.0 m), homogenous or stratified that are not interrupted by any other soil formation with a thickness of more than 5.0m and of lower strength and Vs velocity	≤1.8	Vs:200-450 m/sec N-SPT > 20, Su > 70 KPa
D1	Recent soil deposits of substantial thickness (up to 60m), with the prevailing formations being soft clays of high plasticity index (PI>40), high water content and low values of strength parameters	≤2.0	Vs ≤ 300 m/sec N-SPT < 25, Su < 70KPa
D2	Recent soil deposits of substantial thickness (up to 60m), with prevailing fairly loose sandy to sandy-silty formations with a substantial fines percentage (not to be considered susceptible to liquefaction)	≤2.0	Vs ≤ 300 m/sec N-SPT < 25
D3	Soil formations of great overall thickness (> 60.0m), interrupted by layers of category D1 or D2 soils of a small thickness (5 – 15m), up to the depth of ~40m, within soils (sandy and/or clayey, category C) of evidently greater strength, with Vs≥ 300 m/sec	≤3.0	Vs: 150-600 m/sec

E	Surface soil formations of small thickness (5 - 20m), small strength and stiffness, likely to be classified as category C and D according to its geotechnical properties, which overlie category A formations (Vs ≥ 800 m/sec)	≤0.7	Surface soil layers: Vs ≤ 400 m/sec
X	-Loose fine sandy-silty soils beneath the water table, susceptible to liquefaction (unless a special study proves no such danger, or if the soil's mechanical properties are improved). -Soils near obvious tectonic faults. -Steep slopes covered with loose lateral deposits. -Loose granular or soft silty-clayey soils, provided they have been proven to be hazardous in terms of dynamic compaction or loss of strength. Recent loose landfills. -Soils with a very high percentage in organic material -Soils requiring site-specific evaluations		

The classification of Thessaloniki region based on EC8 and the new classification system is presented in Figure 4.4 and Figure 4.5 respectively. The building blocks of the study area are also shown.

Table 4.2 gives the soil amplification factors for the soil classes of EC8 as they are currently in the code (CEN 2004), as well as the improved soil factors for the EC8 soil classes as they were proposed within SHARE by AUTH (Pitilakis et al. 2012), while Table 4.3 gives the soil amplification factors and the parameters describing the normalized response spectra of the new classification scheme proposed in SHARE by AUTH.

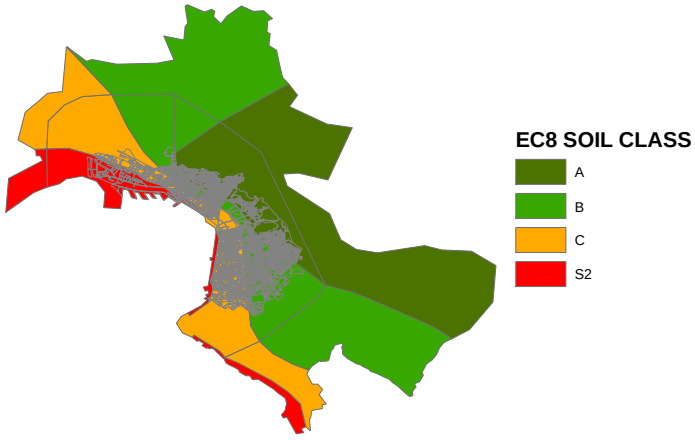

Figure 4.4: Map of EC8 site classes for Thessaloniki compiled utilizing all available geological, geophysical and geotechnical information. Grey polygons illustrate the building blocks of the study area.

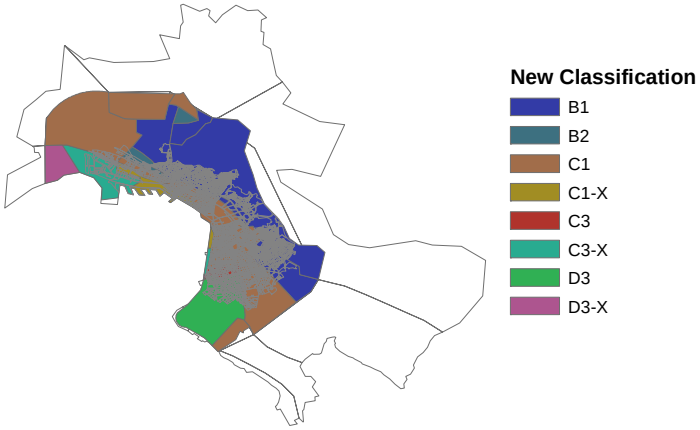

Figure 4.5: Map of new site classes for Thessaloniki compiled utilizing all available geological, geophysical and geotechnical information. Grey polygons illustrate the building blocks of the study area.

Table 4.2 Current and improved soil amplification factors S for the existing EC8 classification scheme (Pitilakis et al. 2012)

EC8 Soil Class	**Type 2 (Ms≤5.5)**		**Type 1 (Ms>5.5)**	
	EC8	**Proposed (Pitilakis et al. 2012a)**	**EC8**	**Proposed (Pitilakis et al. 2012a)**
B	1.35	1.40	1.20	1.30
C	1.50	2.10	1.15	1.70
D	1.80	1.80	1.35	1.35
E	1.60	1.60	1.40	1.40

Table 4.3 Parameters of proposed acceleration response spectra (Pitilakis et al. 2013)

Soil Class	**Type 2 (Ms≤5.5)**					**Type 1 (Ms>5.5)**				
	T_B (sec)	**T_C (sec)**	**T_D (sec)**	**S**	**β**	**T_B (sec)**	**T_C (sec)**	**T_D (sec)**	**S**	**β**
A	0.05	0.3	1.2	1	2.5	0.1	0.4	2	1	2.5
B1	0.05	0.25	1.2	1.2	2.75	0.1	0.4	2	1.1	2.75
B2	0.05	0.3	1.2	1.5	2.5	0.1	0.5	2	1.4	2.5
C1	0.1	0.25	1.2	1.8	2.5	0.1	0.6	2	1.7	2.5
C2	0.1	0.4	1.2	1.7	2.5	0.1	0.6	2	1.3	2.5
C3	0.1	0.5	1.2	2.1	2.5	0.1	0.9	2	1.4	2.5
D	0.1	0.7	1.2	2.0	2.5	0.1	0.7	2	1.8	2.5
E	0.05	0.2	1.2	1.6	2.75	0.1	0.35	2	1.4	2.75

In order to incorporate local site conditions into current rock hazard, the EC8 Type 1 elastic response spectra were applied based on the soil classification of the study area given in Figure 4.4. This hazard is hereinafter referred to as **Hazard 1** (Figure 4.6).

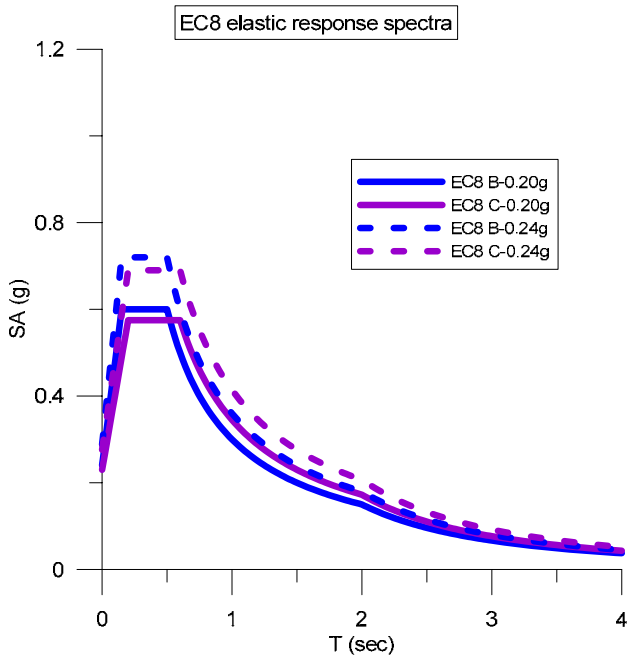

Figure 4.6: EC8 Type 1 elastic response spectra for soil classes B and C and for PGA_{rock}=0.2g or 0.24g (Hazard 1).

Local site conditions were incorporated into the SHARE rock hazard with three different ways:

1. Using EC8 soil classification scheme and the soil amplification factors (S factors) proposed by EC8 in the current version of the code (CEN 2004) (
2. Table 4.2). The EC8 Type 1 elastic response spectra for soil classes B and C were divided with Type 1 elastic response spectra for soil class A and SHARE UHS was multiplied by the corresponding period-dependent soil factors based on the soil classification of the study area given in Figure 4.4 (**Hazard 4**).
3. Using EC8 soil classification scheme and the improved soil amplification factors proposed in SHARE by AUTH (Pitilakis et al. 2012) (
4. Table 4.2). It is reminded that the improvement of the EC8 spectra is related to the proposal of new soil factors (see
5. Table 4.2). The improved Type 1 elastic response spectra for soil classes B and C were divided with Type 1 elastic response spectra for soil class A and SHARE rock UHS was multiplied by the corresponding period-dependent soil factors based on the soil classification of the study area given in Figure 4.4 (**Hazard 5**).
6. Using the new soil classification scheme and the corresponding soil amplification factors proposed in SHARE by AUTH (Table 4.3, Pitilakis et al. 2013). The proposed Type 1 elastic response spectra for new soil classes B1, B2, C1, C3, D3 were divided with Type

1 elastic response spectra for new soil class A and SHARE rock UHS was multiplied by the corresponding period-dependent soil factors based on the soil classification of the study area given in Figure 4.5 (**Hazard 6**).

Figure 4.7 illustrates the comparisons between the elastic response spectra based on EC8, improved EC8 and the new classification system, for the SHARE hazard. Spectra are plotted only for those soil classes which are actually met in the study area. All spectra refer to a return period T=475 years and 5% damping.

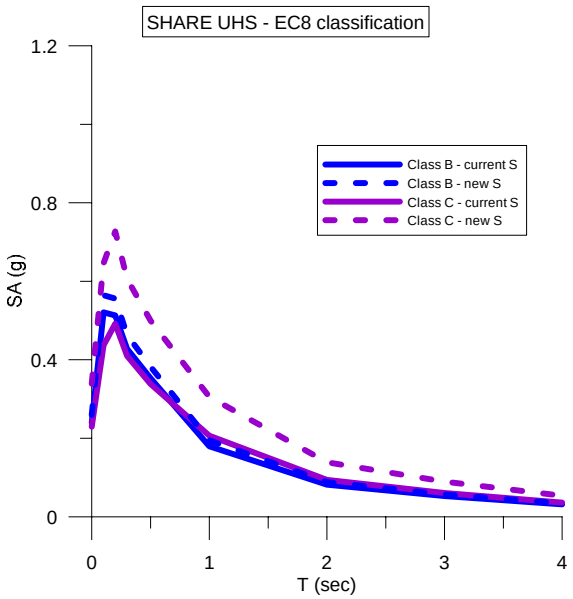

(a)

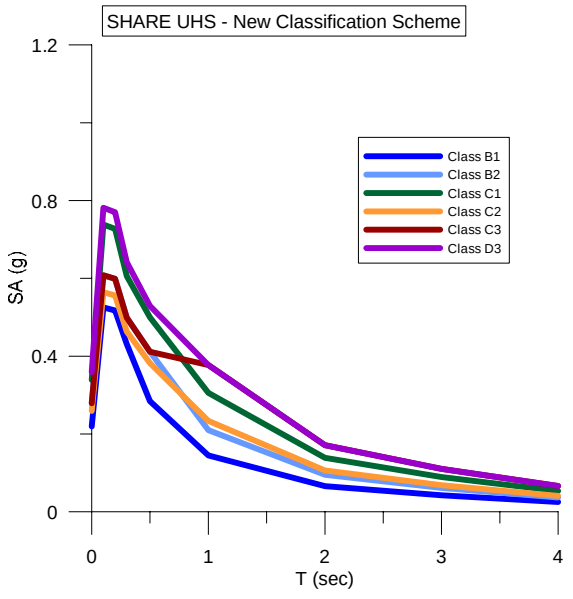

(a)

Figure 4.7: (a) SHARE rock UHS for Thessaloniki amplified with the current (Hazard

4) and the improved (Hazard 5) EC8 soil amplification factors, (b) SHARE rock UHS for Thessaloniki amplified with the soil amplification factors of the new classification system (Hazard 6). All spectra refer to a return period T=475 years.

In Figure 4.8 a comparison between the elastic response spectra of the two components of the accelerograms recorded at City Hotel during the 1978 M=6.5 Thessaloniki earthquake and several design spectra for soil class EC8 C / Greek Seismic Code EAK Γ is shown. SHARE UHS, EC8 spectrum for PGA_{rock}=0.2g and Greek Seismic Code EAK design spectrum for the specific soil class are included. The epicenter of the earthquake was located at a distance of about 25km NE of the city, and the focal depth was about 8 km. The recorded PGA in the station, which was located in the basement of an eight-story building at the shore line of the city was rather low (~0.15g) most probably due to the presence of non linear site effects, while the maximum ground acceleration on stiff soils is estimated to be of the order of 0.30g (Pitilakis et al. 2004).

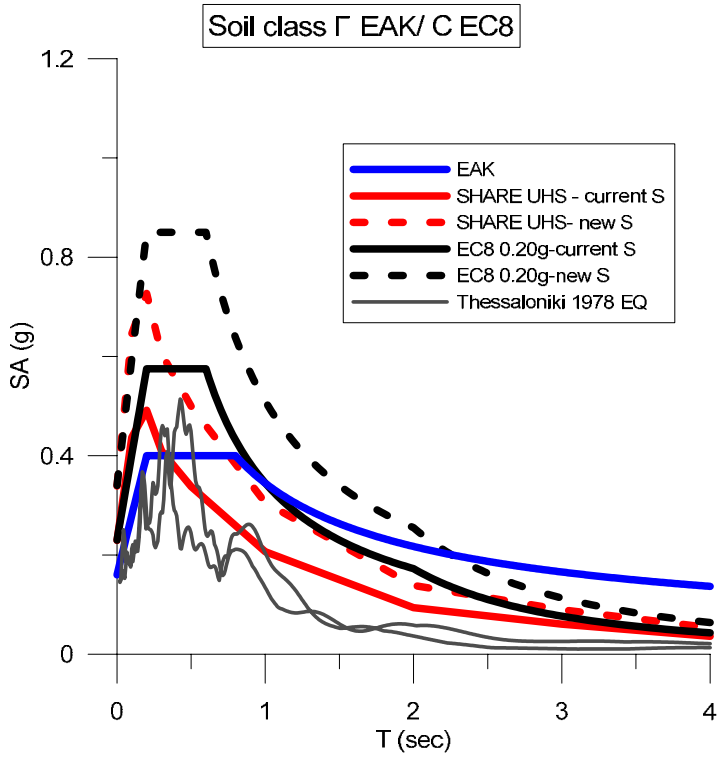

Figure 4.8: Elastic Response Spectra of Thessaloniki 1978 accelerograms recorded at City Hotel compared to various code spectra.

4.1.2. Exposure

Building Exposure

The current detailed building inventory is based on the inventory which was compiled within RISK-UE and LESSLOSS projects, with the improvements and additions that took place for

SYNER-G project. The reference unit of the inventory is the building block (Figure 4.9). The building inventory comprises 2893 building blocks with 27738 buildings, the majority of which (25639) are reinforced concrete (RC) buildings. This is why it was decided to limit the study only to the RC buildings of the inventory.

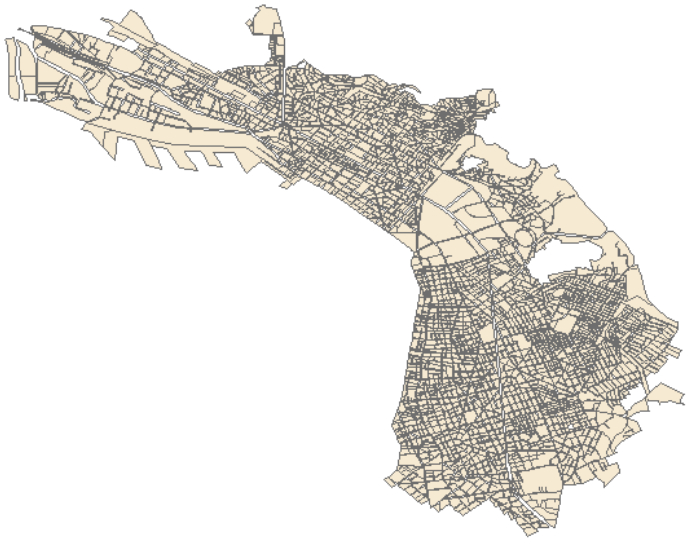

Figure 4.9: Building blocks of Thessaloniki study area.

The classification of RC buildings is based on the Building Typologies Matrix of Kappos et al. 2006, representing practically all common RC building types in Greece (Table 4.4). The same Building Typologies Matrix has also been used for Thessaloniki in the framework of SYNER-G EU project. Regarding the structural system, both frames and frame+shear walls (dual) systems are included, with a further distinction based on the configuration of the infill walls. Regarding the height, three subclasses are considered (low-, medium- and high-rise). Finally, as far as the level of seismic design is concerned, four different levels are considered:

- No code (or pre-code): R/C buildings with very low level of seismic design or no seismic design at all, and poor quality of detailing of critical elements;
- Low code: R/C buildings with low level of seismic design (roughly corresponding to pre-1980 codes in S. Europe, e.g., the 1959 Code for Greece);
- Moderate code: R/C buildings with medium level of seismic design (roughly corresponding to post-1980 codes in S. Europe, e.g., the 1985 Supplementary Clauses of the Greek Seismic Codes) and reasonable seismic detailing of R/C members;
- High code: R/C buildings with enhanced level of seismic design and ductile seismic detailing of R/C members according to the new generation of seismic codes (similar to Eurocode 8).

Table 4.4 R/C Building Typology Matrix (BTM) for Thessaloniki (Kappos et al. 2006)

Type	Structural system	Height	Code level

RC1	Concrete moment frames	(L) Low-rise (1-3) (M) Mid-rise (4-7) (H) High-rise (8+)	(N)o/pre code (L)ow code (M)edium code (H)igh code
RC3	Concrete frames with unreinforced masonry infill walls		
3.1	Regularly infilled frames	(L) Low-rise (1-3) (M) Mid-rise (4-7) (H) High-rise (8+)	(N)o/pre code (L)ow code (M)edium code (H)igh code
3.2	Irregularly infilled frames (pilotis)	(L) Low-rise (1-3) (M) Mid-rise (4-7) (H) High-rise (8+)	(N)o/pre code (L)ow code (M)edium code (H)igh code
RC4	RC Dual systems (RC frames and walls)		
4.1	Bare Systems (no infill walls)	(L) Low-rise (1-3) (M) Mid-rise (4-7) (H) High-rise (8+)	(N)o/pre code (L)ow code (M)edium code (H)igh code
4.2	Regularly infilled dual systems	(L) Low-rise (1-3) (M) Mid-rise (4-7) (H) High-rise (8+)	(N)o/pre code (L)ow code (M)edium code (H)igh code
4.3	Irregularly infilled dual systems (pilotis)	(L) Low-rise (1-3) (M) Mid-rise (4-7) (H) High-rise (8+)	(N)o/pre code (L)ow code (M)edium code (H)igh code

The classification of the RC buildings of the study area based on the BTM of Table 4.4 is illustrated in Figure 4.10. Most of the buildings are either regularly or irregularly infilled dual systems (Building types RC4.2 and RC4.3), while the majority of RC buildings are pre-1980 constructions and thus have been designed with low level of seismic code.

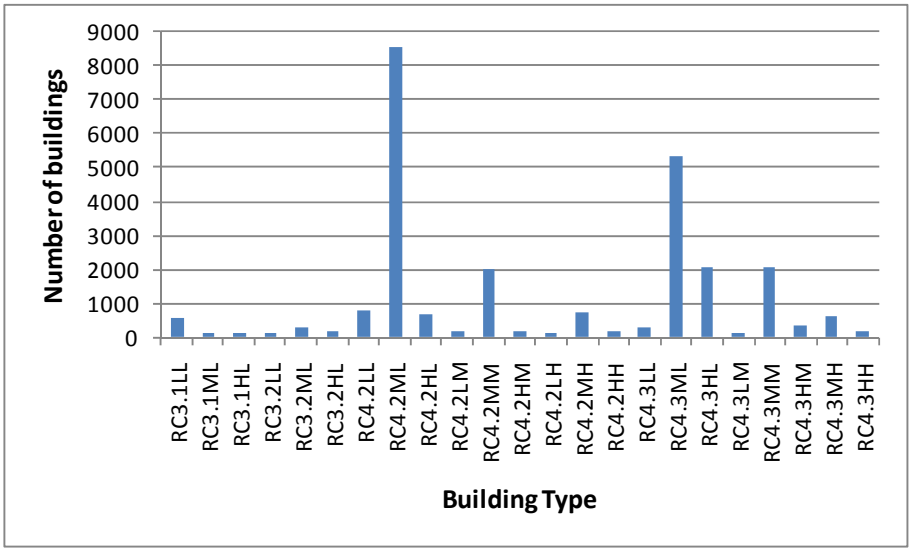

Figure 4.10: Classification of the RC buildings of the study area based on the BTM of Table 4.4 (Kappos et al. 2006). The first letter of each building type refers to the height of the building (L: low, M: medium, H: high), while the second letter refers to the seismic code level of the building (N: no, L: low, M: medium, H: high).

Population Exposure

Based on the Urban Audit Data for Thessaloniki, the population of the area shown in Figure 4.1 is 376589. Since there were no available data for the exact number of inhabitants of each building of the inventory, we assumed a constant number of inhabitants per square meter of floor area for all buildings.

4.1.3. Vulnerability

The Capacity Spectrum Method (CSM) described in Section 2.1 was used to determine the seismic performance of the buildings, by comparing the capacity of the structure with the seismic demand. The capacity and fragility curves developed by the Aristotle University of Thessaloniki and which are described in numerous research works (e.g. Kappos et al. 2006, D' Ayala et al. 2012) were used. These curves have been developed for five damage states: DS1 (slight), DS2 (moderate), DS3 (substantial to heavy), DS4 (very heavy) and DS5 (collapse). Some typical pushover curves and their corresponding bilinear approximations (derived on the basis of equal areas under the curves) used for the present study are given in Figure 4.11. To facilitate direct comparison with earthquake demand (i.e. overlaying the capacity curve with a demand spectrum), the normalized force (normalized base shear) axis was converted to spectral acceleration and the displacement axis was converted to spectral displacement (Kappos et al. 2006). Peak building response expressed in terms of spectral displacement at the point of intersection of the capacity curve and demand spectrum is then used with fragility curves to estimate damage state probabilities. The EarthQuake Risk Model code (EQRM - http://sourceforge.net/projects/eqrm) (Geoscience Australia) was used for the estimation of the expected damages with CSM. The EQRM code has been designed for four damage states (slight, moderate, extensive and complete), while the selected capacity and fragility curves

were available for five damage states. To overcome this, DS1 damage state of Kappos et al. (2006) was selected as representative for slight damage, DS2 for moderate, DS3 for extensive and DS5 for complete, while DS4 damage state of Kappos et al. (2006) was not taken into consideration. Representative plots of the applied fragility curves as a function of spectral displacement (S_d) referring to mid-rise regularly infilled dual systems designed with "low" (RC4.2ML, most frequent typology) and "medium" seismic code provisions (RC4.2MM) are illustrated in Figure 4.12. It should be stressed that the lognormal standard deviation beta value assigned to all fragility curves was equal to 0.4, since this is the default value that EQRM uses for structural damage.

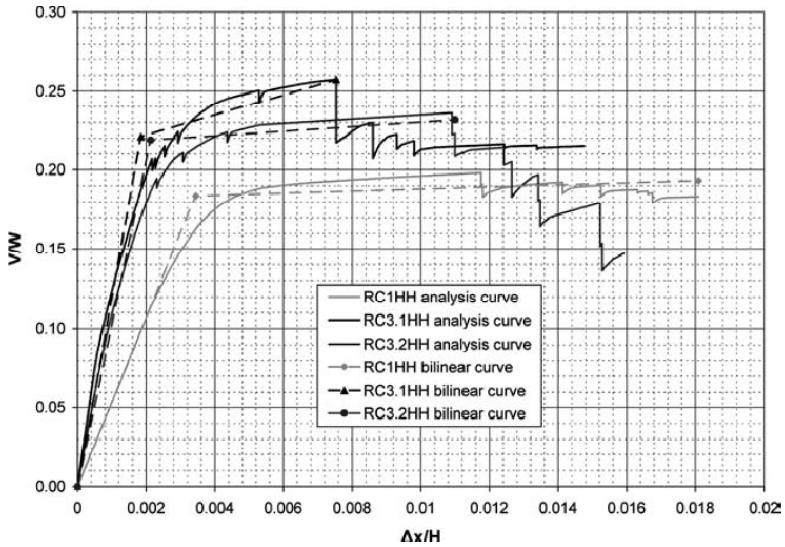

Figure 4.11: Plot of representative pushover curves for high-rise R/C frames designed to high codes (Kappos et al. 2006).

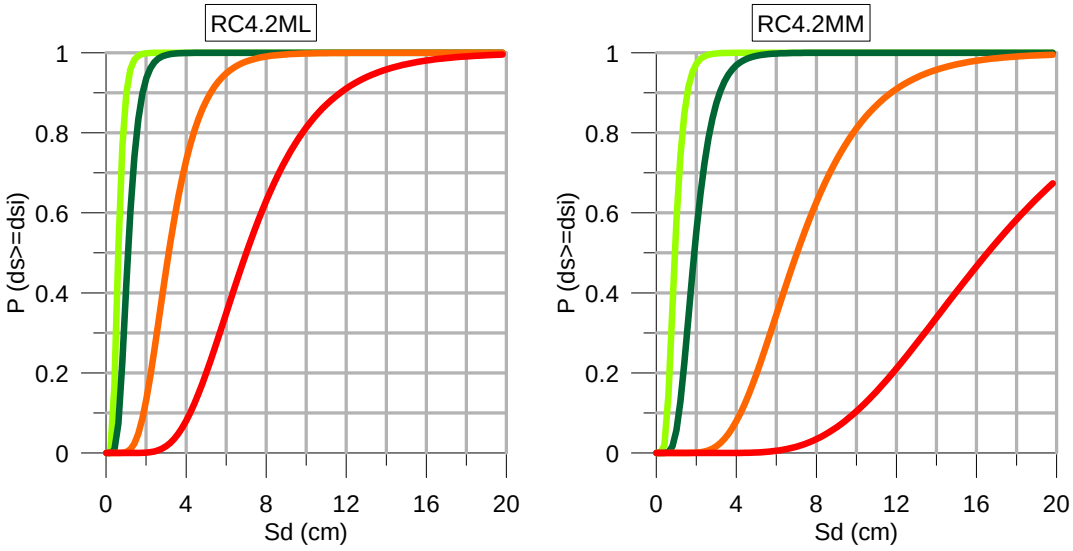

Figure 4.12: Fragility curves for mid-rise regularly infilled dual R/C systems, for (a) "low" and (b) "medium" code design, for a beta value equal to 0.4 (modified after

Kappos et al. 2006).

For the estimation of casualties, Equation 2.1 was applied for the four levels of injury of HAZUS-MH (FEMA, 2003) described in detail in Table *2.1* (light injuries, hospitalization, severe injuries and mortal wounds). The casualty rates used to estimate the social losses are those defined by HAZUS-MH (FEMA, 2003) for reinforced concrete building (Table *2.2*). The following assumptions were made:

- The number of inhabitants of each building is proportional to the floor area of the building (constant number of inhabitants per square meter of floor area for all buildings).
- All buildings are considered to have residential land use.
- 5% of the complete damaged buildings collapse. This value in HAZUS is close to 10% for RC buildings, but it was considered as too high for Greece, where the data from past earthquakes show that very few of the buildings that suffer complete damage actually collapse.

Economic losses are expressed though the estimation of mean damage ratio (MDR), which represents the total cost of repair divided by the cost of reconstruction. For the estimation of MDR, the loss indices (repair cost/replacement cost) used in Kappos et al. (2003) were applied (
Table 4.5). As a result, MDR is calculated using the following equation:

$$\mathrm{MDR} = [\mathrm{D1}] \times 0.005 + [\mathrm{D2}] \times 0.05 + [\mathrm{D3}] \times 0.2 + [\mathrm{D5}] \times 0.8 \qquad 4.1$$

where D1, D2, D3 and D5 are the percentages of surface area in damage grades slight, moderate, extensive and complete, respectively.

Table 4.5 Loss indices for R/C structures (Kappos et al. 2003)

Damage State	Central damage factor (%)
D1	0.5
D2	5
D3	20
D5	80

4.1.4. Seismic Risk

Current seismic hazard

The percentages of the damaged floor area per damage state for each sub-city district for Hazard scenario 1 are illustrated in Figure 4.13. The total percentages of damaged buildings per damage state for the whole study area are given in Table 4.6.

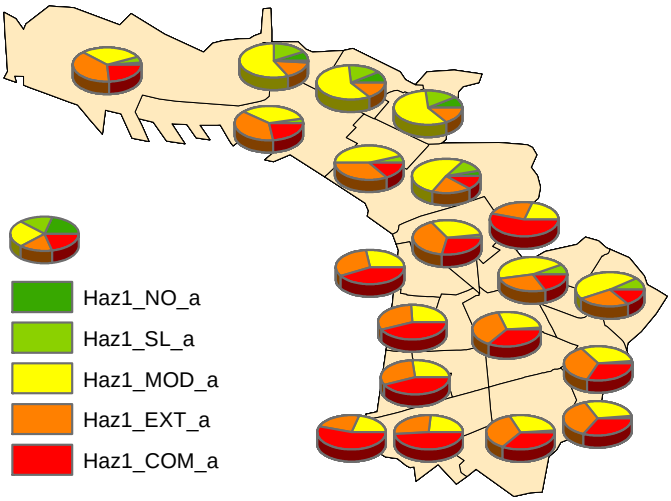

Figure 4.13: Hazard 1: Seismic risk per Sub-City District for a return period of 475 years in terms of the percentage of floor area for no damaged buildings, slight damaged buildings, moderate damage buildings, extensive damaged buildings and, complete damaged buildings.

Table 4.6: Percentages of affected floor area per damage state for the current hazard scenario (Hazard 1), for a return period of 475 years.

	Hazard 1
Slight [D1]	6.22%
Moderate [D2]	39.54%
Extensive [D3]	28.28%
Complete [D5]	24.05%
No	1.91%

Inserting the percentages [D1], [D2], [D3] and [D5] into Equation 4.1, the mean damage ratio (MDR) is calculated (Figure 4.14). The total MDR values for the whole study area is equal to 26.91%. By multiplying this mean damage ratio with the replacement cost, the economic losses can be evaluated. Assuming an average replacement cost equal to 1000€/m^2, the estimated economic losses for hazard scenarios 1 are 9,2 billions €.

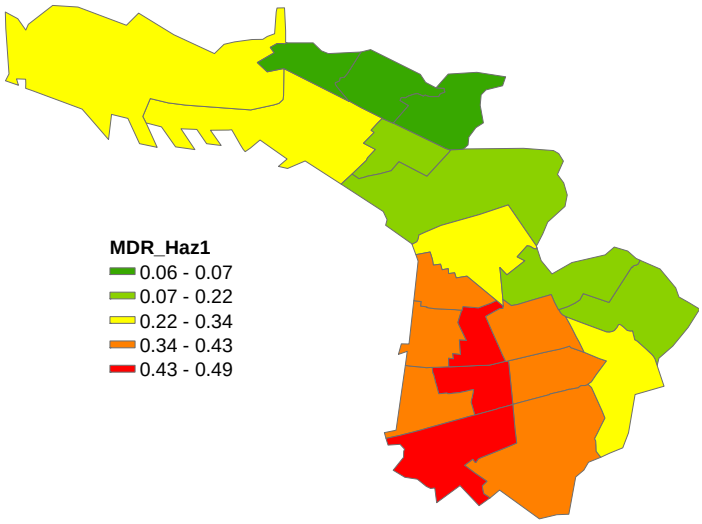

Figure 4.14: Hazard 1: Economic losses per Sub-City District in terms of Mean Damage Ratio (MDR). MDR for the whole study area is estimated as equal to 26.91%

The estimated casualties for the four levels of injury of HAZUS-MH (FEMA, 2003) described in detail in Table *2.1* were calculated using Equation 2.1 and the casualty rates of Table *2.2*. Level 1- Level 4 casualties for hazard scenario 1 (Hazard 1) are given as percentages of the population of each district in Figure 4.15. The total casualties for the whole study area are given in Table 4.7.

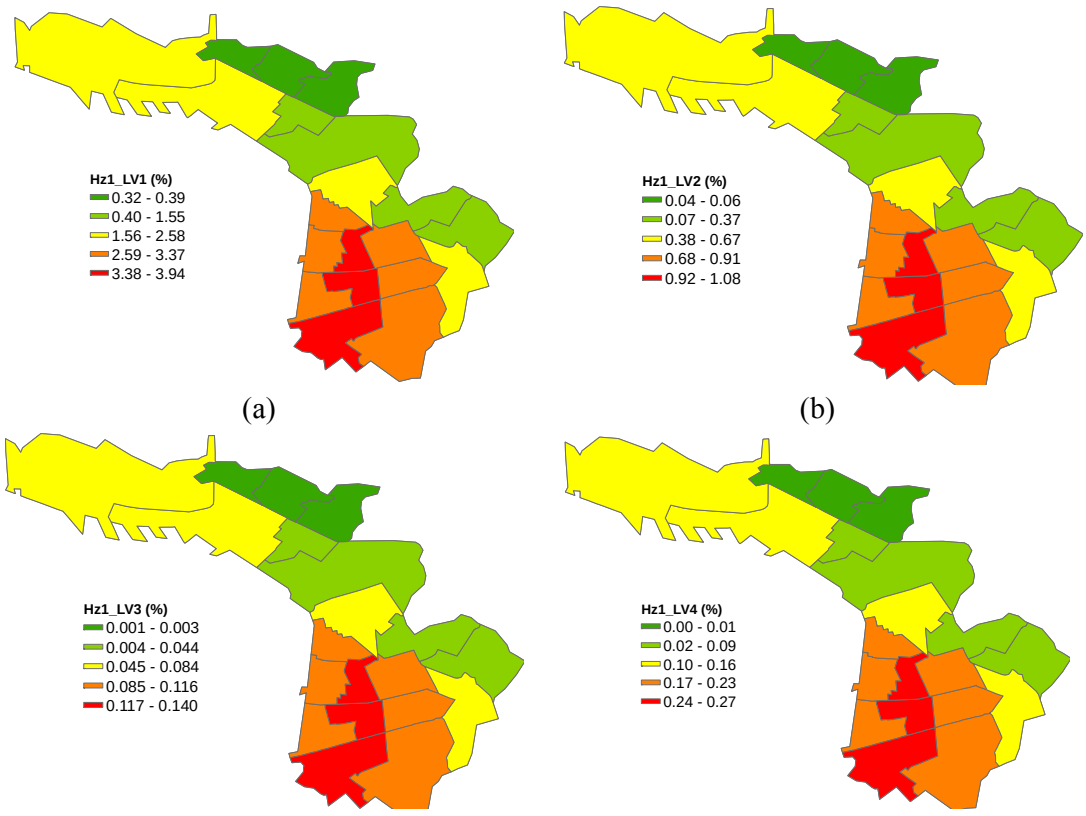

(c) (d)

Figure 4.15: Hazard 1: Percentages of casualties (a) level 1 (b) level 2 (c) level 3 (d) level 4.

Table 4.7: Estimated Level 1 - Level 4 casualties for the current hazard scenario (Hazard 1), for a return period of 475 years

	Hazard 1
Level 1	8683
Level 2	2245
Level 3	280
Level 4	549

SHARE seismic hazard

The percentages of the damaged floor area per damage state for each sub-city district are illustrated in Figure 4.16, Figure 4.17 and Figure 4.18 for Hazard scenarios 4, 5 and 6 respectively. The total percentages of damaged buildings per damage state for the whole study area are given in Table 4.8.

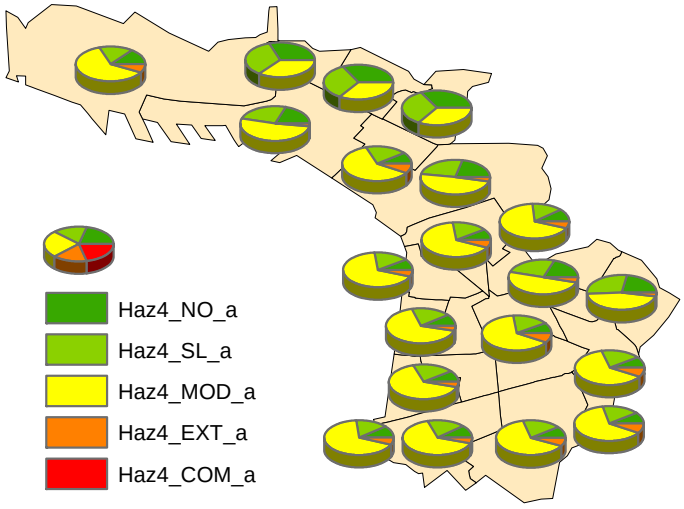

Figure 4.16: Hazard 4: Seismic risk per Sub-City District for a return period of 475 years in terms of the percentage of floor area for no damaged buildings, slight damaged buildings, moderate damaged buildings, extensive damaged buildings and complete damaged buildings.

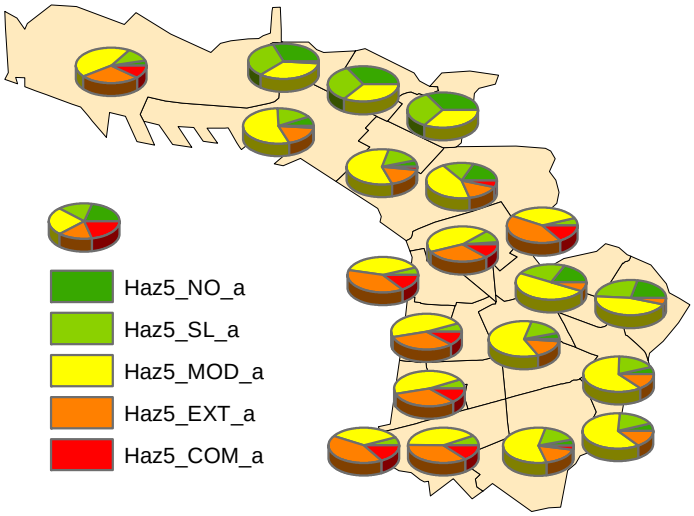

Figure 4.17: Hazard 5: Seismic risk per Sub-City District for a return period of 475 years in terms of the percentage of floor area for no damaged buildings, slight damaged buildings, moderate damaged buildings, extensive damaged buildings and complete damaged buildings.

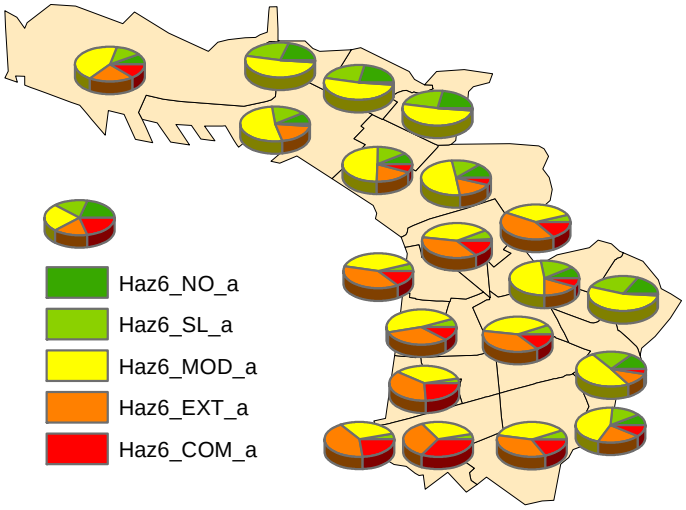

Figure 4.18: Hazard 6: Seismic risk per Sub-City District for a return period of 475 years in terms of the percentage of floor area for no damaged buildings, slight damaged buildings, moderate damaged buildings, extensive damaged buildings and complete damaged buildings.

Table 4.8: Percentages of damaged buildings per damage state for the SHARE hazard scenarios, for a return period of 475 years.

	Hazard 4	Hazard 5	Hazard 6
Slight	23.88%	17.34%	15.31%
Moderate	56.54%	47.81%	45.03%
Extensive	4.17%	18.94%	21.76%
Complete	0.06%	4.64%	9.34%
No	15.36%	11.28%	8.56%

Inserting the percentages [D1], [D2], [D3] and [D5] into Equation 4.1, the mean damage ratio (MDR) for each scenario is calculated (Figure 4.19, Figure 4.20, Figure 4.21). The total MDR values for the whole study area are given in Table 4.9.

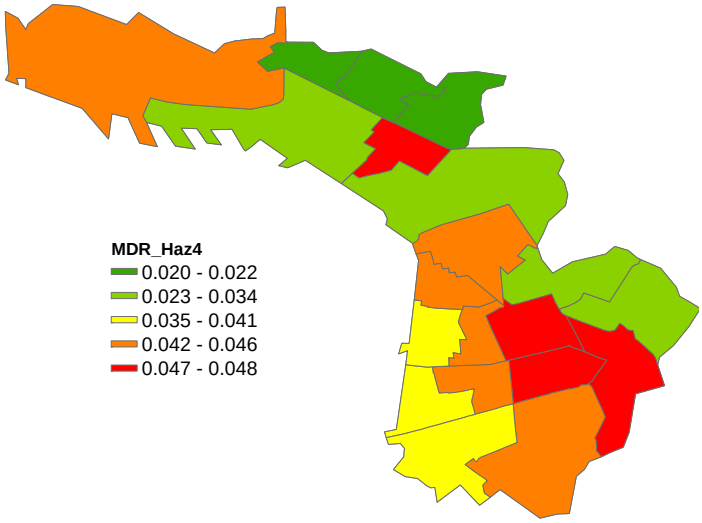

Figure 4.19: Hazard 4: Economic losses per Sub-City District in terms of Mean Damage Ratio (MDR).

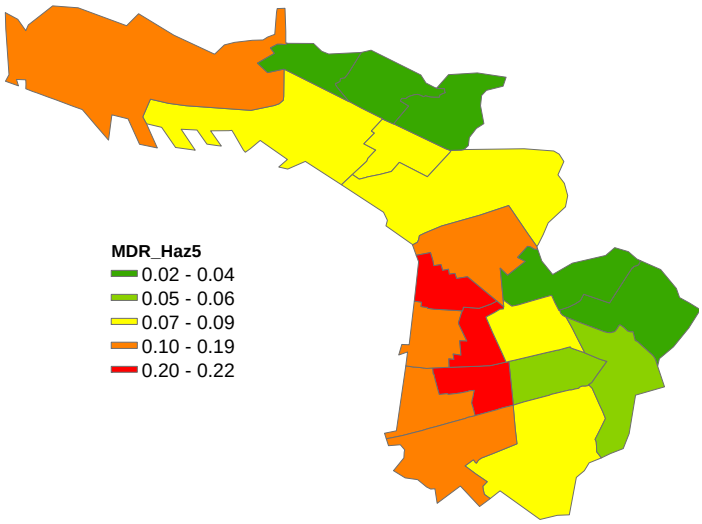

Figure 4.20: Hazard 5: Economic losses per Sub-City District in terms of Mean Damage Ratio (MDR).

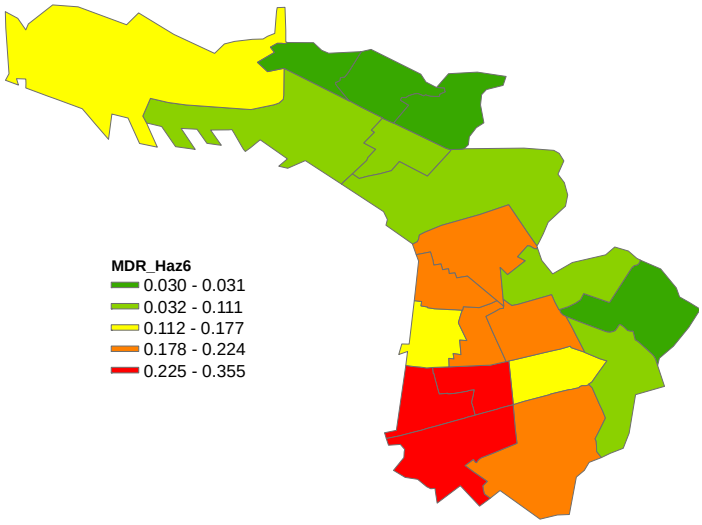

Figure 4.21: Hazard 6: Economic losses per Sub-City District in terms of Mean Damage Ratio (MDR).

Table 4.9: Mean Damage Ratios for the SHARE hazard scenarios (4-6), for a return period of 475 years

	Hazard 4	Hazard 5	Hazard 6
MDR	3.83%	9.98%	14.15%

By multiplying the mean damage ratio with the replacement cost, the economic losses can be evaluated. Assuming an average replacement cost equal to 1000€/m^2, economic losses for hazard scenarios 4-6 are given in Table 4.10.

Table 4.10: Economic losses for the SHARE hazard scenarios (4-6), for a return period of 475 years, assuming an average replacement cost equal to 1000€/m^2

	Hazard 4	Hazard 5	Hazard 6
Economic losses (€)	1.3 billions €	3.4 billions €	4.8 billions €

The estimated casualties for hazard scenarios 4-6 are given as percentages of the population of each district in Figure 4.22 -Figure **4.24**. The total casualties for the whole study area are given in Table 4.11.

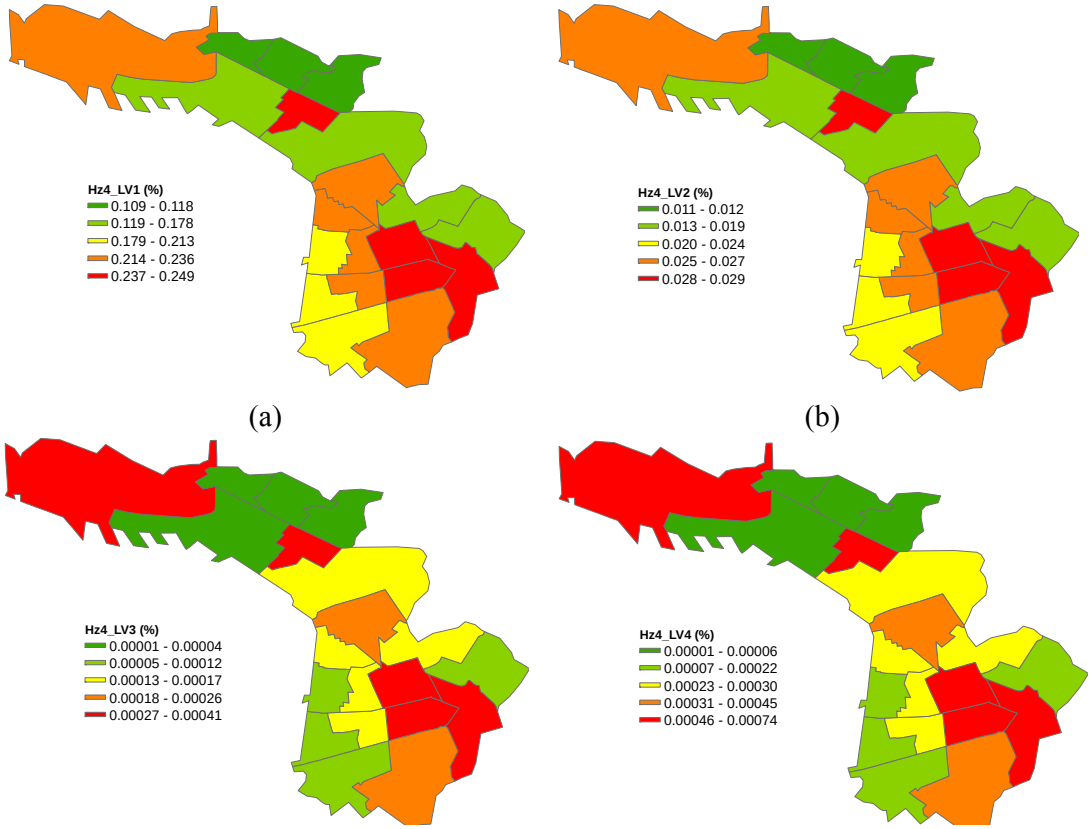

Figure 4.22: Hazard 4: Percentages of casualties (a) level 1 (b) level 2 (c) level 3 (d) level 4.

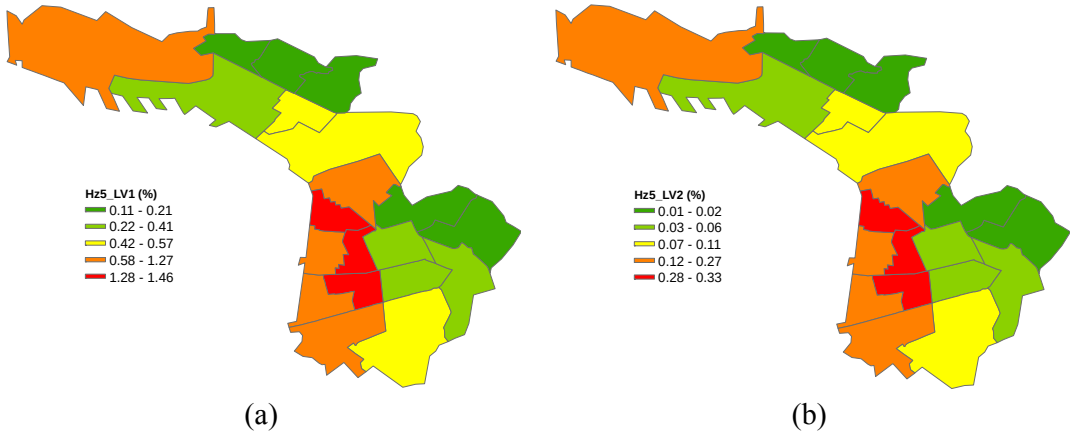

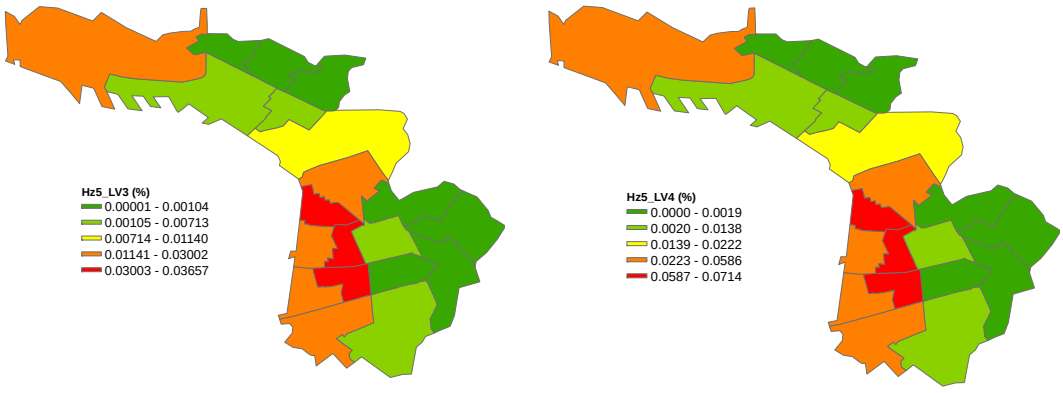

(c) (d)

Figure 4.23: Hazard 5: Percentages of casualties (a) level 1 (b) level 2 (c) level 3 (d) level 4.

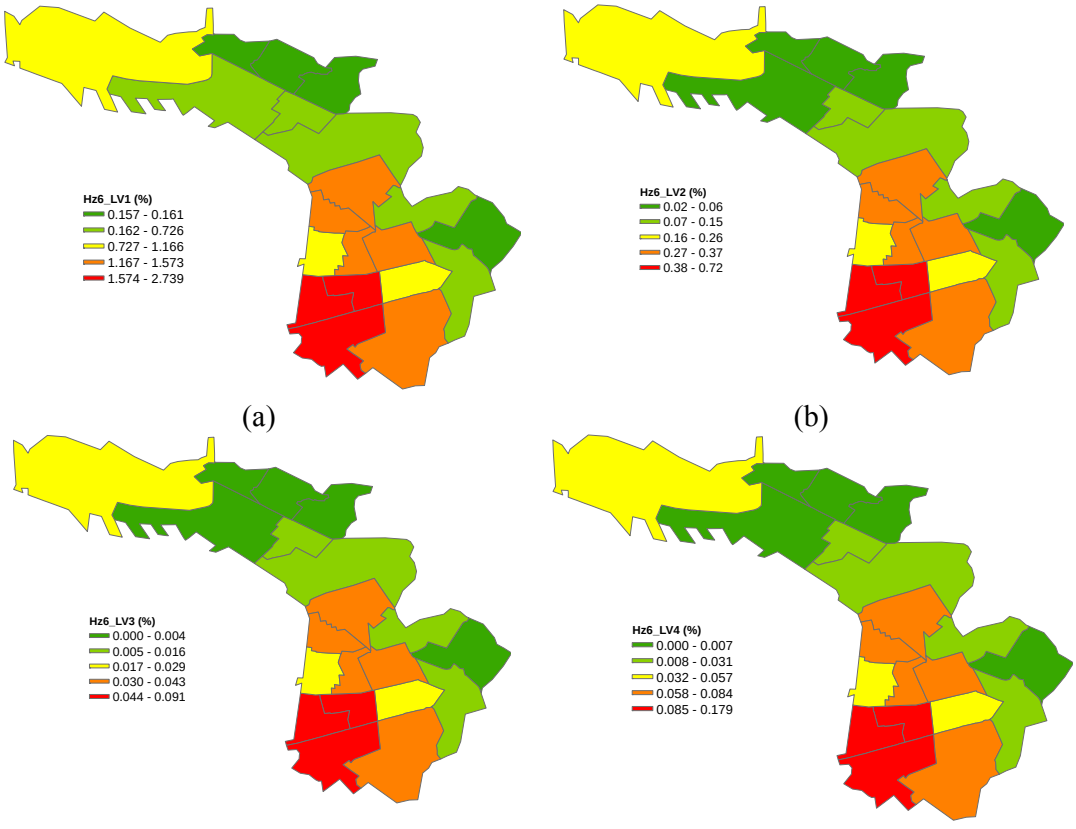

(a) (b)

(c) (d)

Figure 4.24: Hazard 6: Percentages of casualties (a) level 1 (b) level 2 (c) level 3 (d) level 4.

Table 4.11: Estimated Level 1 - Level 4 casualties for the SHARE hazard scenarios (4-6), for a return period of 475 years.

	Hazard 4	Hazard 5	Hazard 6
Level 1	762	2619	4094

Level 2	85	520	932
Level 3	1	52	106
Level 4	1	102	208

The damages presented in the previous paragraph were estimated with Capacity Spectrum Method. The application of this method comprises different steps, and, as a result, encompasses many uncertainties, which originate from different sources. The most crucial sources of uncertainties in the estimation of the expected damages are the following:

- Reduction factors used to reduce the elastic response spectrum to account for the hysteretic damping associated with the inelastic behaviour of structures. In the present application, the damping-based spectral reduction factors by Newmark and Hall (1982) were used, which in the range of 0.1-0.3 damping ratio are higher than the reduction factors resulting from the other methods, and as a result lead to higher displacements (Casarotti et al. 2009);
- Consideration of short, moderate or long earthquake duration. Earthquake duration affects the k factor, which is the factor that defines the effective amount of hysteretic damping. The shorter the duration, the higher the damping value will be. In the present application, earthquake duration was considered as moderate according to HAZUS methodology;
- Capacity curves. The selection of capacity curves highly influences the results. For example, in Figure 4.25 we illustrate the capacity curves of the most frequently present typologies in Thessaloniki, along with the elastic and a representative reduced demand spectrum for Hazard 1 - Soil Class B. We observe that the performance points are close to the ultimate structural displacement capacity, which justifies why the risk analysis leads to many heavy damages for Hazard 1. Higher values of yield acceleration would lead to smaller displacement values at the performance points;
- Demand spectra. The estimated damages are strongly dependent on the demand spectrum. Figure 4.26 illustrates an example of how the performance points for a specific building type differentiate for Hazard 1 and Hazard 4. Such discrepancies in the performance points result to large discrepancies in the estimation of expected damages;
- Fragility curves. The estimated damages are finally strongly influenced by the selected fragility curves. For example, the fragility curves for RC4.2ML (Figure 4.12a) result to be much more severe damages compared to RC4.2MM (Figure 4.12b) for the same level of displacement.

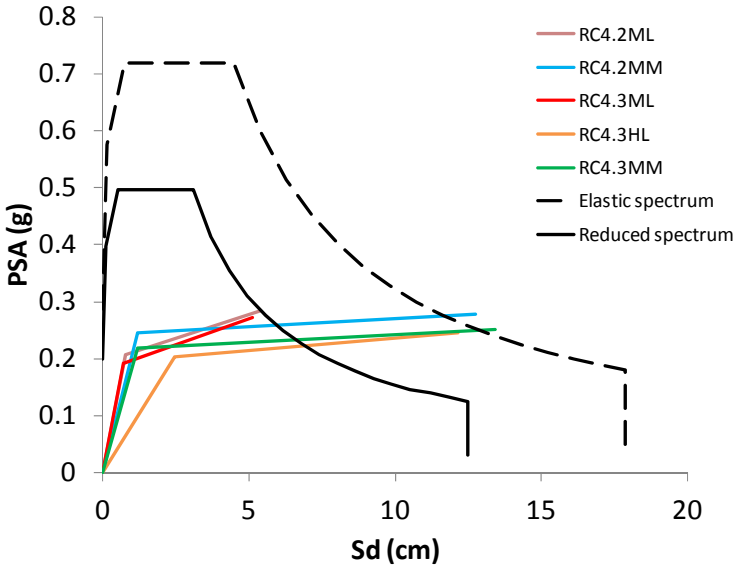

Figure 4.25: Capacity curves for the most frequent RC buildings typologies in Thessaloniki and Hazard 1 elastic and reduced demand spectra.

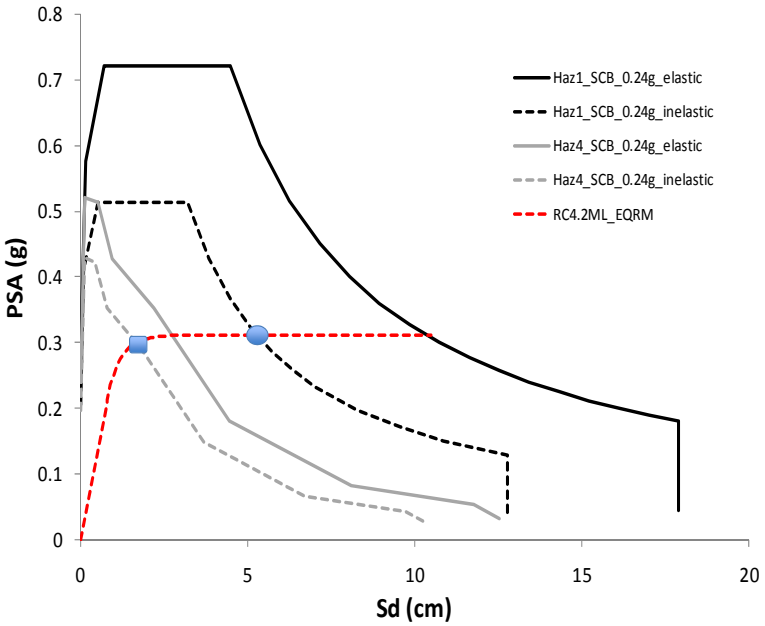

Figure 4.26: Performance points for RC4.2ML building typology located on soil class B, for Hazard 1 (current hazard) and Hazard 4 (SHARE hazard).

In the following the comparison between the results obtained with the current hazard and the SHARE hazard are described and discussed.

Current versus SHARE hazard

Given that the main objective of this deliverable is the comparison between the impact of the SHARE hazard on the seismic risk, comparative maps between Hazard 1 and Hazard 4 have been developed and are shown in Figure 3.9 -Figure 4.29. It is reminded that these two hazard scenarios are equivalent in terms of incorporation of local site conditions (i.e. current EC8 soil

factors). Comparisons are given as differences between the results of the SHARE and current hazard model, i.e. Hazard 4 versus Hazard 1. The percentages of damages, economic and social losses for the whole study area for the 2 hazard models are summarized in Table 4.12-Table 4.15.

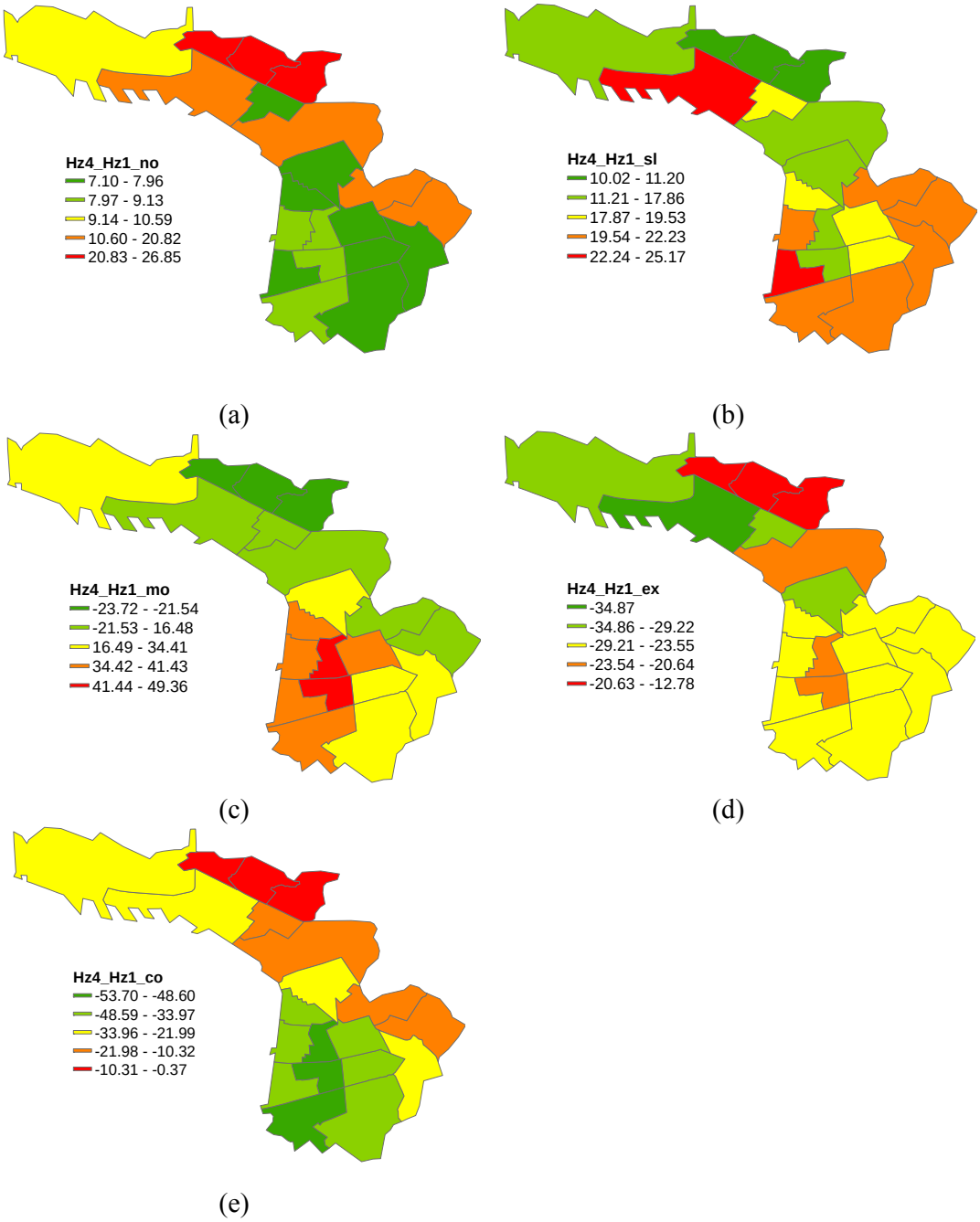

Figure 4.27: Comparative maps. Hazard 4 versus Hazard 1: Conditional seismic risk for a return period of 475 years in terms of (Hazard4-Hazard1) percentages of (a) no damaged floor area (b) slight damaged floor area (c) moderate damaged floor area (d) extensive damaged floor area and (e) complete damaged floor area.

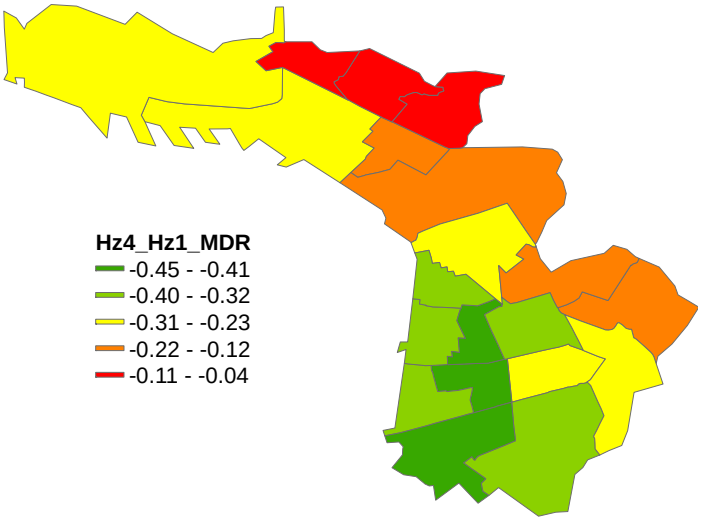

Figure 4.28: Comparative map. Hazard 4 versus Hazard 1: Economic losses per Sub-City District in terms of (Hazard4-Hazard1) Mean Damage Ratio (MDR).

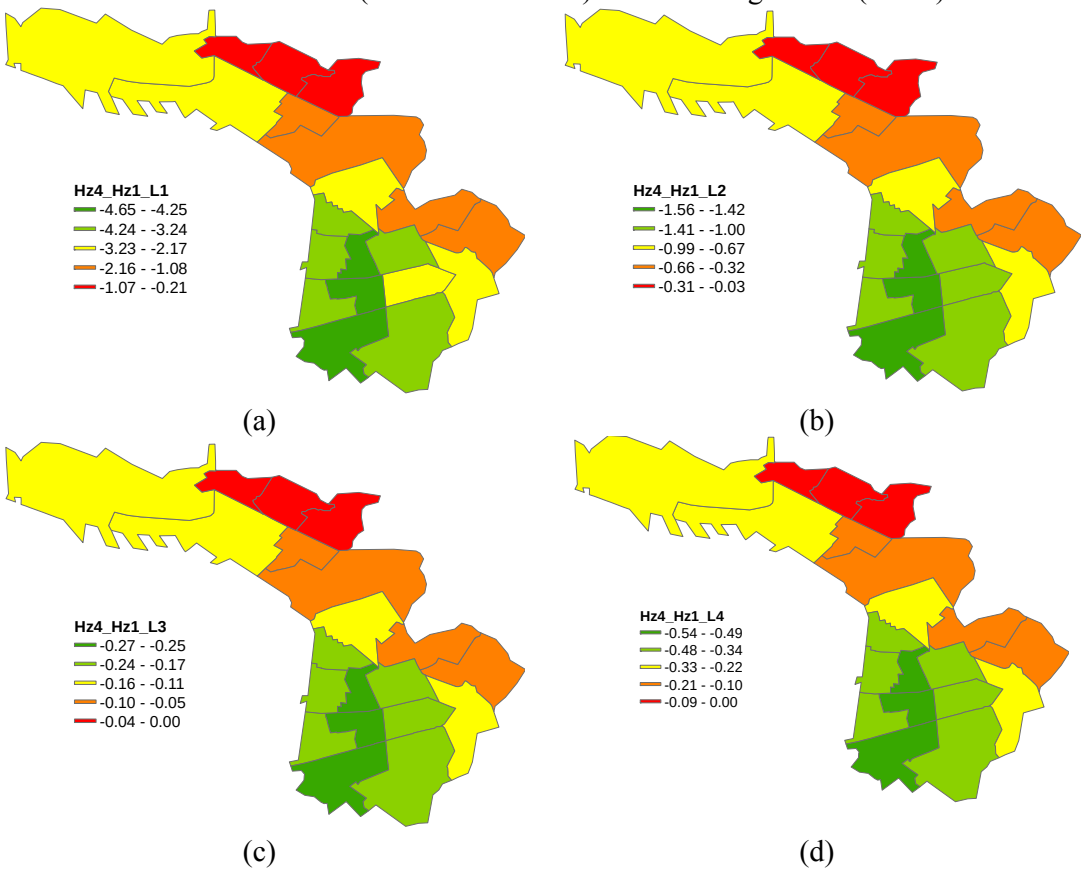

Figure 4.29: Comparative maps. Hazard 4 versus Hazard 1: (Hazard4-Hazard1) percentages of casualties (a) level 1 (b) level 2 (c) level 3 (d) level 4.

Table 4.12: Percentages of damaged buildings per damage state for the current (blue) and the SHARE (red) hazard scenarios, for a return period of 475 years.

	Hazard 1	Hazard 4
Slight [D1]	6.22%	23.88%

Moderate [D2]	39.54%	56.54%
Extensive [D3]	28.28%	4.17%
Complete [D5]	24.05%	0.06%
No	1.91%	15.36%

Table 4.13: Mean Damage Ratios for the current (blue) and the SHARE (red) hazard scenarios, for a return period of 475 years.

	Hazard 1	Hazard 4
MDR	26.91%	3.83%

Table 4.14: Economic losses (in billions €) for the current (blue) and the SHARE (red) hazard scenarios, for a return period of 475 years.

	Hazard 1	Hazard 4
Economic losses (billions €)	9.2	1.3

Table 4.15: Estimated Level 1 - Level 4 casualties for the current (blue) and the SHARE (red) hazard scenarios, for a return period of 475 years.

	Hazard 1	Hazard 4
Level 1	8683	762
Level 2	2245	85
Level 3	280	1
Level 4	549	1

Regarding the impact of the SHARE hazard on seismic risk assessment for Thessaloniki, we observe that the SHARE hazard model (Hazard 4) gives significantly less conservative results in terms of expected damages, economic and human losses, compared to the current hazard model (Hazard 1). This is primarily attributed to the discrepancies between the current and SHARE hazard: SHARE UHS has a much narrower plateau and much lower spectral acceleration values compared to the current hazard spectrum. This results to performance points with much lower displacement values for the SHARE hazard case (Hazard 4), compared to the current hazard case (Hazard 1) (see Figure 4.26).

On the contrary, estimating damages with PGA-based fragility curves (Kappos and Panagopoulos 2010) leads to less significant discrepancies between current and SHARE hazard (see Table 4.16 Table 4.19). This is expected, since the SHARE hazard model is practically the same with the current hazard in terms of PGA for the half of the study area, and differs from the current hazard about 17% for the rest of the study area.

Table 4.16: Percentages of damaged buildings per damage state for the current (blue) and the SHARE (red) hazard scenarios for a return period of 475 years, estimated with PGA-based and Sd-based fragility curves.

	Hazard 1-PGA	Hazard 4-PGA	Hazard 1-Sd	Hazard 4-Sd
Slight	41.05%	45.62%	6.22%	23.88%
Moderate	31.85%	30.88%	39.54%	56.54%
Extensive	24.27%	20.41%	28.28%	4.17%
Complete	0.77%	0.50%	24.05%	0.06%
No	2.05%	2.59%	1.91%	15.36%

Table 4.17: Mean Damage Ratios for the current (blue) and the SHARE (red) hazard scenarios, for a return period of 475 years, estimated with PGA-based and Sd-based fragility curves.

	Hazard 1-PGA	Hazard 4-PGA	Hazard 1-Sd	Hazard 4-Sd
MDR	7.27%	6.25%	26.91%	3.83%

Table 4.18: Economic losses (in billions €) for the current (blue) and the SHARE (red) hazard scenarios, for a return period of 475 years, estimated with PGA-based and Sd-based fragility curves.

	Hazard 1-PGA	Hazard 4-PGA	Hazard 1-Sd	Hazard 4-Sd
Economic losses (billions €)	2.5	2.1	3.3	2.9

Table 4.19: Estimated Level 1 - Level 4 casualties for the current (blue) and the SHARE (red) hazard scenarios, for a return period of 475 years, estimated with PGA-based and Sd-based fragility curves.

	Hazard 1-PGA	Hazard 4-PGA	Hazard 1-Sd	Hazard 4-Sd
Level 1	1487	1272	8683	762
Level 2	184	148	2245	85
Level 3	8	6	280	1
Level 4	16	10	549	1

Comparison with actual damages from the Thessaloniki 1978 earthquake

Table 4.20 compares the estimated damages for Hazards 1, 4, 5 and 6 with the actual recorded damages in Thessaloniki from the 1978 earthquake (Penelis 2008), using the familiar Green,

Yellow, and Red tag scheme. The correspondence between tag colour and damage states was assumed as follows:

• Green: no and slight
• Yellow: moderate and extensive
• Red: complete

Table 4.20: Comparison of damages predicted from Hazard 1 and Hazard 4 with the actual damages from Thessaloniki 1978 EQ

	Hazard 1	Hazard 4	Hazard 5	Hazard 6	Thessaloniki 1978 EQ
"Green"	8 %	39.2 %	28.6%	23.9%	74.5%
"Yellow"	68 %	60.7 %	66.7%	66.8%	21.0%
"Red"	24 %	0.1 %	4.7%	9.3%	4.5%

All hazard models predict significantly fewer "green" buildings and more "yellow" buildings compared to the actual recorded damages. At this point we should emphasize that there are many uncertainties involved in the characterization of a building with one of the tag colours, and that the correspondence between the tag colours and the damage states is not always straightforward. When looking at the "red" buildings percentages, however, we observe that the estimated damages from Hazard 5, which uses the improved soil factors for Eurocode 8 (Pitilakis et al. 2012) are in very good agreement with the recorded damages.

Effect of the incorporation of improved S factors and new classification system in SHARE hazard

Regarding the incorporation of the improved S factors for EC8 or the new classification system, they increase expected damages compared to using the current EC8 S factors (see Table 4.8 - Table 4.11).

4.2. Lisbon

Lisbon is the capital city of Portugal and it is the western largest city located in the European continent. The Lisbon Metropolitan Area (MAL) is divided in 220 civil parishes [INE, 2011], which represent an administrative division smaller than the municipality level. In fact, a parish represents a fourth-order administrative limit that follow the county or municipality, the third-order administrative limit; MAL is divided in 19 counties [INE, 2011] (see Table 4.21). About 2.8 million people live in MAL administrative region and about 3.1 million people live in the broader agglomeration of the MAL (MAL and neighbouring counties), represented in Figure 4.30.

This is the Portuguese region with the highest demographic and economic concentration of elements exposed to earthquakes. Being a moderate seismic hazard region it was affected by severe historical earthquakes, like the emblematic 1755 Lisbon earthquake, with Mw = 8.5 -9.0 [Campos Costa *et al.,* 2010], justifying a recurrent assessment and monitoring of its seismic risk.

Table 4.21: Statistics for MAL [INE, 2002 and INE, 2011].

Census	Region	Counties / parishes	Buildings	Inhabitants
2001	MAL	19 / 216	397 912	2 563 486
	MAL and neighbouring counties	26 / 277	477 170	2 841 067
2011	MAL	19 / 220	460 060	2 837 627
	MAL and neighbouring counties	26 / 281	548 376	3 059 070

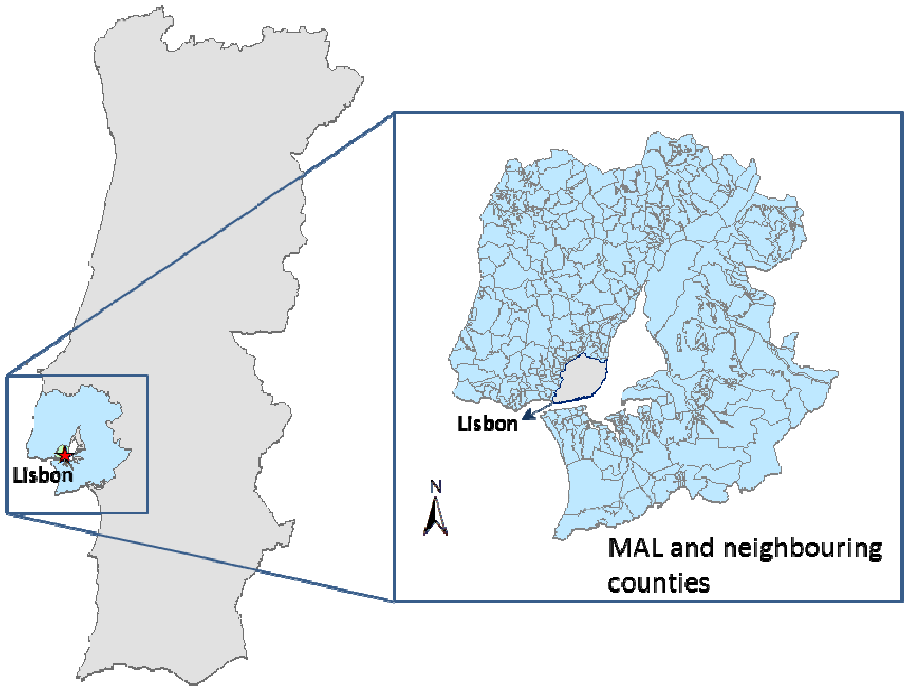

Figure 4.30: Portugal, Lisbon Metropolitan Area and some neighbouring counties (MAL) and Lisbon municipality.

In MAL, loss estimations were obtained using LNECloss that is a computer tool which evaluates losses as a consequence of a user defined ground motion seismic scenario. LNECloss was developed and updated in previous projects [LESSLOSS, 2007]. This automatic tool comprises several modules that model seismic action at the bedrock and considering the influence of soil conditions, simulate earthquake damage to buildings and estimate social and economic losses. The simulation software uses a scientific programming language and was incorporated, as an external application, in a Geographic Information System.

4.2.1. Seismic hazard assessment

The seismic risk will be carried out using two different types of hazard: (i) the seismic hazard present in the Portuguese National Annex of Eurocode 8, simply referred to, in this report, as NA of EC8, and (ii) the new hazard model developed in SHARE. In what follows, a description of the seismic hazard that will be used for the reference situation, the NA of EC8, is provided.

Current seismic hazard map

The Structural Eurocode programme comprises 10 standards. The focus of SHARE project is the EN 1998-1:2004, *Eurocode 8: Design of structures for earthquake resistance - Part 1: General Rules, seismic action and rules for buildings*, herein also referred as EC8 [EN 1998-1: 2004].

The EN 1998-1:2004 comprises 56 left open parameters, the Nationally Determined Parameters (NDPs) to be chosen by each country. Key information regarding the NPDs concerning the present study comprises the seismic zonation map, the values of peak ground acceleration (PGA) and the corner periods that define the basic seismic actions to be considered in structural design. Seismic zonation should be established for a reference PGA on type A ground (rock or other rock-like geological formation, including at most 5 m of weaker material at the surface), ag_R, correspondent to a reference return period, T_{NCR}, of seismic action for the no-collapse requirement, recommended as 475 years.

ENs are translated to each country language and are complemented by National Annexes (NA), providing values for the Nationally Determined Parameters (NDPs). The Portuguese version of EN 1998-1:2004 is the NP EN 1998-1: 2010 [IPQ, 2010], *Norma Portuguesa. Eurocódigo 8 – Projecto de estruturas para resistência aos sismos. Parte 1: Regras gerais, acções sísmicas e regras para edifícios*. Although it was published in 2010, this standard is not yet mandatory in Portugal, while it is expected that, briefly, there is a transition period wherein two codes coexist: (i) the Portuguese code that is presently in force, called RSA[1], [INCM, 1983] and (ii) the NP EN 1998-1: 2010 [IPQ, 2010]; after that period, the NP EN 1998-1:2010 will be the official code for seismic design of structures.

As in RSA [INCM 1983], the NP EN 1998-1:2010 considers two scenarios for the seismic zonation of mainland Portugal: (i) a scenario labelled seismic action Type 1, characterizing earthquakes with epicentres mainly offshore and (ii) a scenario labelled seismic action Type 2, referring to events with epicentres mainly inland and in the Azores Archipelago.

Figure *4.31* illustrates seismic zonation for the Portuguese National Annex of EC8, in what concerns Mainland Portugal. Table 4.22 presents the reference peak ground acceleration, ag_R for the considered seismic zones and for the two scenarios. These are the hazard scenarios, corresponding to the reference situation, called NA of EC8 hazard that is going to be compared with hazard results of SHARE.

[1] RSA, *Regulamento de segurança e acções para estruturas de edifícios e pontes.*

It should be noticed that zones 2.1 and 2.2 are not illustrated in Figure 4.31, because they just refer to the Azores archipelago.

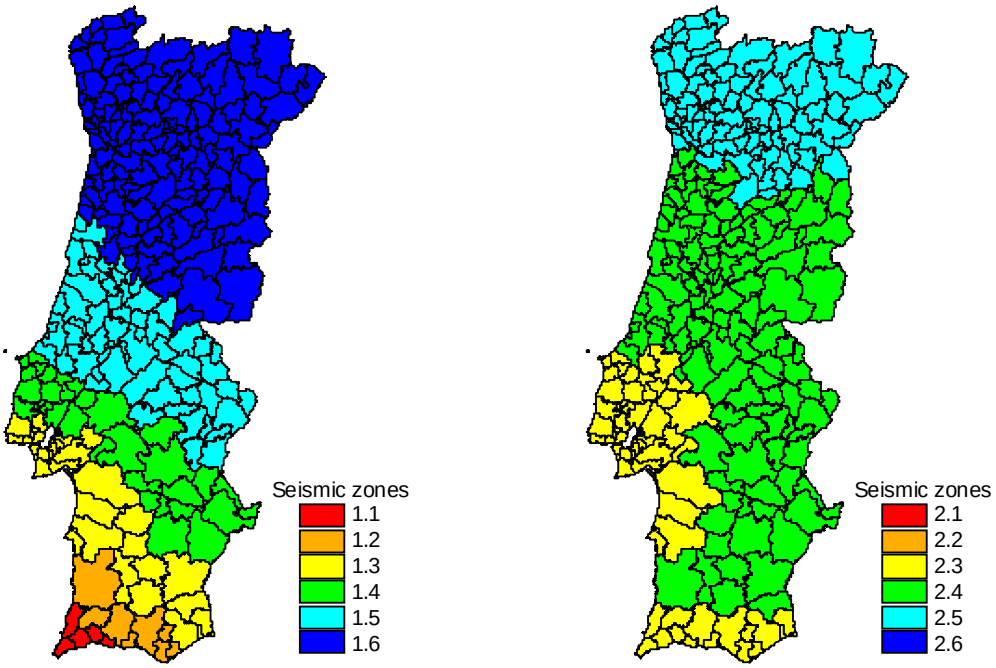

Figure 4.31: Mainland Portuguese seismic zonation (a) seismic action Type 1 (b) seismic action Type 2 [NP EN 1998-1: 2010].

Table 4.22: Reference peak ground acceleration [NP EN 1998-1: 2010].

Seismic action Type 1		Seismic action Type 2	
Seismic Zone	a_{gR} (m/s^2)	Seismic Zone	a_{gR} (m/s^2)
1.1	2.5	2.1	2.5
1.2	2.0	2.2	2.0
1.3	1.5	2.3	1.7
1.4	1.0	2.4	1.1
1.5	0.6	2.5	0.8
1.6	0.35	-	-

Within the scope of EN 1998 the earthquake motion at a given point on the surface is represented by an elastic ground acceleration response spectrum, the "elastic response spectrum", represented in Figure *4.32*.

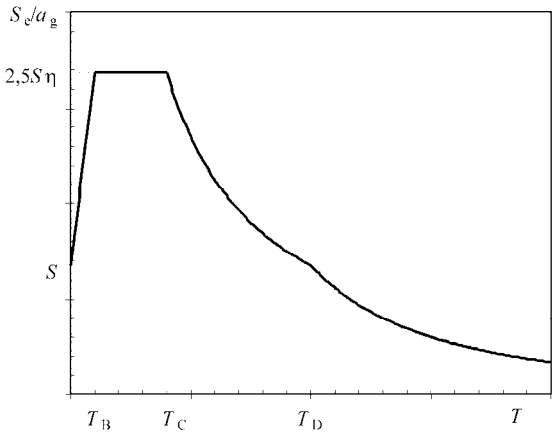

Figure 4.32: Shape of elastic response spectrum [EN 1998-1: 2004].

Table *4.23* presents the values of parameters describing the spectrum, for Portugal, considering soil type A.

Table 4.23: Values of the parameters describing Type 1 and Type 2 elastic response spectra for Portugal; soil type A [NP EN 1998-1: 2010].

Action	S_{max}	T_B (s)	T_C (s)	T_D (s)
Type 1	1.0	0.1	0.60	2.0
Type 2	1.0	0.1	0.25	2.0

Figure *4.33* shows the spectra shape (seismic actions Type 1 and Type 2) for Lisbon, that is located in seismic zones 1.3 and 2.3, as they are defined in the NA of EC8, and considering a soil type A.

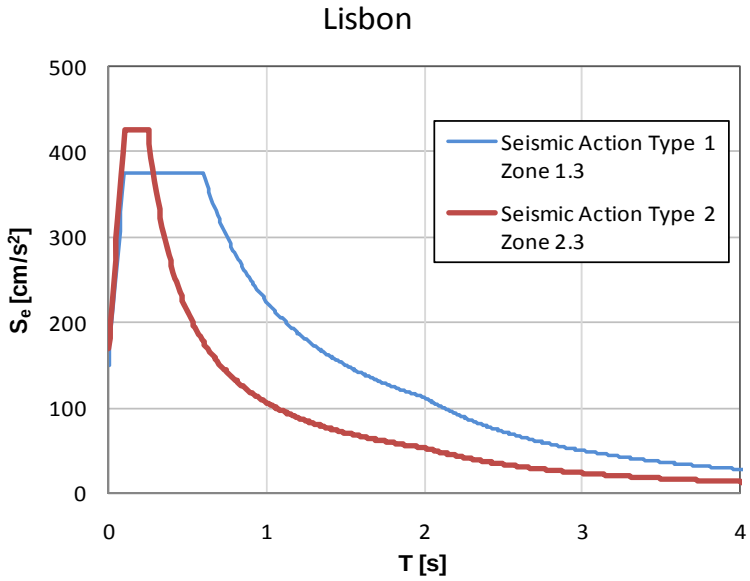

Figure 4.33: Elastic response spectra for Lisbon.

In the framework of a project conducted by the National Civil Protection Authority, in 2002 [Carvalho *et al.*, 2002] it was carried out a geological - geotechnical inquiry to characterize the soil columns for each parish of MAL (37 soil columns units as shown in Figure *4.34*). In this figure, soil unit A also refers to rock or other rock-like geological formation.

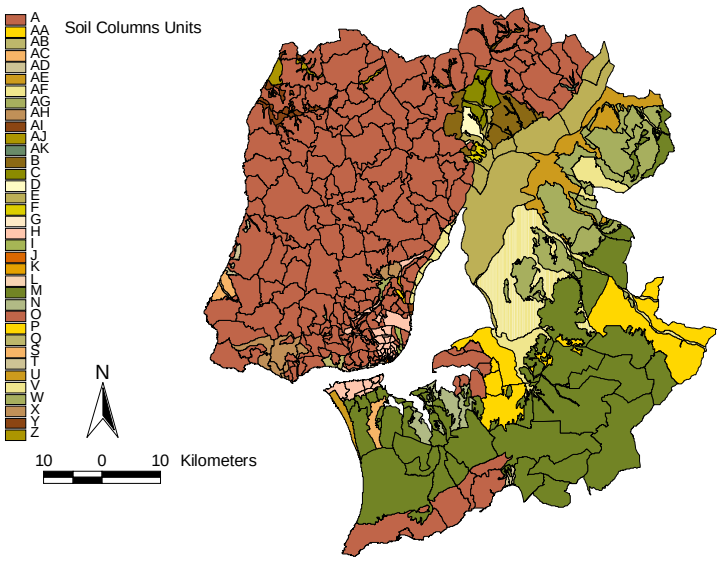

Figure 4.34: Soil types for each parish of MAL [Carvalho et al., 2002].

The computer algorithms developed and implemented in LNECloss introduced some major improvements to take into account site effects due to soil dynamic amplification in a rather efficient way. The elastic response spectrum for each parish is transformed into a Power Spectrum Density Function at the bedrock, using the classical theory of stationary random process. In this case, the elastic response spectrum in the bedrock is the same for all parishes, as we are using the spectra defined in the NA of EC8 for zones 1.3 and 2.3, shown in Figure *4.33*. Site effects are evaluated by means of an equivalent stochastic nonlinear one-dimensional ground response analysis for each stratified soil profile units designed for the region. Each soil unit is characterized by the thickness of their shallow layers, shear waves velocity, density and plastic index. This equivalent stochastic nonlinear one-dimensional ground response analysis will be the procedure applied to evaluate seismic action at surface using both NA of EC8 and SHARE seismic hazard results.

Figure *4.35* and Figure *4.36* illustrate the elastic response spectrum for one parish of the Metropolitan Area of Lisbon (Sesimbra parish) at bedrock and at surface.

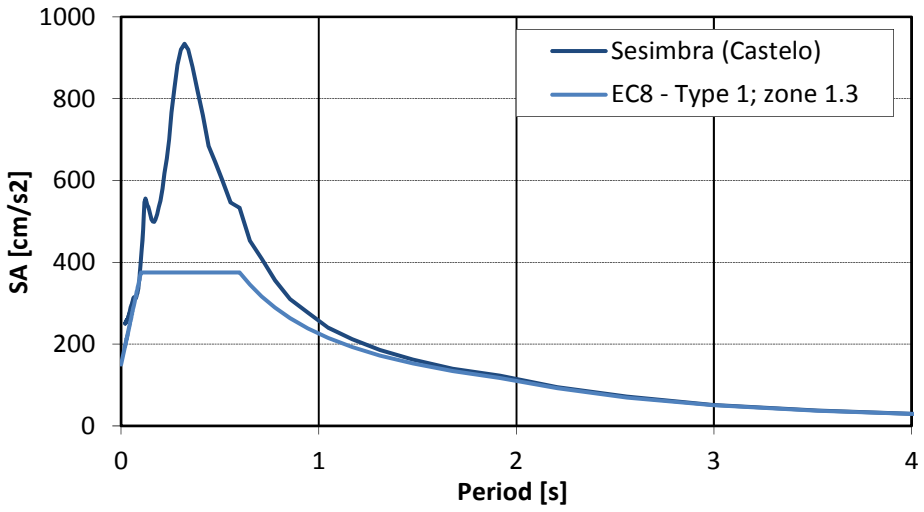

Figure 4.35: Elastic response spectra for Sesimbra, at bedrock and considering soil effects; seismic action Type 1.

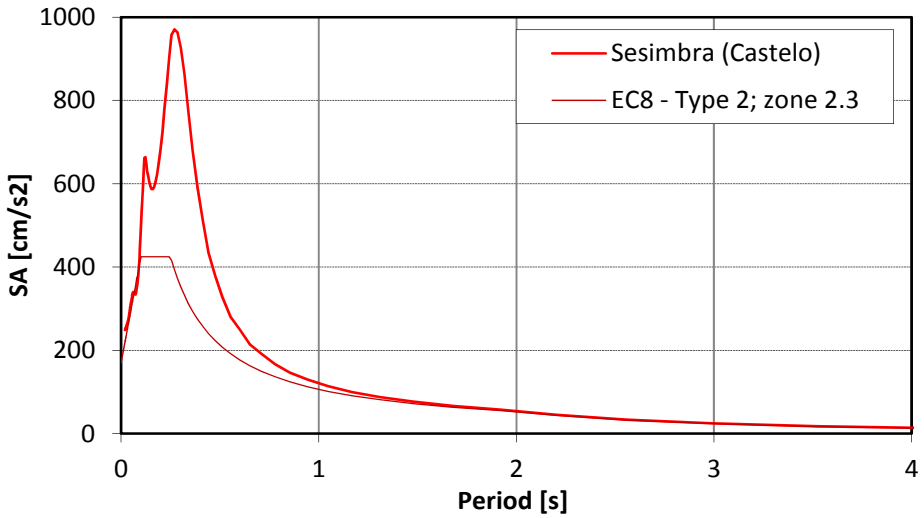

Figure 4.36: Elastic response spectra for Sesimbra, at bedrock and considering soil effects; seismic action Type 2.

Notice that we are considering in MAL a constant value of PGA of 150 cm/s^2 for seismic action Type 1 and of 170 cm/s^2 for seismic action Type 2, as presented in Table *4.22*.
The maps of PGA values at surface (shown in Figure *4.38* top), evidences a reduction of PGA values in some classes of soils and amplification of PGA in others, *e.g.* located south of the Tagus river. In parishes where soil type A (rock) prevails, mainly located to the north and west of Lisbon, there is no evidence of change in PGA values. This variation in PGA is clear for strong ground motions, but not so obvious for weak ground motions, as already was reported in previously studies [Carvalho *et al*., 2008; LESSLOSS, 2007; Zonno et al., 2008], being an indication of nonlinear soil response during earthquakes.

Seismic hazard comparison

Figure *4.37* shows the comparison between the hazard models proposed in SHARE and the design spectra presented in the Portuguese National Annexe of EC8 for Lisbon seismic zone and soil type A.

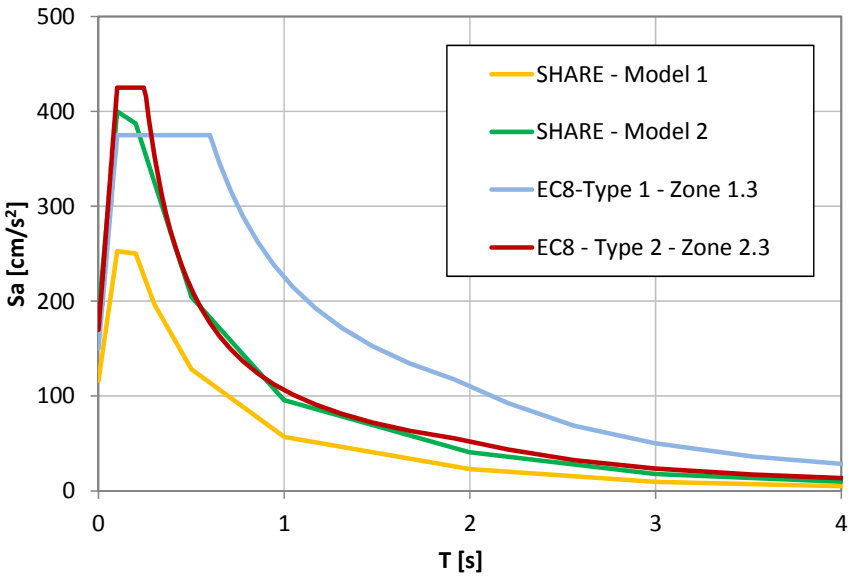

Figure 4.37: *Comparison of NA of EC8 elastic response spectra and SHARE models for Lisbon.*

Figure *4.37* shows that, in Lisbon, the hazard of Model 2 of SHARE is similar to the seismic action Type 2 (inland earthquakes) of the National Annex of EC8, whereas seismic action type 1 of NA of EC8 scenario shows spectral ordinates considerably higher than those of the other spectra, being the dominant spectrum for periods higher than 0.28 s.

This comparison indicates that the seismic action for Lisbon, provided by the Portuguese National Annex of EN 1998-1, exceeds the output specifications of SHARE. It is worthwhile mentioning that the specifications of SHARE correspond to uniform hazard spectra, resulting from seismic hazard studies, whereas the elastic response spectra provided by the National Annex, for each seismic zone, reflect several options adopted in (i) the underlying hazard studies, (ii) the seismic zonation, (iii) expert opinion on structural behaviour and (iv) in some other requirements of EC8. Furthermore, the two hazard models of SHARE are not directly comparable with EC8 elastic spectra, because the former correspond to two different ways to consider the activity rate, whereas the latter does not address global seismic hazard, but two hazard scenario resulting, independently, from the seismicity mainly located offshore, labelled seismic action Type 1, and from the seismicity mainly located inland, labelled seismic action Type 2.

Figure *4.38* presents the comparison of the NA of EC8 seismic hazard maps and SHARE seismic hazard maps, for MAL and for a 475 return period, in terms of PGA at the surface, *i.e.*, considering the influence of soil conditions.

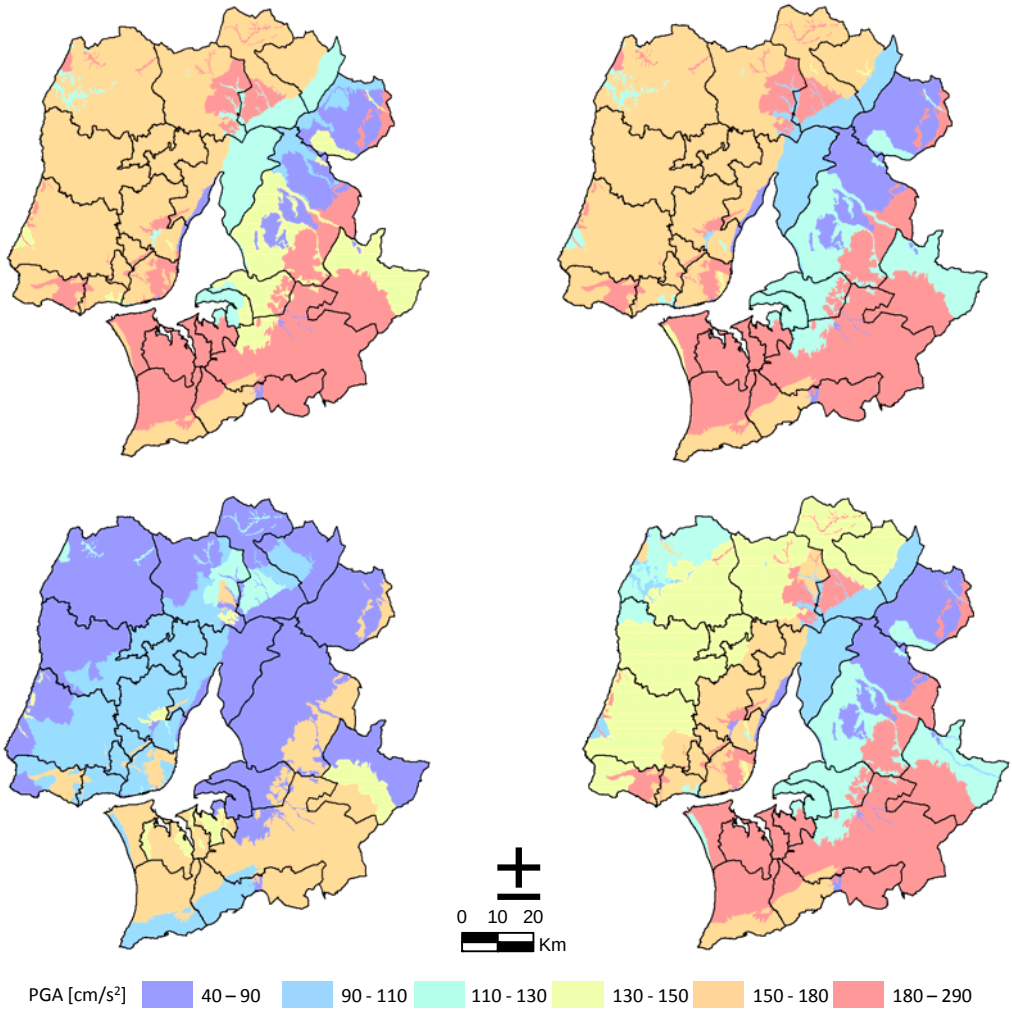

Figure 4.38: Peak ground acceleration at surface for MAL and a return period of 475 years. Top: NP EN 1998-1; left: seismic action Type 1; right: seismic action Type 2. Down: SHARE; left: Model 1; right: Model 2.

Figure *4.39* presents a similar comparison in terms of ordinates for 0.3s spectral period (Sa(0,3s)). This period was chosen because the housing stock in Portugal is mostly low rise (Table *4.26*) and, in some soils, the greatest spectral amplifications were verified around this period (Figure *4.35* and Figure *4.36*).

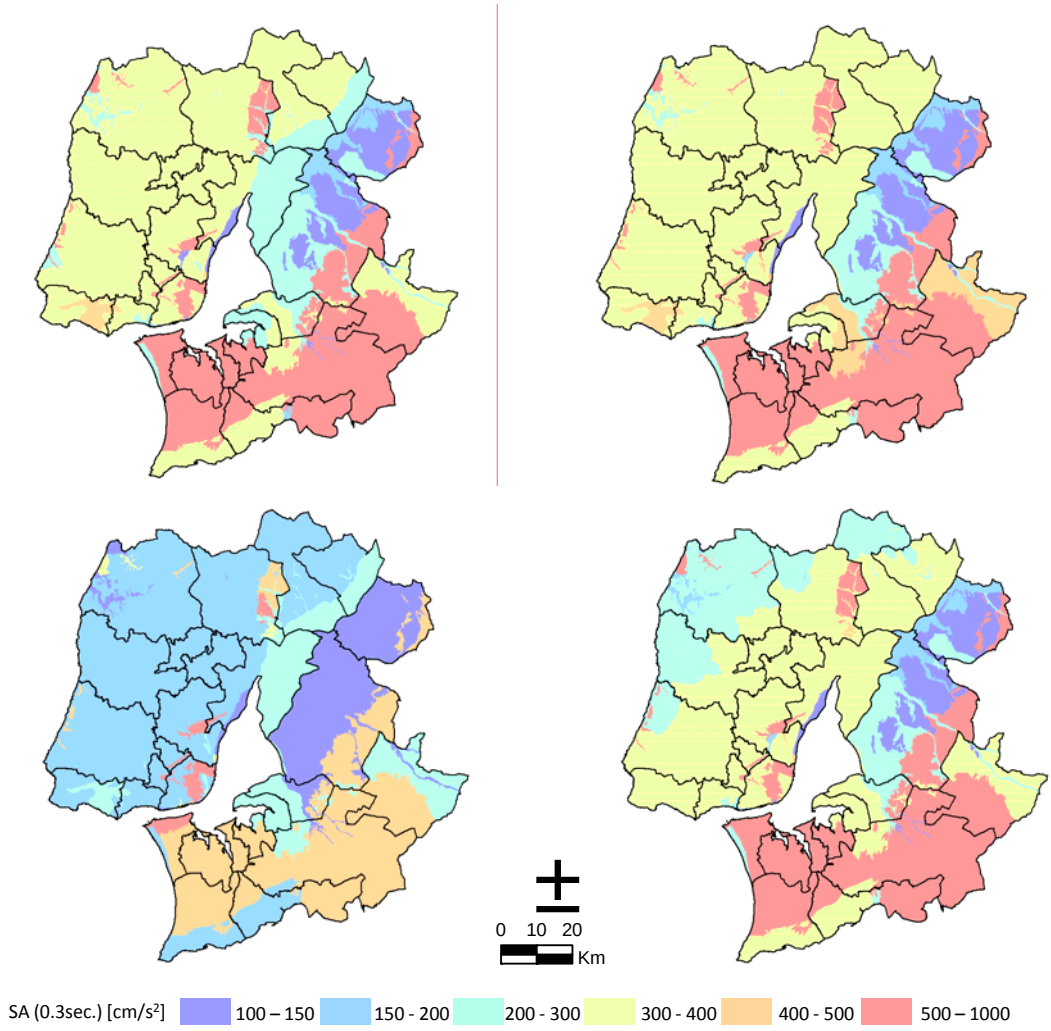

Figure 4.39: Sa(0,3s) ordinates for MAL and a return period of 475 years. Top: NP EN 1998-1. left: seismic action Type 1; right: seismic action Type 2. Down: SHARE; left: Model 1; right: Model 2.

As it was expected from the previous observation of Figure *4.37*, the SHARE model 1 presents lower values of PGA and of spectral acceleration for all municipalities in MAL. Furthermore, soil amplification leads to higher values of PGA and of spectral acceleration in parishes located south of the Tagus River. In addition, the Type 1 scenario of NA of EC8 presents the highest hazard values at surface for most parishes of MAL.

4.2.2. Exposure

Inventory

In 2011, a new statistical survey for population and residential building was conducted in Portugal [INE, 2011]. Despite the fact that, in December 2011, some provisional results are available, only some variables were accessible on that date. Final results were published at the end of year 2012, so it was not possible to obtain, timely, the inventory of buildings of Census 2011, with crossings of the variables relevant to characterize their seismic vulnerability.

Due to these reasons, in this report, the number of residential buildings and individuals, for each typology, or vulnerability class, has been obtained from the database of 2001 Census, whereas the plot of the geographic distribution of the total number of buildings and population will be based on Census 2011. The 2001 inventory was used in seismic risk analysis both to evaluate building damages and social losses.

As referred in Section 4.2, in 2011, about 2.8 millions of people live in MAL administrative region and about 3.1 millions of people live in the broader agglomeration of the MAL and neighbouring counties, representing an increase of 11% and of 8%, respectively, in the number of inhabitants between 2001 and 2011 (see Table 4.21). In what concerns existing buildings, in 2011, there were about 0.46 million buildings in MAL administrative region and about 0.55 million buildings in MAL and neighbouring counties, representing an increase of 16% and of 15%, respectively, in the number of buildings relatively to 2001.

Building exposure

Considering the 2001 survey, the building stock was classified in 315 different typologies crossing, simultaneously, the following variables: *date of construction*, *structural type*, and *number of floors* (9 epochs of construction per 5 structural types and per 7 classes of number of floors – see Table *4.24*) [Carvalho *et al*., 2002; Sousa, 2006; Sousa *et al.*, 2003]. Census databases were also inquired to obtain dwellings and inhabitants classified in those building typologies.

Table 4.24: Vulnerability factors identified in Census 2001 [Carvalho *et al*., 2002; Sousa *et al*., 2003].

Epoch of construction or reconstruction	Structural type	Number of floors
Before 1919	RC	1
1919 – 1945		2
1946 – 1960	Masonry with RC floors	3
1961 -1970	Masonry without RC floors	4
1971 – 1980		5 to 7
1981 – 1985	Adobe and rubble stone	8 to 15
1986 – 1990		More than 15
1991 – 1995	Others	
1996 – 2001		

Following previous research projects, [LESSLOSS, 2007], in order to simplify the analysis of results, the original 325 typologies obtained from Census 2001 were aggregated in 7 typological classes (see Table 4.25), taking into consideration two vulnerability factors referred in Table 4.24: e*poch of construction or reconstruction* and *structural type.* In order to have into consideration the building height in the seismic response of vulnerability classes, each typological class was then subdivided in 7 classes of *number of floors*, obtaining a total of 49 vulnerability classes.

Note that loss estimations were based on the original 325 typologies and the 49 classes were created with the goal of analysing the correlation of losses estimates and building classes [LESSLOSS, 2007].

This classification aims at characterizing Portuguese constructive practices, the evolution of materials and technologies along time and, simultaneously, making the connection with the available inventory. Actually, typological classes presented in Table 4.25 were chosen in order to take in account the evolution of Portuguese seismic regulation, also considering the two years transition period adopted for its application. The first Portuguese seismic code, called RSCCS[2], dates from 1958 [Imprensa Nacional, 1958], was successively updated and substituted by the RSEP in 1961 [Imprensa Nacional, 1961], and by the RSA in 1983 [INCM, 1983] [Carvalho et al., 2002]. Consequently, buildings constructed before 1960 are assumed to have no earthquake-resistant design; buildings constructed between 1961 and 1985 are assumed to be designed and constructed according RSCCS and RSEP codes and buildings constructed after 1985 are assumed to be designed and constructed according to RSA. This is, of course, an overly optimistic assumption for the constructive panorama in Portugal.

Table 4.25: Vulnerability classes for MAL building stock [LESSLOSS, 2007].

Typological classes	Number of floors
Adobe and Rubble Stone	1
Masonry before 1960	2
Masonry 1961 – 1985	3
Masonry 1986 – 2001	4
RC before 1960	From 5 to 7
RC 1961 – 1985	From 8 to 15
RC 1986 – 2001	More than 15

Table *4.26* shows the number of buildings inventoried in 2001, in MAL and neighbouring counties, distributed per vulnerability class, and building totals derived from Census 2011.

[2] RSCCS - Regulamento de Segurança das Construções Contra os Sismos.

RSEP - Regulamento de Solicitações em Edifícios e Pontes.

Table 4.26: Number of residential buildings per vulnerability class.

Number of floors	Adobe + rubble stone	Masonry ≤ 1960	Masonry 1961-85	Masonry 1986-01	RC ≤ 1960	RC 1961-85	RC 1986-01	Total 2001
1	27 277	36 826	55 426	19 084	10 707	42115	20 225	211 660
2	9 468	14 704	26 114	17 115	6 458	38 608	29 585	142 052
3	3 048	5 303	5 691	3 429	3 516	13 482	10 982	45 451
4	1 879	3 956	2 768	1 289	3 273	12 531	6 245	31 941
From 5 to 7	1 088	3 726	138	68	4 868	14 441	9 523	33 852
From 8 to 15	0	0	0	0	847	6 039	4 826	11 712
More than 15	0	0	0	0	0	278	224	502
Total 2001	42 760 (9.0 %)	64 515 (13.5 %)	90 137 (18.9 %)	40 985 (8.6 %)	29 669 (6.2 %)	127 494 (26.7 %)	81 610 (17.1 %)	477 170 (100 %)
Total 2011	548 376							

The main conclusions drawn from the presented information are the following:

- Around 50 % of the housing stock is classified in the reinforced concrete structural type;
- reinforced concrete becomes progressively more important in more recent construction epochs, since its appearance around 1935-40; the opposite has been verified in relation to the masonry structural type;
- the majority of the buildings, 44% and 30%, have 1 and 2 floors, respectively;
- in 2001, about 71% of buildings were constructed after 1961, date assumed to correspond to the start of application of seismic codes.
- There was an increase of 15% in the number of buildings in MAL and neighbouring counties in the last 10 years. If those buildings were designed and constructed according to the last code [RSA, 1983] this would be favourable to the reduction of seismic vulnerability in this region.

However, Carvalho et *al*. [2002] argue that these results should be carefully considered, since it is not possible to assure that all buildings constructed after 1958 follow seismic design requirements, especially with resisting elements different from reinforced concrete. Moreover, those authors also highlight that other aspects should be accounted for, such as building maintenance and construction supervision.

Figure 4.40 presents the geographical distribution of buildings belonging to different vulnerability classes. Percentage of buildings per parish is shown in that Figure. Building totals presented in *Figure 4.40h)* refers to Census 2011.

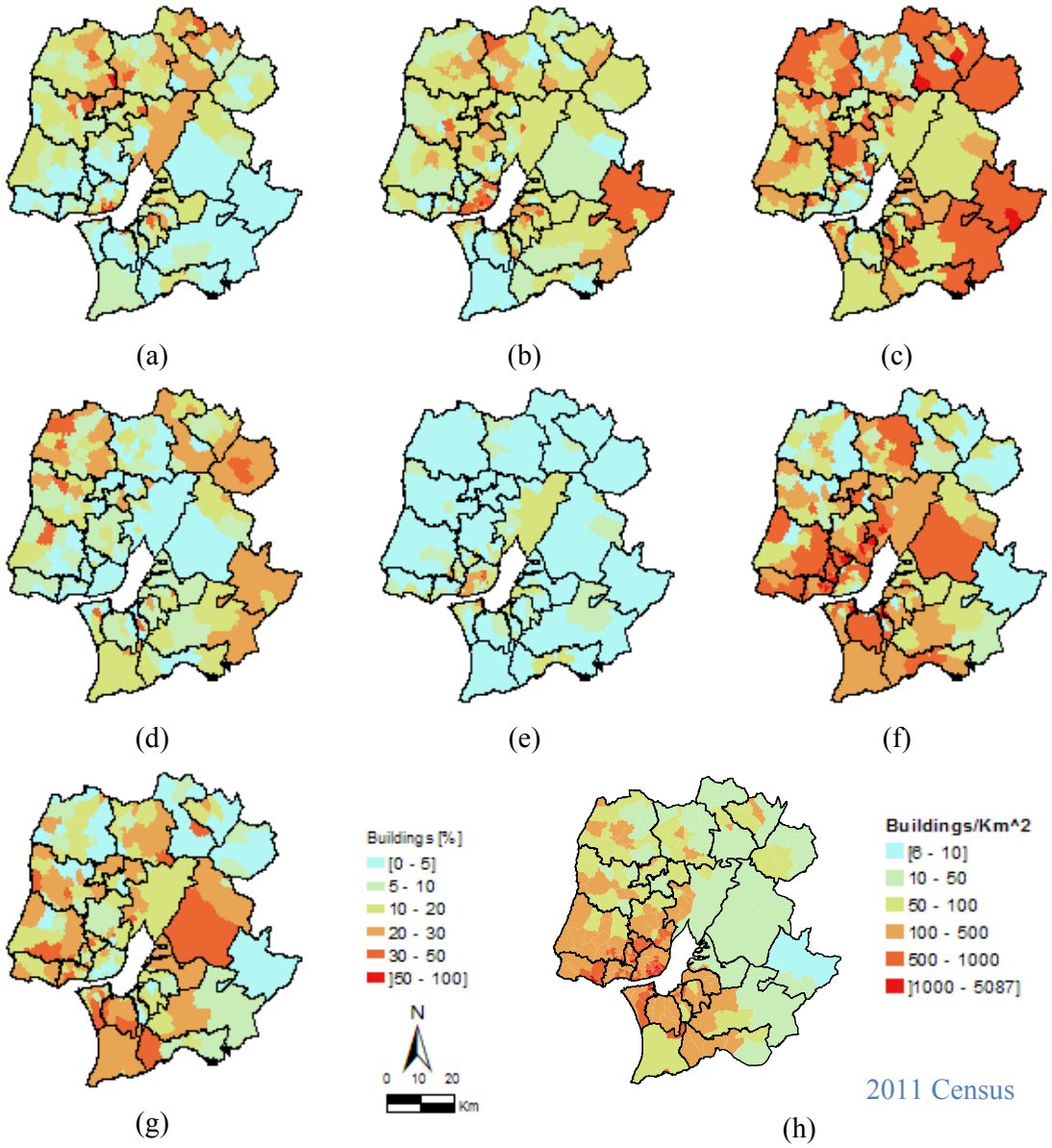

Figure 4.40: Seismic vulnerability maps for MAL; percentages of buildings per parish in each vulnerability classes. Figures (a-g) are based on **2001** inventory a) Adobe and Rubble Stone; b) Masonry before 1960; c) Masonry 1961 – 1985; d) Masonry 1986 – 2001; e) RC before 1960 f) RC 1961 – 1985 g) RC 1986 – 2001; Figure (h) is based on **2011** inventory.

Population exposure

Table *4.27* shows the number of resident individuals inventoried in 2001, in MAL and neighbourhood counties, per vulnerability class, and inhabitants totals derived from Census 2011.

Table 4.27: Number of individuals per vulnerability class.

Number of floors	Adobe + rubble stone	Masonry ≤ 1960	Masonry 1961-85	Masonry 1986-01	RC ≤ 1960	RC 1961-85	RC 1986-01	Total 2001
1	43 348	67 510	121 290	39 715	22 292	98 267	44 084	436 506
2	25 720	42 894	82 872	45 366	21 065	125 044	76 884	419 845
3	16 403	33 706	35 647	17 048	26 911	91 463	54 966	276 144
4	14 734	41 393	42 816	15 363	42 600	209 633	83 012	449 551
From 5 to 7	10 437	53 171	2 650	855	91 717	337 137	209 821	705 788
From 8 to 15	0	0	0	0	22 395	276 399	217 043	515 837
More than 15	0	0	0	0	0	20 913	16 483	37 396
Total 2001	110 642 (3.9 %)	238 674 (8.4 %)	285 275 (10.0 %)	118 347 (4.2 %)	226 980 (8.0 %)	1 158 856 (40.8 %)	702 293 (24.7 %)	2 841 067 (100 %)
Total 2011	3 059 070							

Table *4.27* shows that, in 2001, over 75% of the inhabitants of MAL and neighbouring counties lived in reinforced concrete buildings, which is a much higher percentage than of the buildings belonging to this structural type (50%, as presented in Table *4.26*). On that date, about 80% of the individuals lived in buildings constructed after 1961 (date assumed to correspond to the start of seismic codes application).

Figure *4.41* shows the distribution of people throughout MAL, belonging to different vulnerability classes. Percentages of resident individuals per parish are shown. Population totals presented in Figure *4.41*h) refer to Census 2011.

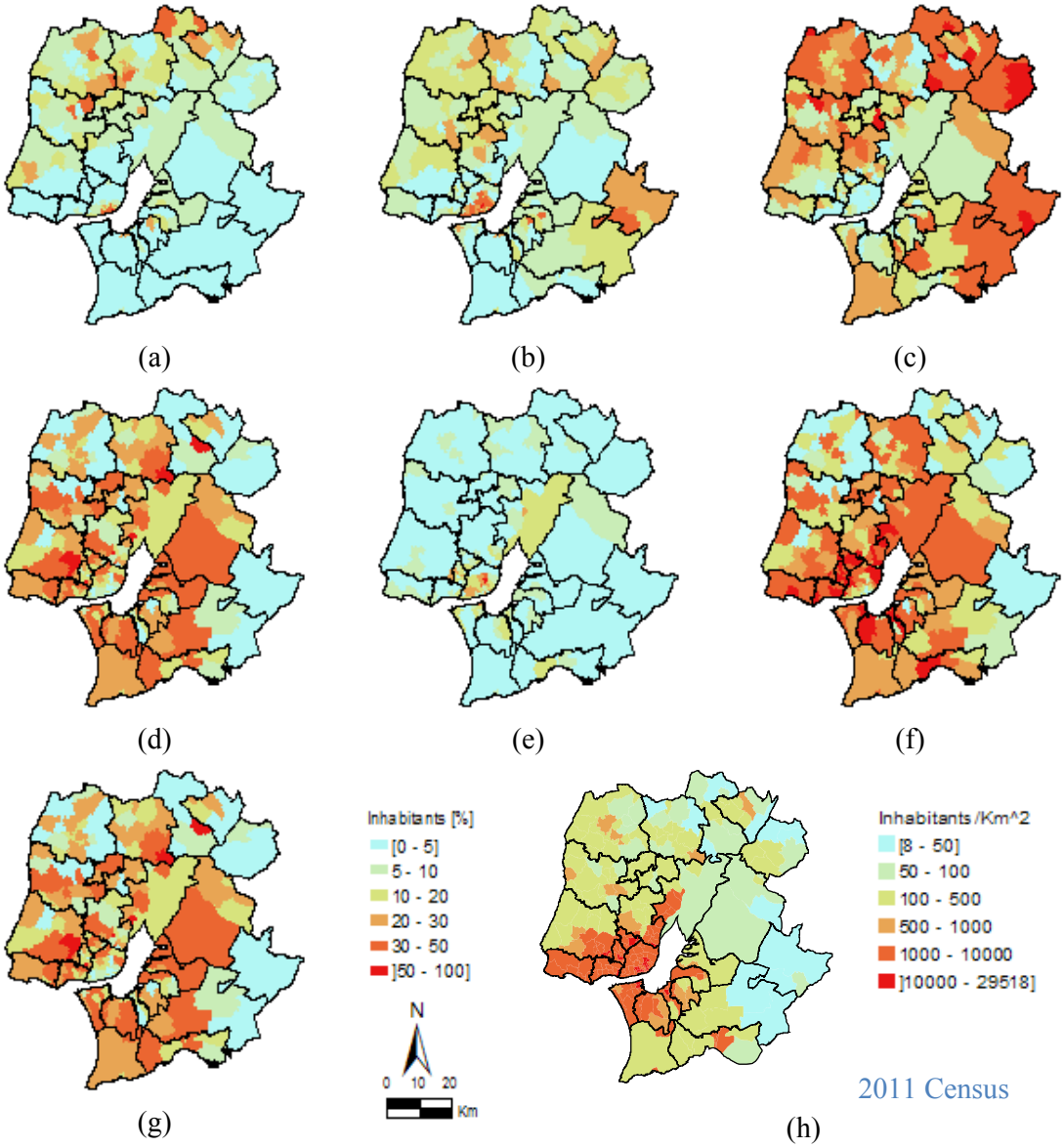

Figure 4.41: Percentages of individuals per MAL's parish in each vulnerability class. Figures (a - g) are based on **2001** inventory; a) Adobe and Rubble Stone; b) Masonry before 1960; c) Masonry 1961 – 1985; d) Masonry 1986 – 2001; e) RC before 1960 f) RC 1961 – 1985 g) RC 1986 – 2001; Figure (h) is based on **2011** inventory.

4.2.3. Vulnerability

LNECloss, which is the software used to compute Lisbon seismic risk, uses the capacity spectrum method [ATC, 1996], worldwide divulged by the HAZUS loss estimation methodology [FEMA & NIBS, 1999; FEMA, 2003], to evaluate building damages.

Carvalho *et al.* [2002] proposed capacity and fragility curves for the 315 typologies identified taking into account (i) a first analysis of Portuguese Census 1991 and (ii) expert opinion in what concerns the Portuguese construction practice, design criteria and the evolution of seismic regulation. Those curves were then updated taking into account the new features

included in Census 2001 and a more reliable classification of the building vulnerability was developed [Campos Costa *et al.,* 2005]. The capacity curves were derived from estimates of acceleration and displacement values corresponding to yield and ultimate capacity (in terms of strength and ductility) of typical buildings. Both these values and the global drift limit values were established by adjusting HAZUS parameters to the characteristics of Portuguese construction [Campos Costa *et al.,* 2005].

Likewise, capacity and fragility curves take into account the number of storeys and the period of construction, except for adobe and rubble stone vulnerability class, which was assumed that construction techniques would be the same for all time periods, varying only with the number of storeys. Design strength coefficient (*Cs*) and the natural frequency of the typical building were based on the analysis of code provisions. Those parameters vary according to seismic zonation in force on the date of building construction. Regarding the RSA code, all counties of the MAL region are located in seismic zone A; this is the zone of higher seismicity in RSA; in what concerns RSCCS code most counties of MAL are located in seismic zone A (of higher seismicity) and a few are located in seismic zone B. Seismic zonation for this Portuguese codes are presented in Annex A.

Error! Reference source not found. also shows the threshold points of four damage limit states. The threshold of those damage states are established in terms of global drift for each building typology. Five damage states were considered, dependent on the typology, «Slight Damage (S), «Moderate Damage» (M), «Extensive damage» (E) and «Complete Damage» (C). Approximately 10 to 25% of the total area of buildings in «Complete Damage» state is likely to collapse totally, whereas the remaining is expected to collapse partially [LESSLOSS, 2007].

Annex B presents, for each vulnerability class, the design strength coefficient (*Cs*), the natural frequency and the height of typical buildings. The others parameters that define capacity and fragility curves were based on FEMA [2003] proposals and on the classification of MAL buildings in HAZUS typologies [see LESSLOSS, 2007]. Variables that define capacity and fragility curves, used in LNECloss to characterize vulnerability of buildings in MAL, are also presented in Annex B. The capacity curves are defined by distinct sections, delimited by the two control points above mentioned, the yield capacity (SD_y, SA_y) and the ultimate capacity (SD_u, SA_u), as it is exemplified in Figure *4.42*. The values adopted values for these control points are presented in Annex B.

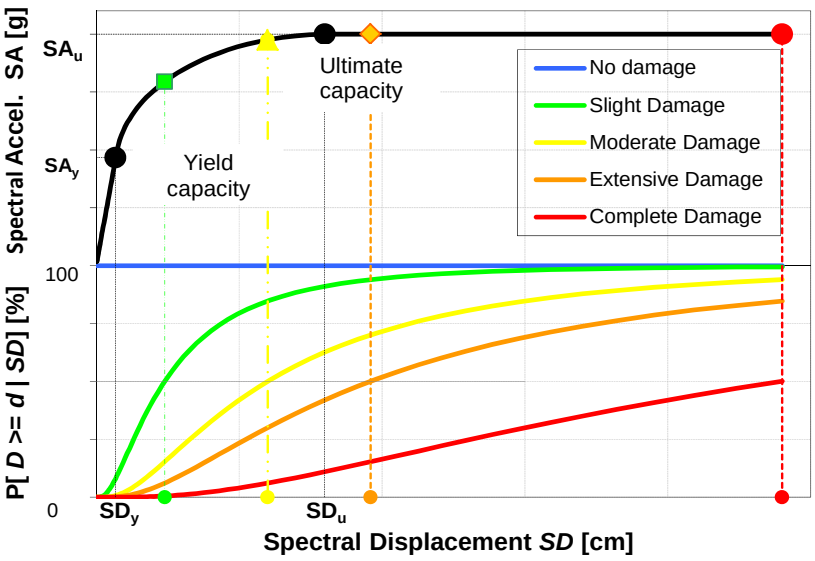

Figure 4.42: (a) Example of a capacity curve (in black) and of fragility curves for 5 damage states.

According to ATC (1996) the evaluation of peak response relies on the intersection of the capacity curve of a given vulnerability class with the seismic spectral demand at the site. The initial elastic response spectrum is iteratively reduced to the so called demand spectra, taking into account the building degradation when exposed to the seismic motion. The procedure is illustrated in *Figure 4.43* [Campos Costa & Sousa, 2010; Campos Costa et al., 2010].

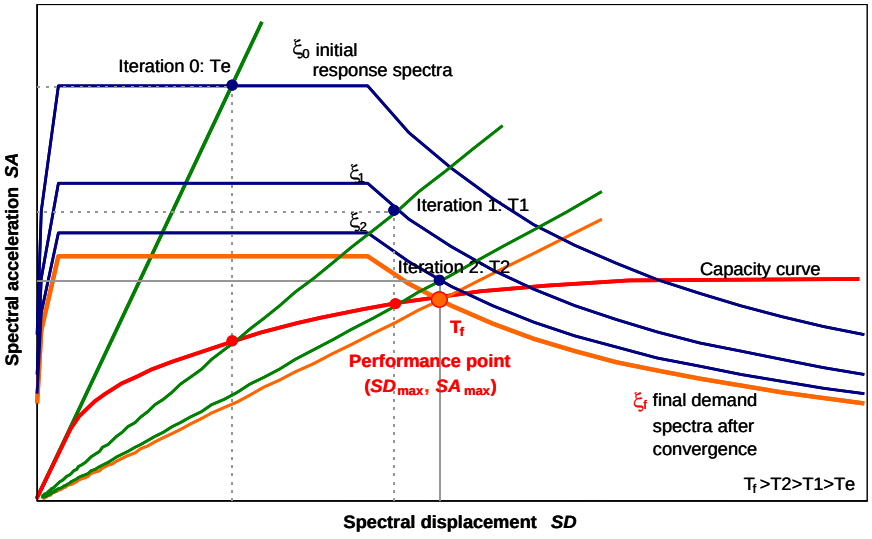

Figure 4.43: Iterative process to obtain the peak of building response in the capacity spectrum method [Campos Costa et al., 2010].

As stated in LESSLOSS [2007] an innovative technique was introduced in LNECloss operational procedure that takes into account an iterative process that estimates sequential

demand spectra, with increasing effective damping, reflecting structure degradation during its cyclic response. While in HAZUS the modifications of spectral demand are represented by reduction factors, in LNECloss those modifications were performed through an iterative equivalent non-linear stochastic methodology. Progressive building responses are obtained over the demand spectra, till the convergence with the median capacity curve is achieved. The performance point, obtained this way, corresponds to the peak of the dynamic response of a structure idealized by a single degree of freedom system.

The authors [LESSLOSS, 2007] also present the main advantages of the equivalent non-linear stochastic approach relatively to the method that relies on the graphic intersection and on the reduction factors: (i) it is more efficient computationally, because it avoids the successive evaluation of the entire reduced demand spectra (ii) it give us an exact evaluation of building peak response, instead of an approximate evaluation obtained by interpolation methods, (iii) it does not use empirical relations to reduce demand spectra due to effective damping and (iv) it allows the explicit inclusion of the duration of seismic demand on the peak response of building.

The abscissa of this performance point corresponds to the effect of seismic action, measured in terms of a spectral displacement, *SDmax*. Mathematical notation is simplified omitting the suffix *max* in the variable spectral displacement, ***i.e.***, $SD_{\max} \equiv SD$. This ground motion value conditions the cumulative lognormal probability distributions of the variable damage, $P_D(d)$, that model building fragility:

$$P_D\left(D \geq d \mid SD\right) = \Phi\left[\frac{1}{\beta_d} \ln\left(\frac{SD}{\overline{SD_d}}\right)\right] \qquad 4.2$$

Building fragility curves allow the evaluation of the probability to exceed the threshold of a given damage state, conditioned by the level of seismic ground motion, *SD*, where Φ is the standard normal cumulative distribution function; $\overline{SD_d}$ is the median of spectral displacement at which the building reaches the threshold of the damage state *d,* presented in Annex B; β_d is the standard deviation of the natural logarithm of spectral displacement of the damage state *d*. Values adopted for this parameter are based on FEMA [2003] proposal.

With regard to social losses, casualty rates are presented in the Annex C by injury level, typology and damage state. The human losses estimation refers to night time, because the only Portuguese building inventory that is exhaustive refers to the housing stock, being necessary to assume that the population is at home when earthquake scenario occurs [LESSLOSS, 2007].

4.2.4. Seismic Risk

Five structural damage states were considered in the analyses, No Damage, Slight, Moderate, Extensive and Complete Damage, and the percentages of the damaged structures, per parish, for each damage state were computed.

Structural damages (Figure *4.44* and Figure 4.47) and social and economic losses (Figure *4.45*, Figure *4.46*, Figure *4.48* and Figure *4.49*) were computed, considering seismic actions Type 1 and 2 present in the NA of EC8. Four levels of severity of injuries were considered, similar to HAZUS-MH [FEMA, 2003]: light injuries, hospitalization, severe injuries and instantaneously killed or mortally injured.

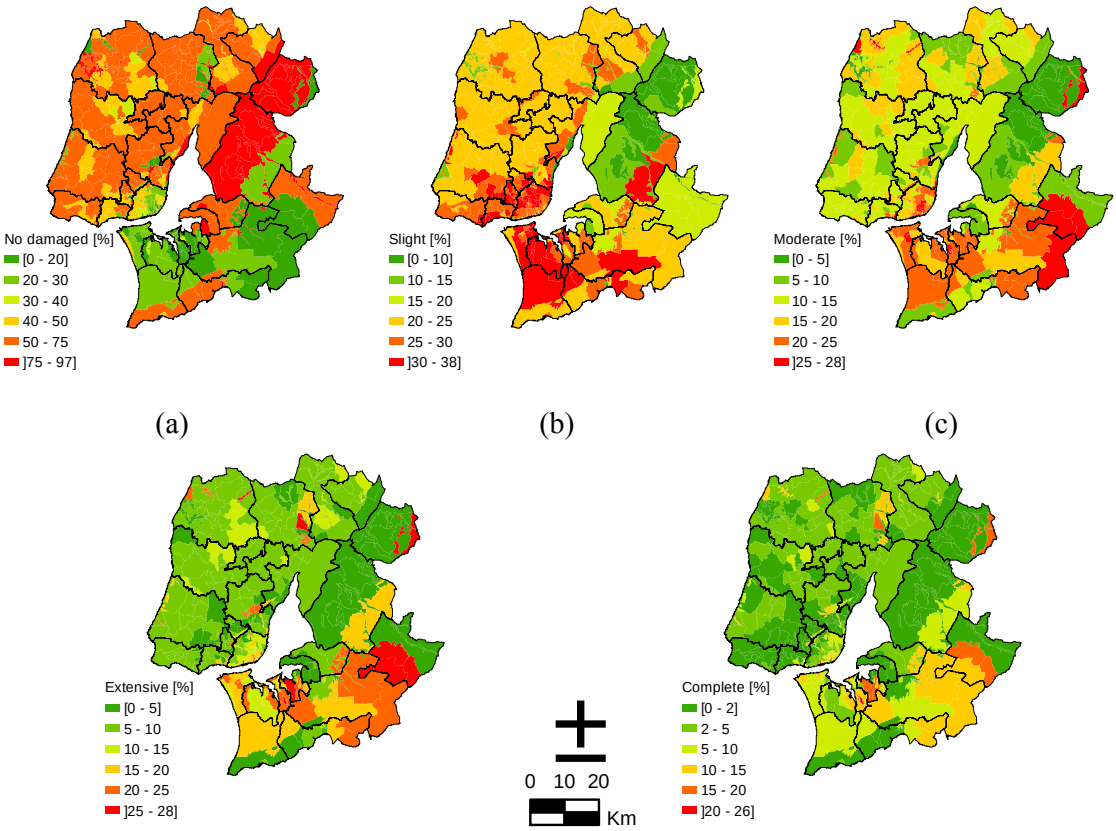

Figure 4.44: Conditional seismic risk for a hazard level of 475 years return period, measured in terms of the percentage of (a) no damaged buildings (b) slight damaged buildings (c) moderate damage buildings (d) extensive damaged buildings and (e) complete damaged buildings. Seismic Action **Type 1** of NA of EC8.

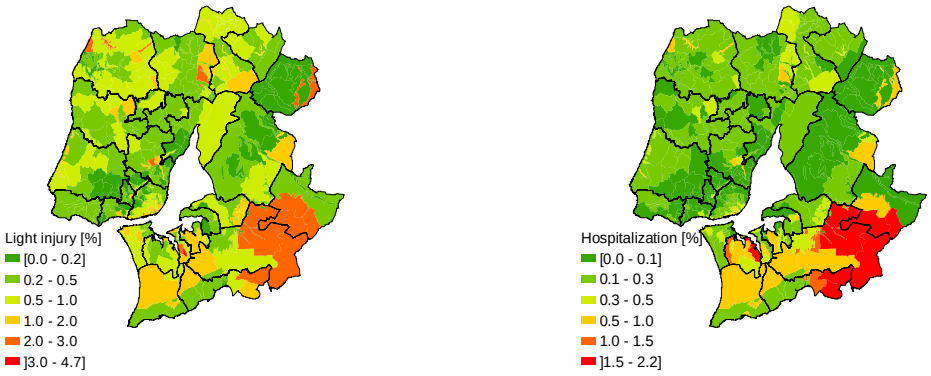

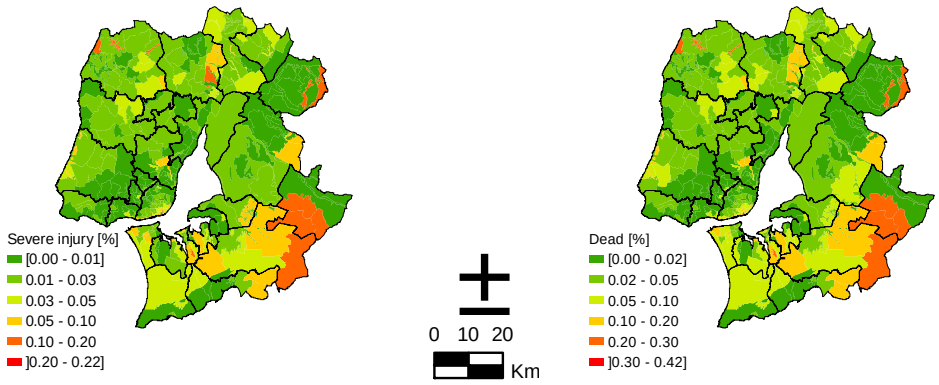

(c) (d)

Figure 4.45: Percentage of casualties conditional on a 475 years return period hazard level: (a) light injury (b) hospitalization (c) severe injury and (d) killed. Seismic Action **Type 1** of NA of EC8.

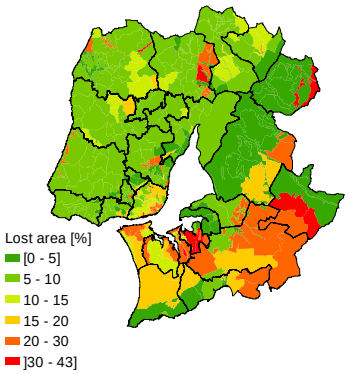

Figure 4.46: Percentage of lost building area conditional on a 475 years return period hazard level. Seismic Action **Type 1** of NA of EC8.

The geographic distribution of aggregated measures of risk, like human losses (*Figure 4.45*) or lost building area(*Figure 4.46*), has a similar pattern to the geographical distribution of the peak ground acceleration at the surface, showing higher losses in parishes located south of the Tagus river. Note that exposure was not taken into consideration in this analysis, since the losses are presented in relative values, normalized by the overall exposure for each parish.

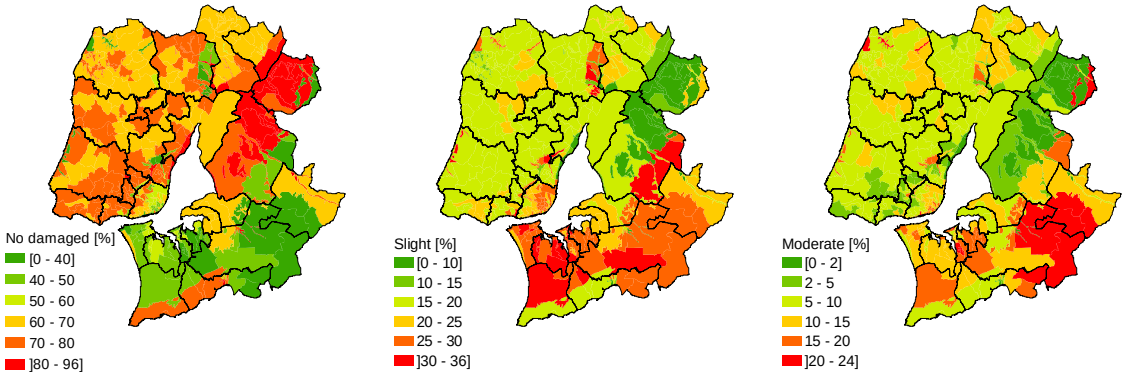

(a) (b) (c)

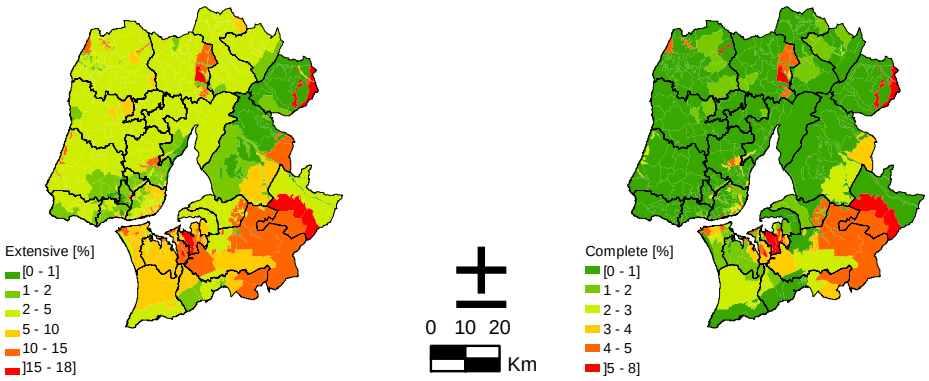

(d) (e)

Figure 4.47: Conditional seismic risk for a hazard level of 475 years return period, measured in terms of the percentage of (a) no damaged buildings (b) slight damaged buildings (c) moderate damage buildings (d) extensive damaged buildings and (e) complete damaged buildings. Seismic Action **Type 2** of NA of EC8.

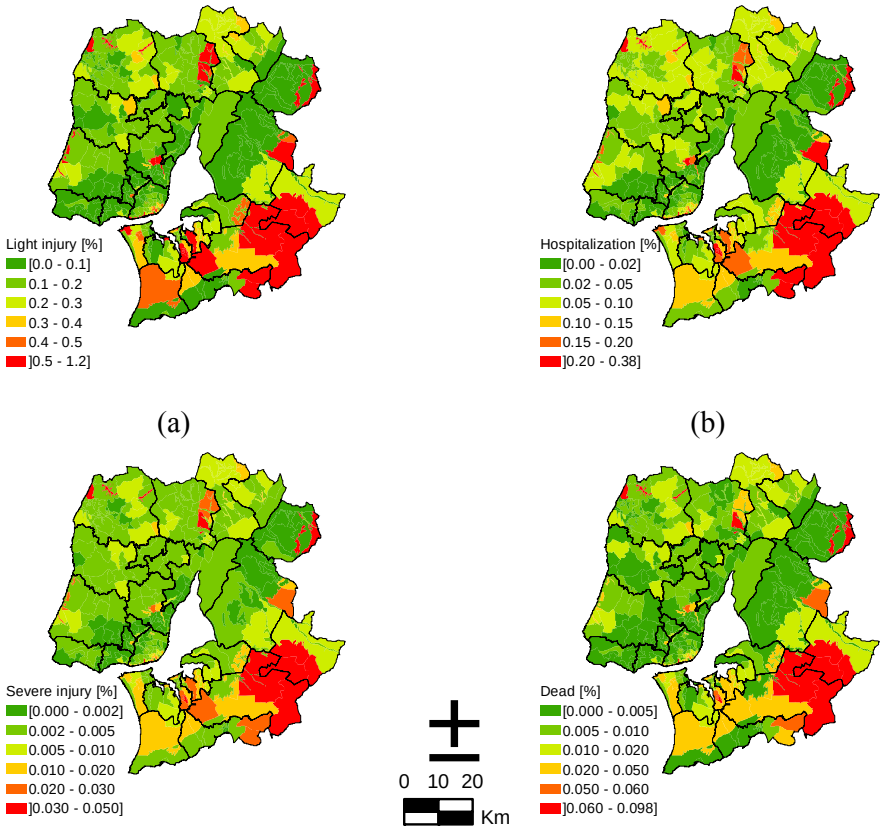

(a) (b)

(c) (d)

Figure 4.48: Percentage of casualties conditional on a 475 years return period hazard level: (a) light injury (b) hospitalization (c) severe injury and (d) killed. Seismic Action **Type 2** of NA of EC8.

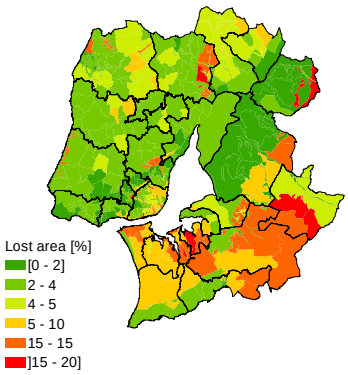

Figure 4.49: Percentage of lost building area conditional on a 475 years return period hazard level. Seismic Action **Type 2** of NA of EC8.

As for the seismic action Type 1, in case of seismic action Type 2 the geographic distribution of human losses (*Figure 4.48*) and lost building area(*Figure 4.49*), has a similar pattern to the geographical distribution of the peak ground acceleration, showing higher losses in parishes located south of the Tagus river.

Seismic risk comparison

Seismic risk scenarios correspondent to the two hazard models of SHARE were compared with the maximum value (envelope) of damages or losses, in each parish, resulting from seismic action scenario Type 1 or Type 2 of the NA of EC8.

Figure 4.50, *Figure 4.51* and Figure *4.52* present the results concerning structural damages, human losses, and lost building area, respectively.

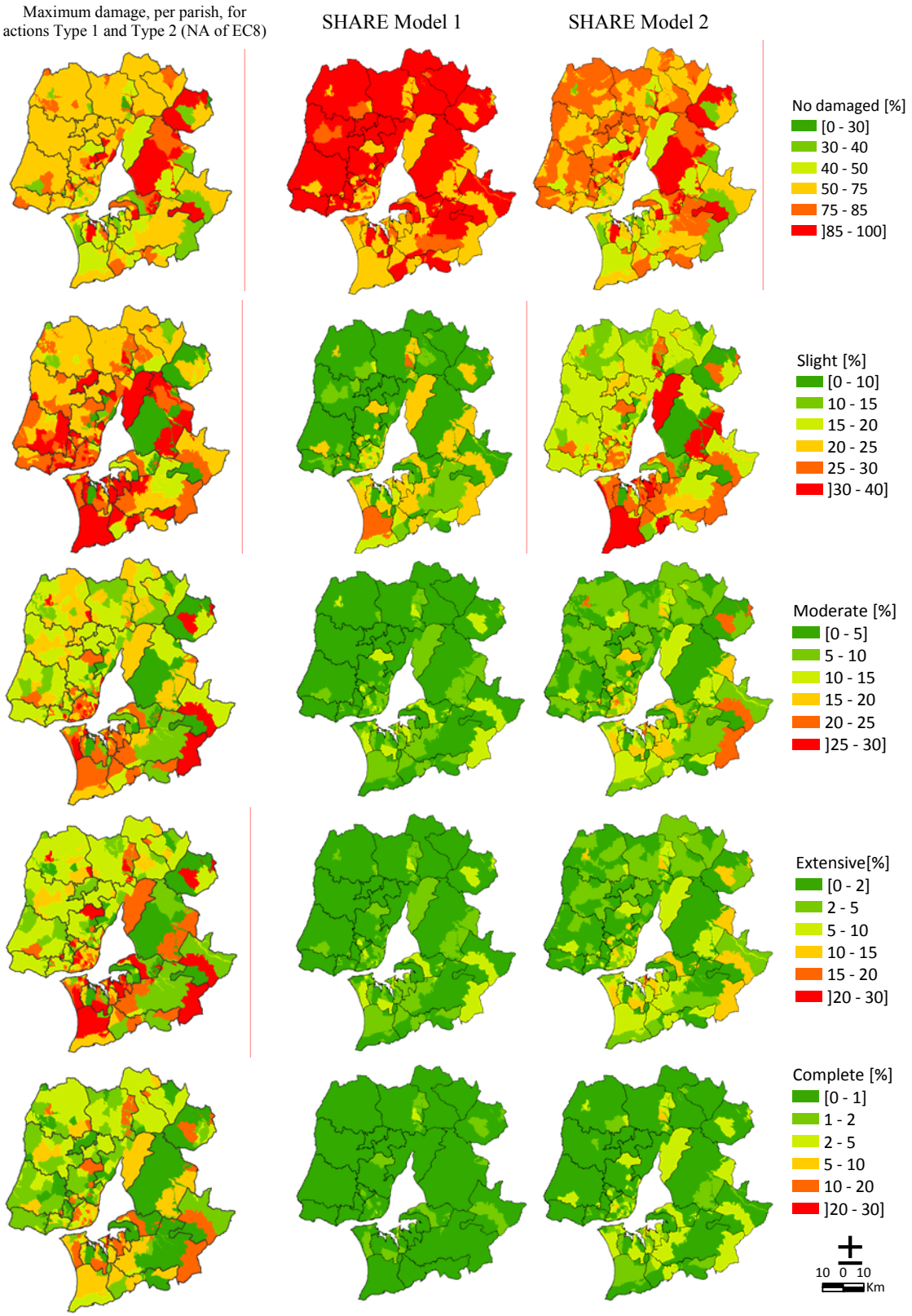

Figure 4.50: Comparative maps: conditional seismic risk for a hazard level of 475 years return period in terms of the percentage of (a) no damaged buildings (b) slight damaged buildings (c) moderate damage buildings (d) extensive damaged buildings and (e) complete damaged buildings.

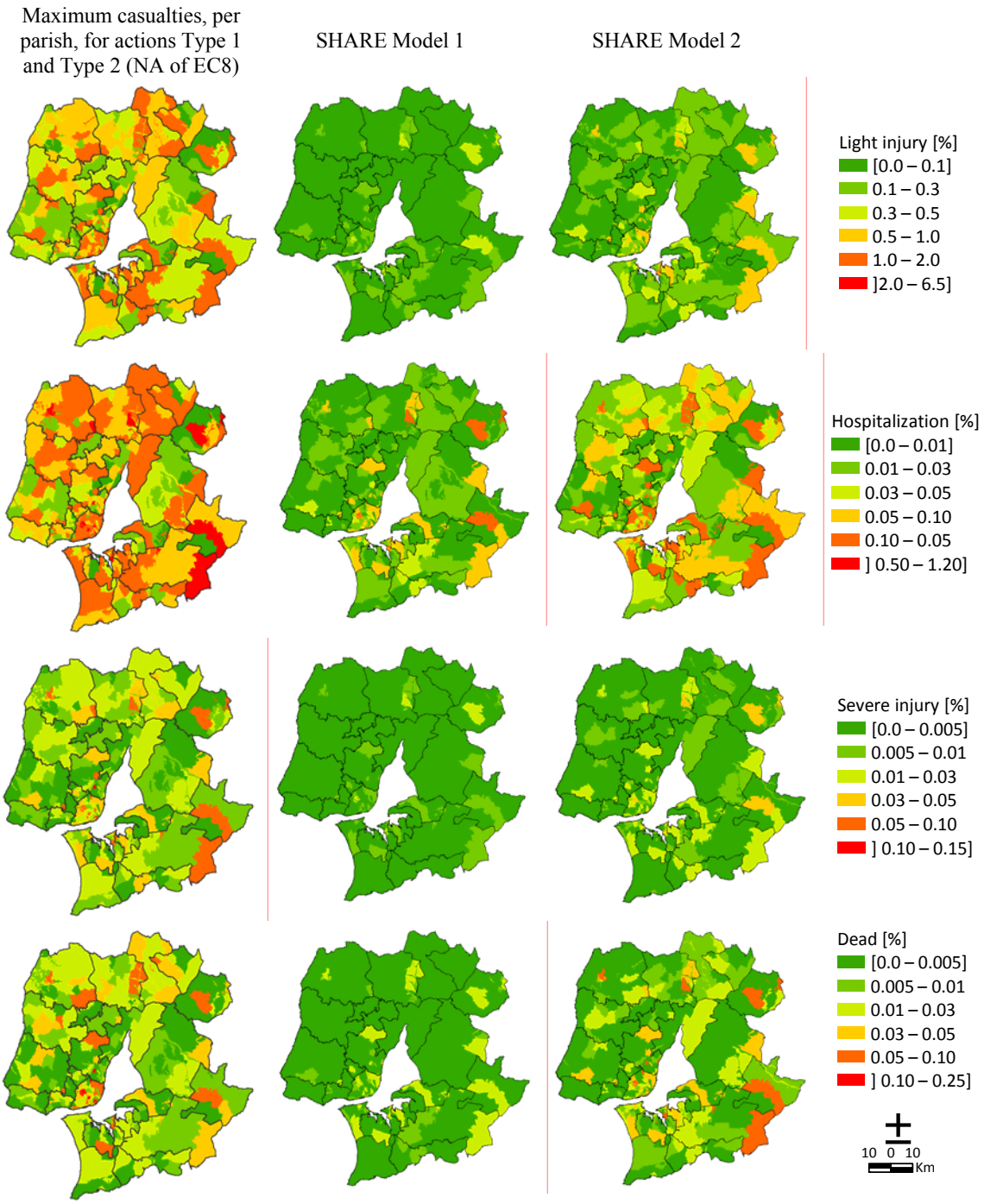

Figure 4.51: Comparative maps: percentage of casualties conditional on a hazard level of 475 years return period: (a) light injury (b) hospitalization (c) severe injury and (d) killed.

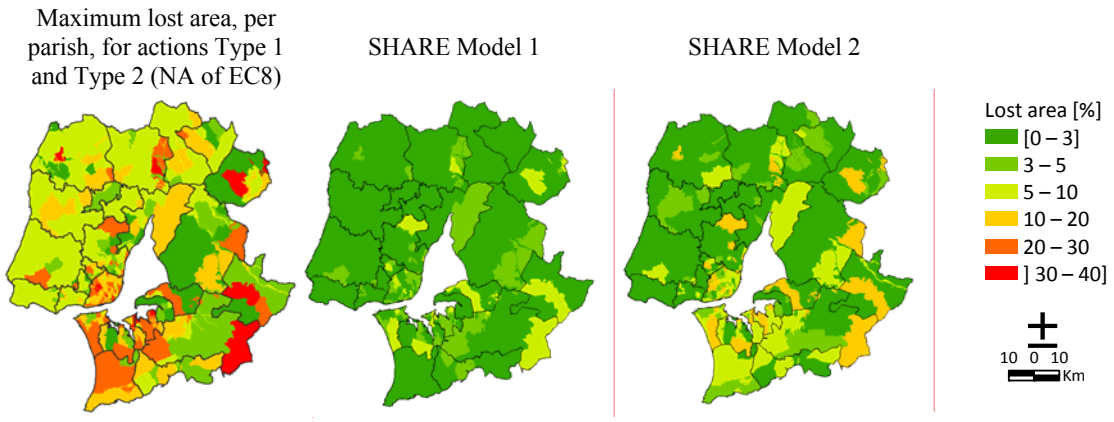

Figure 4.52: Comparative maps: percentage of lost building area conditional on a hazard level of 475 years return period.

These maps show that maximum losses and damages resulting from hazard models of NA of EC8 are higher, in general, than losses and damages resulting from both hazard models of SHARE. There are a few exceptions in some southeast parishes of MAL, when comparing the number of fatalities.

Table *4.28* summarizes the results of the comparative seismic risk analysis for MAL.

Table 4.28: Seismic risk for MAL considering the hazard specification of the NA of EC8 and SHARE hazard output.

Risk dimension	Losses [#]	NA of EC8 seismic action				SHARE			
		Type 1		Type 2		Model 1		Model 2	
		Total	[%]	Total	[%]	Total	[%]	Total	[%]
Damage	No damaged	214978	45.05	302512	63.4	390005	81.73	316116	66.25
	Slight	123913	25.97	104606	21.92	60349	12.65	98488	20.64
	Moderate	71972	15.08	43545	9.13	18727	3.92	39362	8.25
	Extensive	47288	9.91	21080	4.42	6812	1.43	18524	3.88
	Complete	19019	3.99	5428	1.14	1278	0.27	4680	0.98
Human Losses	No victims	2822314	99.34	2835790	99.81	2839458	99.94	2836421	99.84
	Light injury	15534	0.55	4440	0.16	1185	0.04	3410	0.12
	Hospitalization	2623	0.09	695	0.02	351	0.01	969	0.03
	Severe injury	285	0.01	67	0	25	0	90	0
	Killed	311	0.01	75	0	48	0	177	0.01
Economic Losses	Lost building area [m^2]	1.1×10^7	10.97	4.8×10^6	4.70	1.7×10^6	1.63	4.3×10^6	4.16

Table *4.29* presents the variation of conditional risk, showing the difference between loss values resulting from SHARE models and maximum losses resulting from hazard specifications of NA of EC8, normalized by the latter results, using the following equation:

$$\Delta\ Risk[\%] = [(SHARE\ losses - \max(NA\ of\ EC8\ losses)) / \max(NA\ of\ EC8\ losses)]*100 \quad 4.3$$

Table 4.29: Relative differences of seismic risk for MAL, considering the hazard specifications of the NA of EC8 and SHARE hazard output.

Risk dimension	Losses	Δ *Risk* [%]	
		SHARE Model 1	SHARE Model 2
Damage	Slight	-51.3	-20.5
	Moderate	-74.0	-45.3
	Extensive	-85.6	-60.8
	Complete	-93.3	-75.4
Human Losses	Light injury	-92.4	-78.0
	Hospitalization	-86.6	-63.1
	Severe injury	-91.2	-68.4
	Killed	-84.6	-43.1
Economic Losses	Lost building area	-85.2	-62.1

The main conclusion of the present analysis is that, since the relative differences are negative, in future, seismic risk will increase in MAL, if the SHARE approach is adopted for design purposes. In fact the assessment of the seismic risk computed with the SHARE hazard gives lower values. This conclusion is valid for all dimensions of risk that were analysed: damage on buildings, social losses, and economic losses. Furthermore, if Model 1 of SHARE is adopted the risk will increase more than if Model 2 is adopted. For instance, the relative negative variation of Complete damaged buildings, comparing Model 1 of SHARE with losses envelope for the reference situation, reaches more than 93%.
Notice that this conclusion relies on the analysis made for the 475 years return period that is the return period of the reference seismic action for the no-collapse requirement adopted in the NP EN 1998-1: 2010.

5. Conclusions

Seismic risk assessment has been computed for the four case studies selected within this task both with the seismic hazard maps currently employed in those regions as well as the new hazard model developed and proposed in the SHARE project. It has to be reminded that the SHARE hazard values used in the seismic risk analyses are the results that were made available in November 2012. These values do not represent the final outcome from SHARE, especially for what concerns model 2 (expert opinion based). Nevertheless, it is not expected that the main conclusions of this study would change with the use of the final SHARE results.
The hypotheses on the exposure and on the vulnerability and the methodology used to calculate the building damage, the social losses and the economic losses are the same for the two approaches (current seismic hazard and SHARE seismic hazard). Given that, it is reasonable to say that different results obtained from the analyses are influenced only by the

applied seismic hazard. The common trend is that a lower seismic risk is found across Europe both at a regional level and at an urban level. In general, the SHARE uniform hazard spectra have lower spectral acceleration values compared to the currently employed hazard spectra and this means that a lower performance point will be computed. It has to be noted that the SHARE PGA values do not substantially differ from the currently employed PGA values in the selected case studies, but the difference becomes significant when spectral accelerations are considered. This is due to a general lower value of T_C (constant velocity corner period) and consequently a much narrower plateau. For this reason, when a spectral acceleration based fragility curve is taken into account the different shape in the spectrum is of a great importance. Such discrepancies could be caused by the different GMPEs utilized in the logic tree of SHARE which are much more modern than the equations used in the local hazard studies. Then, it has to be noted that the resolution chosen for the SHARE project (0.1°) is different from the resolution utilized in the current employed code of the countries and this factor adds uncertainty in the calculation of the spectrum that has to be used in the analyses.

The authors recognize that there are many possibilities to compute the seismic risk and that the uncertainty on different methodologies, capacity curves and fragility curves should be taken into account, but it has to be said that the main focus of this task was the comparison between seismic risk assessments to understand the impact of the SHARE outcome on the seismic risk. For this purpose, the authors decided to fix simple hypotheses on exposure, vulnerability and methodology and to concentrate on the comparison between results.

One positive outcome of this study, i.e. lower levels of risk being estimated with the SHARE results, can be thought of as beneficial to risk mitigation, since the overestimation of risk may have a counter-productive effect, given that the lack of resources available to tackle such high levels of risk may lead to the postponement of mitigation policies.

This study, together with the other tasks developed in work package number 2, namely Engineering Requirements and Applications, has been of help to recognize and understand the recommendations to supply to the EC8 committee (see Deliverable 2.7 for details).

REFERENCES

Ambraseys, N.N., Simpson, K.A., Bommer, J.J. (1996). Prediction of horizontal response spectra in Europe. Earthquake Engineering and Structural Dynamics, 25(4), 371-400

ATC-40 (1996). Seismic evaluation and retrofit of concrete building. Applied Technology Council, Redwood City, California.

Borzi, B., Pinho, R., Crowley, H. (2008a). Simplified pushover-based vulnerability analysis for large scale assessment of RC buildings. Engineering Structures, 30(3), 804-820

Borzi, B., Crowley, H., Pinho, R. (2008b). Simplified pushover-based earthquake loss assessment (SP-BELA) for masonry buildings. International Journal of Architectural Heritage, 2(4), 353 – 376

Campos Costa, A., Sousa, M.L., Coelho, E., 2005. "Building Stock Inventory and Vulnerability Data for Lisbon Metropolitan Area". Report 423/2005, DE/NESDE, LNEC, Lisbon.

Campos Costa, A., Sousa, M.L., Carvalho, A., Coelho, E., 2010. "Evaluation of seismic risk and mitigation strategies for the existing building stock: application of LNECloss to the Metropolitan Area of Lisbon". Bulletin of Earthquake Engineering (BEE), vol. 8, pp. 119–134 (DOI 10.1007/s10518-009-9160-3), Springer.

Campos Costa A., Sousa, M.L., 2010. "Estudo de estratégias de mitigação de risco sísmico de âmbito regional". Reabilitar 2010, Encontro Nacional Conservação e Reabilitação de Estruturas, LNEC, Lisbon.

Carvalho, A., Zonno, G., Franceschina, G., Bilé Serra, J., Campos Costa, A., 2008. "Earthquake shaking scenarios for the metropolitan area of Lisboa". Soil Dynamics and Earthquake Engineering (SDEE), n. 28, pp 347-364 (DOI 10.1016/j.soildyn.2007.07.009), Elsevier.

Carvalho, E.C., Campos Costa, A., Sousa, M.L., Martins, A., Serra, J.B., Caldeira, L., Coelho, A.G., 2002. "Caracterização, vulnerabilidade e estabelecimento de danos para o planeamento de emergência sobre o risco sísmico na Área Metropolitana de Lisboa e nos municípios de Benavente, Salvaterra de Magos, Cartaxo, Alenquer, Sobral de Monte Agraço, Arruda dos Vinhos e Torres Vedras". Relatório final. Report 280/02 – G3ES. LNEC, Lisbon.

Carvalho, E.C., Coelho E., Campos Costa, A., Sousa, M.L., Candeias, P. (2002b). "Vulnerability Evaluation of Residential Buildings in Portugal." Proceedings of 12° European Conference on Earthquake Engineering, London.

Casarotti, C., Monteiro, R., Pinho, R. (2009). Verification of spectral reduction factors for seismic assessment of bridges. Bulletin of the New Zealand Society for Earthquake Engineering, Vol. 42, No. 2, pp. 111-121.

CEN (European Committee for Standardization) (2004). Eurocode 8: Design of structures for earthquake resistance, Part 1: General rules, seismic actions and rules for buildings. EN 1998-1:2004. Brussels, Belgium.

Coburn, A.W. & Spence, R., 2002. "Earthquake protection". John Wiley & Sons, LTD, Great Britain.

D'Ayala, D., Kappos, A., Crowley, H., Antoniadis, P., Colombi, M., Kishali, E., Panagopoulos, G., Silva, V. (2012). Providing building vulnerability data and analytical fragility functions for PAGER, Final Technical Report.

EN 1998-1: 2004. "Eurocode 8. Design of Structures for Earthquake Resistance – Part 1: general rules, seismic actions and rules for buildings". Comité Européen de Normalisation (CEN), Brussels.

Faccioli, E., Pessina, V. (2000). The Catania project: earthquake damage scenarios for high risk areas of the Mediterranean. CNR – gruppo Nazionale per la Difesa dai Terremoti, Rome.

FEMA (2003). HAZUS-MH Technical Manual, Federal Emergency Management Agency, Washington D.C.

FEMA & NIBS, 1999. "Earthquake loss estimation methodology – HAZUS 99". Federal Emergency Management Agency and National Institute of Buildings Sciences, Washington DC.

Frassine, L., Giovinazzi, S. (2004). Databases compared in the vulnerability assessment of residential buildings: an application to the city of Catania. Proceedings of the XI Congresso Nazionale "L'ingegneria sismica in Italia", Genova (in Italian).

Gruppo di Lavoro CPTI (2004). Catalogo Parametrico dei terremoti italiani, 2004 version (CPTI04), INGV Bologna. http://emidius.mi.ingv.it/CPTI04 (in italian)

Gruppo di Lavoro MPS (2004). Redazione della mappa di pericolosità sismica prevista dall'Ordinanza PCM 3274 del 20 marzo 2003. Rapporto Conclusivo per il Dipartimento della Protezione Civile, INGV, Milano-Roma, aprile 2004, 65 pp. + 5 appendici

Imprensa Nacional, 1958. "Regulamento de Segurança das Construções Contra os Sismos." (RSCCS) Decreto nº 41 658. Imprensa Nacional. Lisbon.

Imprensa Nacional, 1961. "Regulamento de Solicitações em Edifícios e Pontes". (RSEP) Decreto nº 44 041. Imprensa Nacional, Lisbon.

INCM, 1983. "Regulamento de segurança e acções para estruturas de edifícios e pontes." (RSA), Decreto Lei nº 235/83 de 31 de Maio e Decreto Lei nº 357/85 de 2 de Setembro. Imprensa Nacional - Casa da Moeda (INCM), 1986. Lisboa. Portugal.

INE, 2002 "Recenseamento da população e da habitação (Portugal) - Censos 2001". Instituto Nacional de Estatística. Lisbon.

INE, 2011. http://censos.ine.pt/xportal/xmain?xpid=CENSOS&xpgid=censos2011_apresentacao.

INGV-DPC S1 (2007a) Continued assistance to the DPC for the completion and management of seismic hazard maps foreseen in the Ordinance PCM 3274 and planning of future developments. http://esse1.mi.ingv.it (in Italian)

IPQ, 2010. "NP EN1998-1: 2010. Eurocódigo 8 – Projeto de estruturas para resistência aos sismos. Parte 1: Regras gerais, acções sísmicas e regras para edifícios." Instituto Português da Qualidade. Caparica, Portugal.

Kappos, A.J., and Panagopoulos, G. (2010). Fragility curves for reinforced concrete buildings in Greece. Structure and Infrastructure Engineering 6 (1-2), pp. 39–53.

Kappos, A.J., Panagopoulos, G. and Penelis, G. (2008). Development of a seismic damage and loss scenario for contemporary and historical buildings in Thessaloniki, Greece, Soil Dynamics and Earthquake Engineering 28:836-850.

Kappos, A.J., Panagiotopoulos, C., Panagopoulos, G. and Papadopoulos, E. (2003). RISK-UE WP4 - Reinforced Concrete Buildings (Level I and II analysis).

Kappos, A.J., Panagopoulos, G., Panagiotopoulos, C., and Penelis, G. (2006). A hybrid method for the vulnerability assessment of R/C and URM buildings, Bulletin of Earthquake Engineering 4 (4): 391-413, DOI 10.1007/s10518-006-9023-0.

Kircher, C.A., Nassar, A. A., Kustu, O. & Holmes, W.T., 1997. "Development of building damage functions for earthquake loss estimation". Earthquake Spectra, Vol. 13, 4: 663-682.

LESSLOSS, 2007. “Earthquake Disaster Scenario Prediction and Loss Modelling for Urban Areas”. Editor Robin Spence, IUSS Press, Pavia, Italy, ISBN 978-88-6198-011-2.

Meroni, F., Petrini, V., Zonno, G. (2000). National distribution of vulnerability. Vulnerability of buildings: assessment of the seismic vulnerability of ordinary buildings at a national scale. Bernardini A. (ed) CNR- Gruppo Nazionale per la Difesa dai Terremoti, Rome, 175 pp+CD-ROM (in Italian)

Montaldo, V., Meletti, C., Martinelli, F., Stucchi, M., Locati, M. (2007). On-line seismic hazard data for the new Italian building code. Journal of Earthquake Engineering, 11(Sp.Issue 1),119-132

NP EN 1998 – 1: 2010. “Norma Portuguesa, Eurocódigo 8 – Projecto de estruturas para resistência aos sismos. Parte 1: Regras gerais, acções sísmicas e regras para edifícios”. IPQ, Lisbon.

NTC08 (2008). Norme tecniche per le costruzioni. D. M. 14 Gennaio 2008, Suppl. Ord. alla G.U. 4.2.2008 n. 30 (in Italian)

Newmark, N.M. and HallW.J. (1982). Earthquake Spectra and design. Technical report. Earthquake Engineering Research Institute (EERI), Oakland, CA

Ordinanza del Presidente del Consiglio dei Ministri (OPCM) (2006). Criteria for the identification of seismic zones for the production and updating of lists of the aforementioned zones. Ordinance no. 3519 of the 28th April 2006 (in Italian)

Papaioannou, C. (2004). Deliverable 3B: Probabilistic Seismic Hazard Analysis. SRM-LIFE (2003-2007). Development of a global methodology for the vulnerability assessment and risk management of lifelines, infrastructures and critical facilities. Application to the metropolitan area of Thessaloniki. General Secretariat for Research and Technology, Greece (in Greek).

Penelis, G. (2008). Thessaloniki 1978 earthquake. Turning point in seismic protection of Greece. Proceedings of 30 years after the Thessaloniki earthquake. Memoirs and perspectives, Polytechnic School of Aristotle University of Thessaloniki, May 2008 (in Greek).

Pitilakis, K., Kappos, A., Hatzigogos, Th., Anastasiadis, A., Anastasiadis, A., Alexoudi, M., Argyroudis, S., Penelis, G., Panagiotopoulos, Ch., Panagopoulos, G., Kakderi, K., Papadopoulos, I., Dikas N. (2004). RISK-UE. An advanced approach to earthquake risk

scenarios with applications to different European towns. Synthesis of the application to Thessaloniki city.

Pitilakis, K., Riga, E. and Anastasiadis, A. (2012). Design spectra and amplification factors for Eurocode 8, Bulletin of Earthquake Engineering 10 (5): 1377-1400, DOI: 10.1007/s10518-012-9367-6.

Pitilakis, K., Riga, E. and Anastasiadis, A. (2013). New code site classification, amplification factors and normalized response spectra based on a worldwide earthquake database, Bulletin of Earthquake Engineering (in press).

RISK-UE (2001-2004). An advanced approach to earthquake risk scenarios with applications to different European towns.

Sabetta, F., Pugliese, A. (1996). Estimation of response spectra and simulation of nonstationary earthquake ground motions. Bulletin of Seismological Society of America, 86(2), 337-352

SHARE, 2011. “Seismic Hazard Harmonization in Europe”. http://www.share-eu.org/.

Sousa, M.L., 2006. “Risco Sísmico em Portugal Continental”. PhD thesis, IST, Lisbon.

Sousa, M.L., Carvalho, A., Bilé Serra, J.& Martins, A., 2010. "Simulation of seismic scenarios in Algarve region”. 14th European Conference on Earthquake Engineering, Ohrid.

Sousa, M.L., Martins, A. & Campos Costa, A., 2003. "Levantamento do Parque Habitacional de Portugal Continental para o Estudo da sua Vulnerabilidade Sísmica com Base nos Censos 2001". Relatório 205/2003, DE/NESDE. Proc. 0305/14/13733, LNEC, Lisbon.

Zonno, G., Carvalho, A., Franceschina, G., Akinci, A., Campos Costa, A., Coelho, E., Cultrera, G., Pacor, F., Pessina, V., Cocco, M., 2008. “Simulating earthquake scenarios using Finite-fault model for the Metropolitan Area of Lisbon (MAL). “ pp 233-244. Book: The 1755 Lisbon earthquake: revisited. Ed. L. Mendes-Victor, C. Sousa Oliveira, J. Azevedo & A. Ribeiro; Series Geotechnical, Geological and Earthquake Engineering, V. 7, publisher: Springer.

13° Censimento Generale della Popolazione e delle Abitazioni. ISTAT (Istituto Nationale di Statistica) www.istat.it. (in Italian)

ANNEX A – Seismic zonation for the first Portuguese earthquake resistant codes

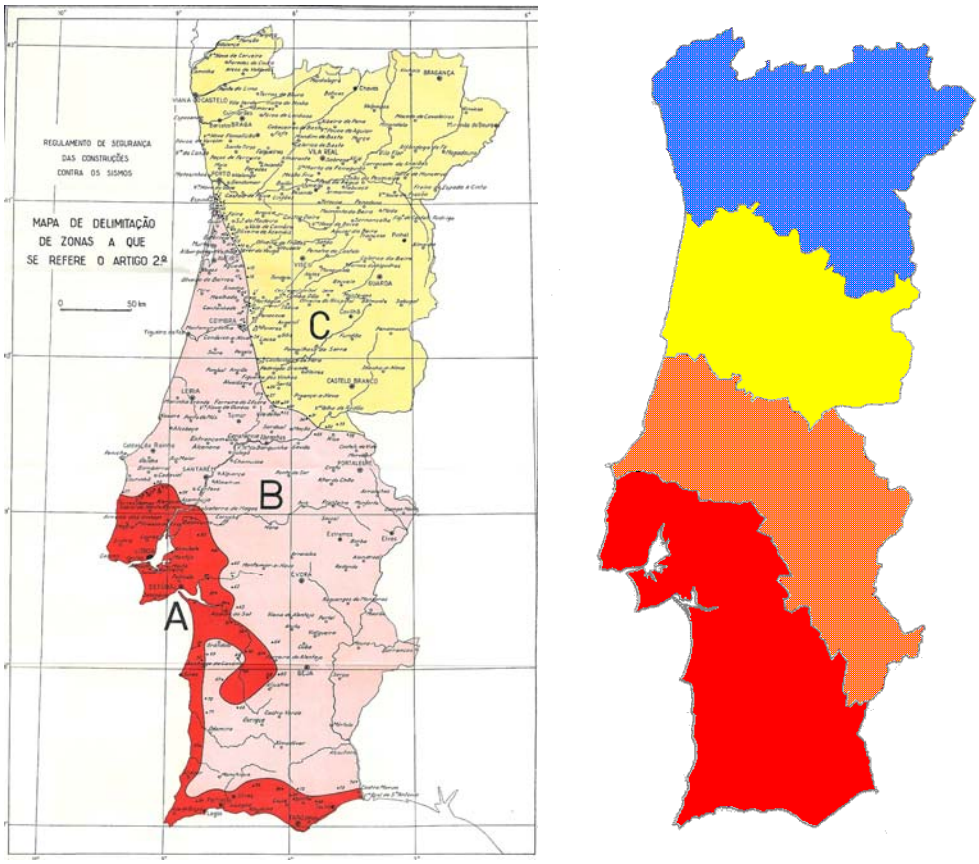

a) *b)*

Figure A.1 – Seismic zonation in a) RCSSC [1958] and b) RSA [1983].

ANNEX B – Parameters of building damage model

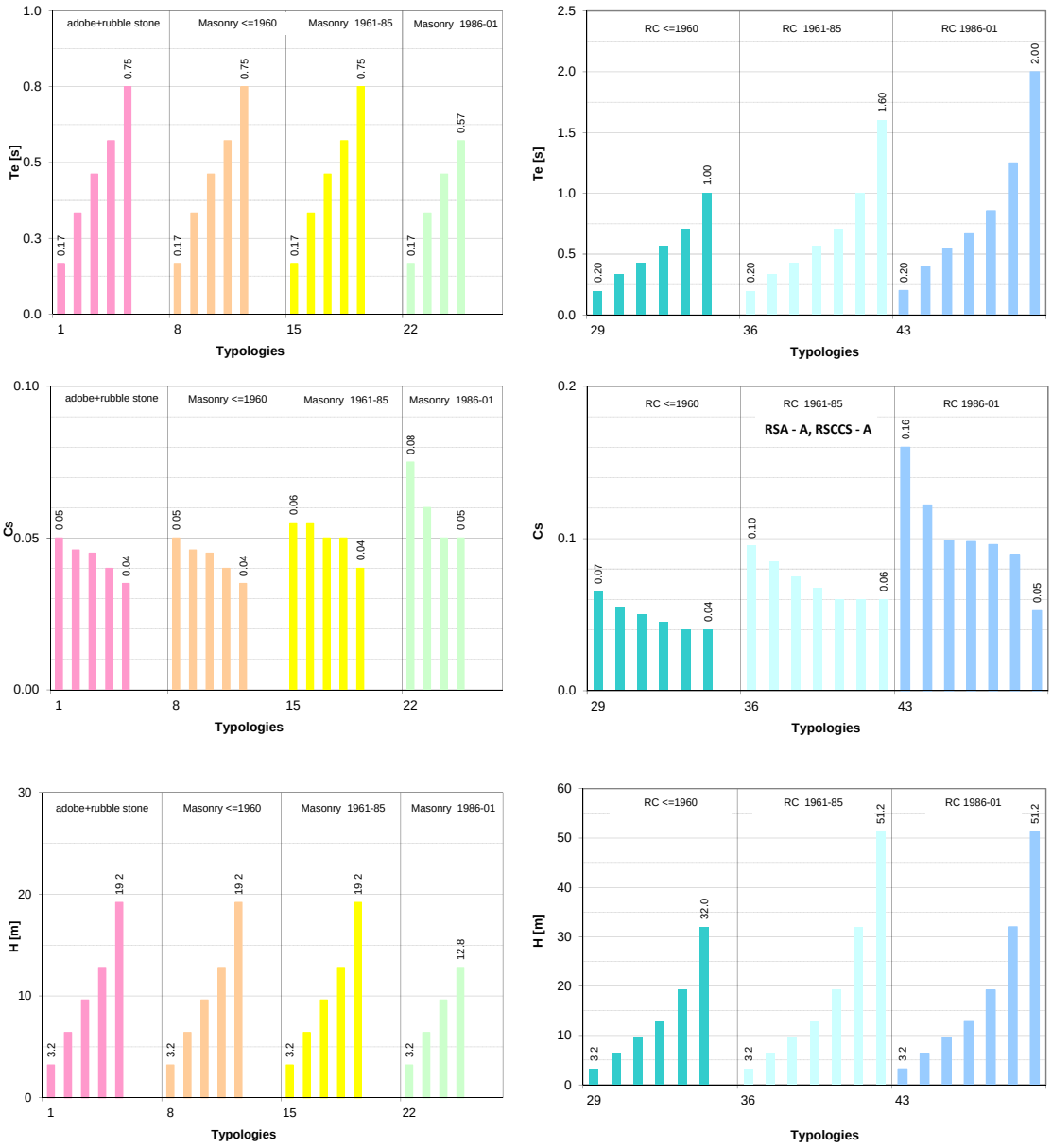

Figure B.1 – Parameters of capacity curves by vulnerability class / typology.

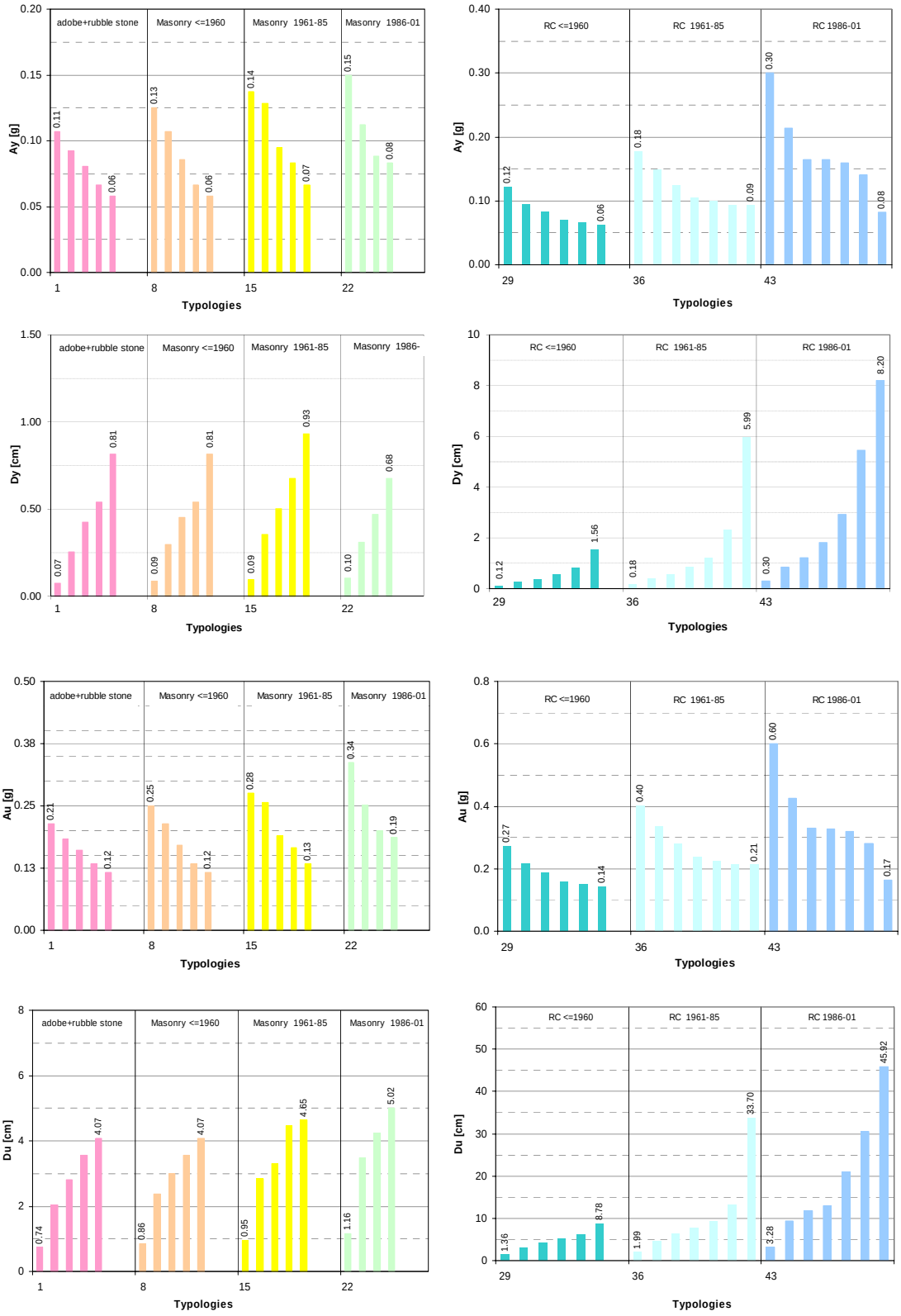

Figure B.2 – Variables that define capacity by vulnerability class / typology [LESSLOSS, 2007].

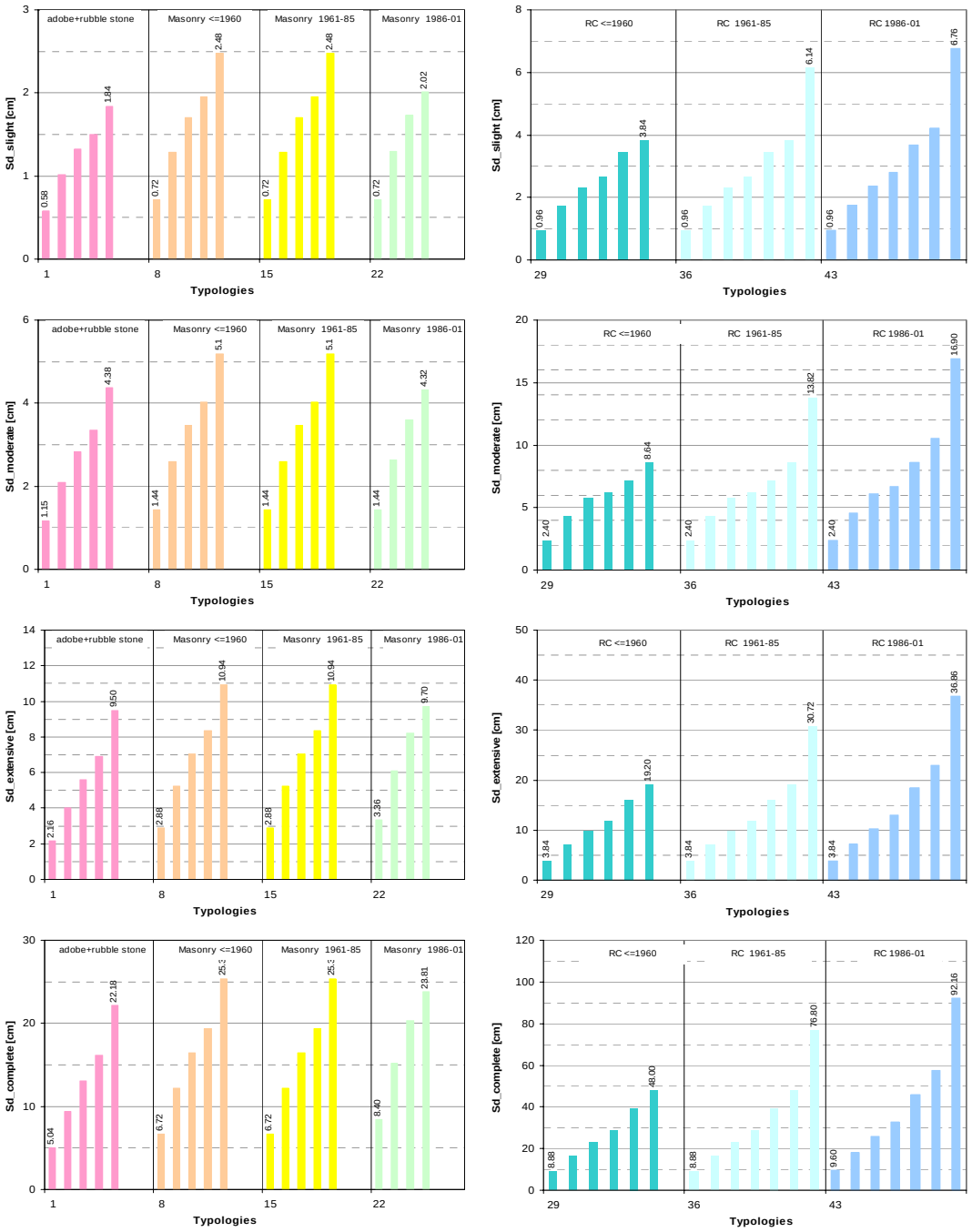

Figure B.3 – Parameters of fragility curves by vulnerability class / typology - median of spectral displacement [LESSLOSS, 2007].

ANNEX C – Parameters of social loss model

Table C.1 – Probability of human losses by injury severity level, typology and damage state [adapted from FEMA, 2003].

Damage state		Typology No. of Floors	Typological class	Injury severity level [%]			
				Slight Injuries	Injuries requiring Hospitalization	Severe Injuries	Deaths
Slight		All	All	0.05	0.0	0.0	0.0
Moderate		All	Adobe + rubble stone + Masonry till 1985 + Others	0.35	0.4	0.01	0.01
		All	Masonry 1986-01	0.2	0.05	0.0	0.0
			RC	0.25	0.03	0.0	0.0
Extensive		All	Adobe + rubble stone + Masonry till 1985 + Others	2.0	0.2	0.001	0.001
		All	Masonry 1986-01 + RC	1.0	0.1	0.002	0.002
Complete	Partial Collapse	All	Adobe + rubble stone + Masonry till 1985 + Others	10.0	2.0	0.02	0.02
		All	Masonry 1986-01 + RC	5.0	1.0	0.01	0.01
	Total Collapse	1-2	ATAPS + Others	40.0	20.0	5.0	10
		1-2	Masonry + RC				
		+ 2	Masonry + RC				

Table C.2 – Probability of collapse in the Complete damage state [adapted from FEMA 2003].

Typological class	**No of floors**	**[%]**
Adobe + rubble stone + Others	All	15.0
Masonry till 1985	All	15.0
Masonry till 1986-01	1-3	15.0
	4-7	13.0
	+ de 7	10.0
RC	1-3	13.0
	4-7	10.0
	+ 7	5.0